

Application of LiDAR DEM Metrics to Estimate Road-stream Sediment Connectivity in
Alberta Eastslopes Salmonid Habitats

by

Liz Fedra Huayta Hernani

A thesis submitted in partial fulfillment of the requirements for the degree of

Master of Science
In
Water and Land Resources

Department of Renewable Resources
University of Alberta

© Liz Fedra Huayta Hernani, 2019

Abstract

In forest lands, through surface erosion and stream fragmentation, roads can be an important source of sediment generation and supply to streams. Disturbances on salmonid habitats and downstream values such as drinking water are considered to be one of the major concerns of road sediment pollution in streams from the east slopes of the Canadian Rocky Mountains. Current models for evaluating road sediment connectivity require field data input, which is often limited for extensive areas. Therefore, in this research, I evaluated sediment connectivity from the unpaved road surface by means of LiDAR-derived DEM metrics only. Sediment connectivity modeling included two components: sediment production and sediment plume length predictions. The road slope and roughness (weighting factor) were key variables used to structure the sediment production model, and a method based on roughness and slope corridors served to estimate sediment plume traveling distance downslope. Furthermore, different roughness methods were examined with the purpose of improving sediment connectivity performance. When compared with field data, predicted results showed that sediment production normalized by the flow-directional measure of roughness based on the median absolute difference (MAD) has a good performance ($r^2=0.77$) as well as the Standard Deviation (SD) of the Slope & Aspect roughness for sediment plume length ($r^2=0.64$). The combination of both roughness indexes was named MSA (Mad and Slope & Aspect). Therefore, by applying MSA roughness, predictions of resource roads proximity to the streams resulted in "a lot of connection" with approximately 60% of sediment input into watercourses. The model was designed in an attempt to overcome the limitations of field data and provides insights for future studies to support salmonid habitats and stream values protection by using DEM metrics.

Acknowledgments

I would like to thank my enthusiastic supervisor, Dr. Axel Anderson (Department of Renewable Resources, University of Alberta), whose expertise was invaluable in the formulating of the research topic, for his patient guidance, encouragement, and useful critiques of this research work.

Similar, profound gratitude goes to my second supervisor, Mr. Rick Pelletier (Department of Renewable Resources, University of Alberta), who has been a truly dedicated mentor in GIS always willing to help me, and whose constant faith, invaluable comments, and edition have made this thesis worth it.

I express my thankfulness to the Bolivian Ministry of Education for the financing support to conduct this work. To the Foothills Research Institute for supporting the field work. To the staff of the Alberta Environment and Parks for the digital data provided for this research.

I am also hugely appreciative to Caitlin Tomaszewski, especially for the field work. She has willingly helped me out collecting the field data.

Special mention goes to Cassio Iishi for having taken me to the field observations. To Milad Moradi for his continuous encouragement through the process of researching and writing this thesis. To Eufemia Jallasi and Renzo Aruquipa for providing some distractions to rest my mind outside of my research.

Finally, thanks go to my mother Beddy Hernani Jarandilla, I believe she would be happy for this achievement.

Table of Contents

Chapter 1: Thesis Introduction.....	1
1.1 Roads Effects on Streams Values	1
1.2 Roads as a Source of Sediment Generation	2
1.3 Resource Road Sediment Transportation and Connectivity	3
1.4 LiDAR for Sediment Connectivity Assessment	5
1.5 Research Justification	5
1.6 Overview of Thesis Chapters.....	6
References	7
Chapter 2. Road-Stream Sediment Connectivity Prediction	11
2.1 Introduction.....	11
2.2 Methods and Materials	12
2.2.1 <i>Study Area</i>	12
2.2.2 <i>Data Overview</i>	13
2.2.3 <i>Modeling Framework</i>	14
2.3 Statistical Analysis.....	30
2.4 Results.....	31
2.4.1 <i>DEM vs Field Sediment Production</i>	31
2.4.2 <i>DEM vs Field Sediment Plume Length</i>	33
2.4.3 <i>DEM vs Field Sediment Connectivity</i>	34
2.4.4 <i>DEM vs Field Sediment Delivery</i>	34
2.5 Discussion.....	35
2.5.1 <i>Sediment production</i>	35
2.5.2 <i>Sediment Plume Length</i>	36
2.5.3 <i>Connectivity</i>	37
2.6 Conclusions.....	37
Tables and Figures.....	39
References	69

Chapter 3. Sediment Connectivity Adjustment Based on LiDAR-derived DEM

Terrain Roughness.....	75
3.1 Introduction.....	75
3.2 Overview of Topographic Roughness Modeling.....	76
3.2.1 <i>Cell Size</i>	76
3.2.2 <i>Optimal Cell Size</i>	76
3.2.3 <i>Moving Window</i>	77
3.3 Methods and Materials	77
3.3.1 <i>Study Area</i>	77
3.3.2 <i>Data Source</i>	77
3.3.3 <i>Modeling</i>	79
3.4 Results.....	82
3.4.1 <i>Sediment production</i>	82
3.4.2 <i>Sediment plume length</i>	83
3.4.3 <i>Sediment Connectivity</i>	84
3.5 Discussion.....	85
3.6 Conclusion	86
Tables and Figures.....	87
References	103
Chapter 4: Road-stream sediment connectivity for fish critical habitat assessment	107
.....	107
4.1 Roads and the Fish Habitat Fragmentation and Degradation	107
4.2 Effects of Roughness on Sediment Movement.....	108
4.3 Road Sediment Connectivity and LiDAR-derived DEM Metrics	108
4.4 Conclusion and Future Research	110
References	116
References.....	118
Appendix	129

List of Tables

Table 2-1. Compilation of sediment production models applied to different research contexts.	39
Table 2-2. Compilation of models associated with sediment plume traveling downslope.	40
Table 2-3. Sub-watersheds constituting the study area for sediment connectivity assessment	41
Table 2-4. Road disturbance in the Oldman watershed	42
Table 2-5. Sampling areas selected in relation to the total areas of each sub-basin.	42
Table 2-6. Road sediment production - field measurement attributes	43
Table 2-7. Sediment plume length - field measurement attributes	44
Table 2-8. Road-stream connectivity - field measurement attributes	44
Table 2-9. Connectivity valuation	45
Table 2-10. Summary for exploratory data analysis: sediment production, sediment plume length, sediment connectivity, and delivery	46
Table 2-11. DEM ~ Field sediment production fitting assessment	47
Table 2-12. DEM ~ Field sediment plume length fitting assessment	48
Table 2-13. DEM ~ Field sediment connectivity and delivery fitting assessment summary.	49
Table 3-1. LAS point characteristics for ground and low vegetation.	87
Table 3-2. Summary of exploratory data analysis for sediment production weighed by roughness.	88
Table 3-3. Correlation statistics for sediment production normalized by roughness against the field sediment production estimates.	88
Table 3-4. Summary of statistics for sediment plume length weighed by roughness.	89
Table 3-5. Correlation statistics for sediment plume length normalized by roughness against the field sediment plume length estimates.	89
Table 3-4. Summary of statistics for road-stream sediment connectivity weighed by roughness.	90

List of Figures

Figure 2-1. Road drainage structure on forest roads.	50
Figure 2-2. Slope characterization for the model: slope of the road and slope of the watershed area.....	50
Figure 2-3. Representation of the method for flow accumulation calculation from DEM cells.	51
Figure 2-4. Schematic portraying the upslope components for road sediment production estimation.	51
Figure 2-5. Schematic describing the components for sediment transportation from erosion initiation points P1 and P2 to Px point.	52
Figure 2-6. Sediment plume flowing directions for potential connectivity to streams affected by downhill topographic conditions.	52
Figure 2-7. Location of the study area.	53
Figure 2-8. Location of the sampling area.	54
Figure 2-9. Volume of sediment production (m^3) predicted from DEM versus the sediment production (m^3) estimated from the field at the corresponding site (N=196). No topographic roughness was applied for the predicted production values from the DEM.	55
Figure 2-10. Sediment plume travel distance (m) predicted from the DEM versus the plume length estimated from the field at the corresponding sites (N=51).	56
Figure 2-11. Number of sediment plumes found in each sub-basin.	57
Figure 2-12. The volume of sediment delivery estimated from DEM versus Field sediment delivery at the sites (N= 44).	58
Figure 2-13. Connectivity estimated from Field and Connectivity predicted from the DEM with no roughness (no weighting factor applied) and with roughness (weighted factor applied) (N= 44).....	59
Figure 2-14. Sediment production predicted from roads (m^3) based on the DEM and field (N=196).	60
Figure 2-15. DEM predicted percentage of roads classified by their sediment delivery status: delivered and non-delivered.	61
Figure 2-16. DEM predicted percentage of roads classified by their connectivity level.	61

Figure 2-17. Roads classified by their estimated percentage of sediment plumes length versus their connectivity class.	62
Figure 2-18. DEM vs. Field sediment production fitting results.....	63
Figure 2-19. DEM vs. Field sediment plume length fitting results	64
Figure 2-20. DEM vs. Field connectivity fitting results.....	65
Figure 2-21. DEM vs. Field delivery fitting results.....	66
Figure 2-22. Sediment production, delivery, and connectivity for Livingstone sub-basin.	67
Figure 2-23. Sediment production, delivery, and connectivity for Dutch sub-basin.....	68
Figure 3-1. Cartesian polar coordinate used to define the angular derivatives to calculate the Slope & Aspect roughness.....	91
Figure 3-2. Road surface sediment production normalized by using different DEM-derived roughness.....	92
Figure 3-3. Approximate sediment production from road surface (m ³) using different DEM-derived terrain roughness.....	93
Figure 3-4. Sediment plume traveling distance from road surface normalized by using different roughness.....	94
Figure 3-5. Prediction of road-stream sediment connectivity as a result of using DEM terrain and DSM vegetation roughness.....	95
Figure 3-6. Approximates of road surface sediment delivery (m ³) by using DEM terrain and DSM vegetation roughness.....	96
Figure 3-5. Approximate values of road sediment delivery in relation to the delivery from the field by using DEM and DSM roughness.....	97
Figure 3-6. Sediment connectivity per type of roughness including the MSA roughness.	98
Figure 3-7. Allison Sub-basin. Road sediment production comparison using the Mad flow directional roughness and the Slope & Aspect roughness (directional statistics).	99
Figure 3-8. Allison Sub-basin. Sediment connectivity comparison using the Mad flow directional roughness and the Slope & Aspect roughness (directional statistics).	100
Figure 3-9. Race Horse Sub-basin. Road sediment production comparison using the Mad flow directional roughness and the Slope & Aspect roughness (directional statistics).	101

Figure 3-10. Race Horse Sub-basin. Road sediment connectivity comparison using the Mad flow directional roughness and the Slope & Aspect roughness (directional statistics).....102

Figure 4-1. Upper Oldman Sub-basin. Road sediment production comparison using the MAD flow-directional roughness and the Slope & Aspect roughness (directional statistics).112

Figure 4-2. Upper Oldman Sub-basin. Road sediment connectivity comparison using the Mad flow directional roughness and the Slope & Aspect roughness (directional statistics).....113

Figure 4-3. Upper Oldman Sub-basin. Sediment production, sediment plume length, sediment connectivity prediction by applying the MSA roughness. Colors sediment production high (red), medium (light orange), and low (white). High connected road areas (purple) and low connected (white). Sediment plume length shows low movement (black ramp) and high movement (gray or no color)114

Figure 4-4. Upper Oldman Sub-basin. Prediction sediment connectivity mapping and pictures from the field.115

Chapter 1: Thesis Introduction

1.1 Roads Effects on Streams Values

The increased construction of roads to establish access for developing activities presents a challenge for water management and aquatic wildlife habitat conservation (Grace et al., 1998; Grace and Clinton, 2007; Rex & Petticrew, 2011). In forested landscapes, roads are considered the dominant source of anthropogenic sediment generation and stream fragmentation due to forest management activities (logging, timber transportation), and recreational activities (Ramos-Scharrón and MacDonald, 2005; Sugden et al., 2007; van Meerveld et al., 2014; Al-Chokhachy et al., 2016). Unpaved roads with high levels of surface erosion are considered an issue of great concern due to the potential generation of fine sediment (Reid and Dunne, 1984; Lisle, 1989; Rex and Petticrew, 2011) can disturb stream characteristics that are very important for fish and macroinvertebrate habitats (Grace et al., 1998; Motha et al., 2004; McCaffery et al., 2007) and increased suspended solids and turbidity can impact drinking source water quality (Lane and Sheridan, 2002). Roads characterized by silty loam and silty-clay loam (62.5 μm) soil texture (Baird et al., 2012) can be able to generate a higher amount of sediment than that from gravelly loam roads (Luce and Black, 1999)

Studies carried out by Hurkett (2009) and Oldman Watershed Council (2010) found that the eastern slopes of the Canadian Rocky Mountains have critical habitats for native Bull trout (*Salvelinus confluentus*) and Cutthroat trout (*Oncorhynchus clarkii lewisii*) and sediment from roads and trails may be a factor in the reduction in their population attributed primarily to the existence of roads. Ripley et al. (2005) pointed out that unpaved forest roads resulted in a negative relation between Bull trout occurrence and road density (e.g., if road density < 1.6 km/km², Bull trout occurrence > 0.1). Thus, road-derived sediment can potentially threaten fish passage, reduction of spawning areas, the survival of salmonid eggs and alevins leading to reductions in salmonid populations (Bilby et al., 1989; Lisle, 1989; Miller, 2014; Alder et al., 2015). Similarly, McCaffery et al. (2007) cited that macroinvertebrate communities also respond negatively to fine sediments. Suspended sediment can prevent the photosynthesis and the growth of aquatic plants (Kemp et al., 2011); thus, it limits the ability for fish to find food,

1.2 Roads as a Source of Sediment Generation

Roads can generate sediment through surface erosion and road use (Schiess, 2001). While erosion from active road use can depend on human-related activities (e.g., traffic, vegetation removal), surface erosion depends mainly on the erosive factors governing the detachment of soil from road surface under conditions of natural mechanisms. Particle detachment has been attributed to the energy of the flowing water (Moore and Burch, 1986; Baird et al., 2012), the road drainage characteristics (Wemple et al., 1996), and the road surface erodibility potential as pointed out by Luce and Black (1999). In undisturbed forest lands, sediment production tends to have low rates by approximately less than 0.27 t/ha/year (Grace et al., 1998); nevertheless, through surface erosion, sediment generation potentially increases even years after road construction and varies from large orders of magnitude (Megahan et al., 2001; Ramos-Scharrón and MacDonald, 2005; Thompson et al., 2008). Even though sediment is produced from all components of the road surface - road surface, hillslope, cutslope, and ditches (Grace et al., 1998)-, findings from Reid and Dunne (1984) pointed out that the sediment generation from road surface can be significant compared to that from the off-road sources.

Sediment production from road surface is attributed to a number of controlling factors. Erosion factors such as precipitation, runoff, and slope along with traffic, road maintenance activities and vegetation removal are some of the factors that can lead to a significant amount of sediment generation. For example, on steep road surfaces, sediment is more likely to be generated at exponential levels as pointed out by Ramos-Scharrón and MacDonald (2005). Luce and Black (1999) noted that on an aggregate surfaced road with well-vegetated ditches, sediment production is generated at low rates while the removal of vegetation from the cutslope and ditch is able to generate up to 7 times more sediment than that from road surface. On the other hand, sediment production by road use can be attributed to factors such as road maintenance and road grading which according to (Luce and Black, 2001) can increase erosion at the time of the activities. Another controlling factor is attributed to the intensity of road use such as traffic. Reid and Dunne (1984) found that highly active roads can produce sediment up to 130 times more than non-active roads.

1.3 Resource Road Sediment Transportation and Connectivity

According to Bilby et al. (1989), the forces that move the material and the sediment availability are the two main factors controlling whether the sediment from the road surface can successfully reach the streams. For example, studies identified that sediment transportation capacity depends primarily on the overflow source strength such as runoff intensity (Croke and Mockler, 2001; Croke and Hairsine, 2006; Sosa-Pérez and MacDonald, 2017) while sediment availability can depend on the potential of erosive factors such as precipitation or traffic intensity to separate particles from road surface. Additionally, Bilby et al. (1989) reported that sediment retention within the channels was inversely related to particle size which means that coarse particles movement rates are low compared to the fine particles as mentioned by Luce and Black (1999).

Therefore, sediment connectivity between a road and stream can be represented by the capacity for the sediment particle to travel a certain distance from the road surface with the expectation to reach the stream downslope (Hooke, 2003; Croke et al., 2005; Bracken and Croke, 2007; Baird et al., 2012; Bracken et al., 2015). The concept of connectivity has been commonly used to evaluate natural process relationships and dynamics. Researchers have also denoted the sedimentological connectivity as “the physical transfer of sediments and attached pollutants through the drainage basin” (Baartman et al., 2013; Alder et al., 2015).

Roads near stream buffers can be highly connected due to the short traveling distance (Bilby et al., 1989; La Marche & Lettenmaier, 2001; Baird et al., 2012) whereas for road far from streams, road sediment connectivity can be controlled by the capacity for the sediment plume to move a distance under the conditions of the pathway surface downslope (Croke et al., 2005; Croke and Hairsine, 2006; Borselli et al., 2008). Therefore, Anderson and Anderson (1987) highlighted that steep and disturbed areas promote sediment movement. Similarly, sediment transportation pathways characteristics such as the presence of barriers, sinks, dense vegetation cover, surface roughness, and soil infiltration capacity are also significant for characterizing sediment connectivity. (Hooke, 2003; Borselli et al., 2008; Bracken et al., 2015). For example, minimal rates at which the soil surface cannot absorb water can highly facilitate sediment flow downstream.

Sediment connectivity can happen either directly into streams through channels, gullies, ditches, or indirectly through diffuse overland flow paths (Croke et al., 2005; Croke and Hairsine, 2006; Borselli et al., 2008). Therefore, as in Wemple et al. (1996) connectivity occurs when road sediment reaches the stream through (1) direct pathways connected to a stream (e.g., channelized) and (2) indirect pathways connected to a stream due to gully occurrences in the hillslope area. Bracken and Croke (2007) indicated that channels originated from gullies can promote overflow generation downhill even when low or moderate rainfall events occur. Additionally, connectivity also occurs (3) through diffuse pathways (Wemple et al., 1996; Bracken and Croke, 2007; Baartman et al., 2013). As underlined by Bracken and Croke (2007), when overland flow pathways are characterized by diffusiveness, the surface has limited capacity to absorb water and infiltrates at a low rate as the sediment flow moves. Normally diffuse sediment flows are wide and shallow (Croke and Hairsine, 2006).

Consequently, as in Bracken and Croke (2007), the degree of connectivity not only depends on the overflow amount and energy and the infiltration capacity of the surface but also on the pathways characteristics as indicated by Croke and Mockler (2001). For example, La Marche and Lettenmaier (2001) found that road-stream sediment transfer capacity was mainly influenced by hillslope topography and downslope distance to the channels. Likewise, Borselli et al. (2008) attributed the surface infiltration capacity to vegetation cover. Overall, this can be summarized in one main factor, surface roughness. Pathway surface irregularities can significantly determine whether the sediment plume has the capacity to reach the streams.

To assess pathways heterogeneities, roughness values have been calculated and used for a better characterization of the sediment plume movement (Borselli et al., 2008; Cavalli et al., 2013). Methods to measure landscape heterogeneities are based on topographic and surface roughness. Topographic roughness is usually measured by means of the standard deviation of the slope (Grohmann et al., 2011), residual topography (Cavalli et al., 2013), cropping and management practices (Borselli et al., 2008), variograms (Trevisani and Rocca, 2015), and among others related to terrain characteristics; on the other hand, surface roughness measurement can also involve the vegetation roughness length (Raupach, 1994; Faivre et al., 2017).

1.4 LiDAR for Sediment Connectivity Assessment

The existence of many roads distributed over a heterogeneous landscape makes the sediment dynamic evaluation a challenging issue. On heterogeneous landscapes, erosion and sediment processes are stochastic, scale-dependent, and display spatial variability. Accordingly, detailed data and field surveys can be limited to only very specific and small local areas. Therefore, the use of Airborne Light Detection and Ranging (LiDAR) has become an important key for the analysis of not only roughness values but sediment production and transportation over large spatial extents (Burnett and Miller, 2007; Borselli et al., 2008; White et al., 2010; Baartman et al., 2013; Alder et al., 2015; Cantreul et al., 2017; Cavalli et al., 2017).

LiDAR data has made sediment connectivity modeling approaches more feasible than ever before. A high-resolution terrain data can expose landscape features effectively allowing more precise extraction of the slope, flow direction, and distance values among other metrics. Various approaches using LiDAR technologies along with Geographic Information Systems (GIS) tools have been proposed to address the issue of the sediment connectivity. Gravity-driven processes have been mostly the main source of sediment supply to streams that have been studied by many researchers. For instance, a study carried out by Burnett and Miller (2007) suggested a probabilistic model examine the spatial distribution of potential for debris-flow points and their transportation to a downslope point under the influence of topography. Borselli et al. (2008) proposed an Index of Connectivity (IC) to estimate debris flow connectivity in alpine environments; to assess the degree of connectivity, this model links the upslope contributing area and the downslope drainage pathway characteristics. Similarly, Cavalli et al. (2013) and Trevisani and Cavalli (2016) modeled sediment connectivity based on Borselli et al. (2008). The use of topographic roughness and the multidirectional concept of downhill sediment movement have gained importance in sediment connectivity assessments (Cantreul et al., 2017; Cavalli et al., 2017) allowing the examination of the degree of connection of the sediment source to streams.

1.5 Research Justification

The eastern slopes of the Canadian Rocky Mountains have been considered as the native habitats for Bull trout (*Salvelinus confluentus*) and Cutthroat trout (*Oncorhynchus clarkii lewisii*) and as

the region of high-quality drinking water supplies; however, due to the increase of extensive unpaved road network for forestry and oil management activities, it is important to evaluate the sediment connectivity from resource road to streams by identifying the roads with a potential for sediment production and contribution to streams.

Through this study, I expect to contribute to the protection of vulnerable Bull trout, and Cutthroat trout species in Alberta's east slopes and in the Oldman watershed by modeling road-stream sediment connectivity which can serve as a baseline for future researchers in consecutive sediment connectivity assessments.

1.6 Overview of Thesis Chapters

In order to evaluate a model that allows the prediction of sediment connectivity through DEM metrics and considering the roads surfaces as a source of sediment supply to streams, I present the following chapters:

In Chapter 2, I present a modeling approach to assess road-stream sediment connectivity from unpaved roads in Alberta's East Slopes through the applicability of high-resolution DEM data. I adapt landslide connectivity models to be applicable to sediment supply from road surfaces. Thus, I focus on the evaluation of the following road-stream sediment connectivity components: sediment production from road surface (upslope component) and sediment plume traveling distance (downslope component). Additionally, I compared the predicted data with the field data to validate the model performance.

In Chapter 3, I evaluate the performance of various roughness indexes calculated from Lidar-derived DEM data to predict the road-stream sediment connectivity. The roughness values represent the significance in terrain variations which denotes an impediment for sediment to move; therefore, values of roughness were used as a weighting factor for sediment production up and road-stream sediment transportation downslope.

References

- Al-Chokhachy, R., Black, T. A., Thomas, C., Luce, C. H., Rieman, B., Cissel, R., ... Kershner, J. L. (2016). Linkages between unpaved forest roads and streambed sediment: why context matters in directing road restoration. *Restoration Ecology*, *24*(5), 589–598. <https://doi.org/10.1111/rec.12365>
- Alder, S., Prasuhn, V., Liniger, H., Herweg, K., Hurni, H., Candinas, A., & Gujer, H. U. (2015). A high-resolution map of direct and indirect connectivity of erosion risk areas to surface waters in Switzerland-A risk assessment tool for planning and policy-making. *Land Use Policy*, *48*, 236–249. <https://doi.org/10.1016/j.landusepol.2015.06.001>
- Anderson, P., & Anderson, R. (1987). Erosion potential index : a method for evaluating sheet erosion at stream crossings. Edmonton : Alberta Forestry, Lands and Wildlife. <https://doi.org/10.5962/bhl.title.110391>
- Baartman, J. E. M., Masselink, R., Keesstra, S. D., & Temme, A. J. A. M. (2013). Linking landscape morphological complexity and sediment connectivity. *Earth Surface Processes and Landforms*, *38*(12), 1457–1471. <https://doi.org/10.1002/esp.3434>
- Baird, E. J., Floyd, W., Van Meerveld, I., & Anderson, A. E. (2012). Road Surface Erosion, Part 1 : Summary of Effects, Processes, and Assessment Procedures. *Streamline Watershed Management Bulletin*, *15*(1), 1–35. Retrieved from <http://www.forrex.org/publications/streamline%0AProject>
- Bilby, R. E., Sullivan, K., & Duncan, S. H. (1989). The generation and fate of road-surface sediment in forested watersheds in southwestern Washington. *Forest Science*, *35*(2), 453–468. <https://doi.org/doi.org/10.1093/forestscience/35.2.453>
- Borselli, L., Cassi, P., & Torri, D. (2008). Prolegomena to sediment and flow connectivity in the landscape: A GIS and field numerical assessment. *Catena*, *75*(3), 268–277. <https://doi.org/10.1016/j.catena.2008.07.006>
- Bracken, Louise J., and Croke, J. (2007). The concept of hydrological connectivity and its contribution to understanding runoff-dominated geomorphic systems, *21*, 2267–2274. <https://doi.org/10.1002/hyp.6313>
- Bracken, L. J., Turnbull, L., Wainwright, J., & Bogaart, P. (2015). Sediment connectivity: A framework for understanding sediment transfer at multiple scales. *Earth Surface Processes and Landforms*, *40*(2), 177–188. <https://doi.org/10.1002/esp.3635>
- Burnett, K. M., & Miller, D. J. (2007). Streamside policies for headwater channels: An example considering debris flows in the Oregon coastal province. *Forest Science*, *53*(2), 239–253. <https://doi.org/doi.org/10.1093/forestscience/53.2.239>
- Cantreul, V., Bielders, C., Calsamiglia, A., & Degré, A. (2017). How pixel size affects a sediment connectivity index in central Belgium. *Earth Surface Processes and Landforms*. <https://doi.org/10.1002/esp.4295>
- Cavalli, M., Goldin, B., Comiti, F., Brardinoni, F., & Marchi, L. (2017). Assessment of

- erosion and deposition in steep mountain basins by differencing sequential digital terrain models. *Geomorphology*, 291, 4–16. <https://doi.org/10.1016/j.geomorph.2016.04.009>
- Cavalli, M., Trevisani, S., Comiti, F., & Marchi, L. (2013). Geomorphometric assessment of spatial sediment connectivity in small Alpine catchments. *Geomorphology*, 188, 31–41. <https://doi.org/10.1016/j.geomorph.2012.05.007>
- Croke, J. C., & Hairsine, P. B. (2006). Sediment delivery in managed forests: a review. *Environmental Reviews*, 14(1), 59–87. <https://doi.org/10.1139/a05-016>
- Croke, J., & Mockler, S. (2001). Gully initiation and road-to-stream linkage in a forested catchment southeastern Australia. *Earth Surface Processes and Landforms*, 26(2), 205–217. [https://doi.org/10.1002/1096-9837\(200102\)26:2<205::AID-ESP168>3.0.CO;2-G](https://doi.org/10.1002/1096-9837(200102)26:2<205::AID-ESP168>3.0.CO;2-G)
- Croke, J., Mockler, S., Fogarty, P., & Takken, I. (2005). Sediment concentration changes in runoff pathways from a forest road network and the resultant spatial pattern of catchment connectivity. *Geomorphology*, 68(3–4), 257–268. <https://doi.org/10.1016/j.geomorph.2004.11.020>
- Faivre, R., Colin, J., & Menenti, M. (2017). Evaluation of methods for aerodynamic roughness length retrieval from very high-resolution imaging LIDAR observations over the Heihe Basin in China [Remote Sens., 9, (2017) 63]. *Remote Sensing*, 9(2), 1–25. <https://doi.org/10.3390/rs9020157>
- Grace, J. I., & Clinton, B. . (2007). Protecting soil and water in forest road management. *Transactions of the American Society of Agricultural and Biological Engineers ASABE*, 50(5), 1579–1584. Retrieved from <http://digitalcommons.unl.edu/usdafsfacpub/58>
- Grace, J. I., Rummer, B., Stokes, B. J., & Wilhoit, J. (1998). Evaluation of Erosion Control Techniques on Forest Roads. *American Society of Agricultural Engineers*, 41(2), 383–391. Retrieved from <https://www.fs.usda.gov/treearch/pubs/65>
- Grohmann, C. H., Smith, M. J., & Riccomini, C. (2011). Multiscale analysis of topographic surface roughness in the Midland Valley, Scotland. *IEEE Transactions on Geoscience and Remote Sensing*, 49(4), 1200–1213. <https://doi.org/10.1109/TGRS.2010.2053546>
- Hooke, J. (2003). Coarse sediment connectivity in river channel systems: A conceptual framework and methodology. *Geomorphology*, 56(1–2), 79–94. [https://doi.org/10.1016/S0169-555X\(03\)00047-3](https://doi.org/10.1016/S0169-555X(03)00047-3)
- Hurkett, B. (2009). Bull Trout Population Assessment in the Upper Oldman River Drainage. Lethbridge, Alberta. Retrieved from <https://www.ab-conservation.com/publications/report-series/bull-trout-population-assessment-in-the-upper-oldman-river-drainage-2009/>
- Kemp, P., Sear, D., Collins, A., Naden, P., & Jones, I. (2011). The impacts of fine sediment on riverine fish. *Hydrological Processes*, 25(11), 1800–1821. <https://doi.org/10.1002/hyp.7940>
- La Marche, J. L., & Lettenmaier, D. P. (2001). Effects of forest roads on flood flows in the Deschutes River, Washington. *Earth Surface Processes and Landforms*, 26(2), 115–134.

[https://doi.org/10.1002/1096-9837\(200102\)26:2<115::AID-ESP166>3.0.CO;2-O](https://doi.org/10.1002/1096-9837(200102)26:2<115::AID-ESP166>3.0.CO;2-O)

- Lane, P. N. J., & Sheridan, G. J. (2002). Impact of an unsealed forest road stream crossing: Water quality and sediment sources. *Hydrological Processes*, 16(13), 2599–2612. <https://doi.org/10.1002/hyp.1050>
- Luce, C. H., & Black, T. a. (1999). Sediment production from forest roads in western Oregon. *Water Resources Research*, 35(8), 2561. <https://doi.org/10.1029/1999WR900135>
- Luce, C. H., & Black, T. A. (2001). Effects of traffic and ditch maintenance on forest road sediment production. In *Seventh Federal Interagency Sedimentation Conference* (pp. 67–74). Reno, Nevada. Retrieved from <http://www.treesearch.fs.fed.us/pubs/23963>
- McCaffery, M., Switalski, T. A., & Eby, L. (2007). Effects of Road Decommissioning on Stream Habitat Characteristics in the South Fork Flathead River, Montana. *Transactions of the American Fisheries Society*, 136(3), 553–561. <https://doi.org/10.1577/T06-134.1>
- Miller, D. J., & Burnett, K. M. (2008). A probabilistic model of debris-flow delivery to stream channels demonstrated for the Coast Range of Oregon, USA. *Geomorphology*, 94(1–2), 184–205. <https://doi.org/10.1016/j.geomorph.2007.05.009>
- Moore, I. D., & Burch, G. J. (1986). Physical Basis of the Length-slope Factor in the Universal Soil Loss Equation. *Soil Science Society of America Journal*, 50(5), 1294. <https://doi.org/10.2136/sssaj1986.036159950050000500042x>
- Oldman Watershed Council. (2010). Oldman River State of the Watershed Report 2010. Lethbridge, Alberta. Retrieved from www.oldmanbasin.org
- Ramos-Scharrón, C. E., & MacDonald, L. H. (2005). Measurement and prediction of sediment production from unpaved roads, St John, US Virgin Islands. *Earth Surface Processes and Landforms*, 30(10), 1283–1304. <https://doi.org/10.1002/esp.1201>
- Raupach, M. R. (1994). Simplified expressions for vegetation roughness length and zero-plane displacement as functions of canopy height and area index. *Boundary-Layer Meteorology*, 71(1–2), 211–216. <https://doi.org/10.1007/BF00709229>
- Reid, L. M., & Dunne, T. (1984). Sediment production from forest road surfaces. *Water Resources Research*, 20(11), 1753–1761. <https://doi.org/10.1029/WR020i011p01753>
- Rex, J. F., & Petticrew, E. L. (2011). Fine Sediment Deposition at Forest Road Crossings: An Overview and Effective Monitoring Protocol. In D. A. Manning (Ed.), *Sediment Transport in Aquatic Environments* (2011th ed., p. 332). INTECH. Retrieved from <http://www.intechopen.com/books/sediment-transport-in-aquatic-environments%0AIn>
- Ripley, T., Scrimgeour, G., & Boyce, M. S. (2005). Bull trout (*Salvelinus confluentus*) occurrence and abundance influenced by cumulative industrial developments in a Canadian boreal forest watershed. *Canadian Journal of Fisheries and Aquatic Sciences*, 62(11), 2431–2442. <https://doi.org/10.1139/f05-150>
- Schiess, P. (2001). Road Management Strategies to Reduce Habitat Impacts: A Case for Engineered Cable Yarding Operations and Harvest Schedules. In U. Arzberger & M.

- Grimoldi (Eds.), *New Trends in Wood Harvesting with Cable Systems for Sustainable Forest Management in The Mountains*. Ossiach, Austria June 18 to 24 June 2001: Forestry Training Centre, Government of Austria. Retrieved from <http://www.fao.org/3/Y9351E/Y9351E32.htm#ch32>
- Sosa-Pérez, G., & MacDonald, L. H. (2017). Reductions in road sediment production and road-stream connectivity from two decommissioning treatments. *Forest Ecology and Management*, 398, 116–129. <https://doi.org/10.1016/j.foreco.2017.04.031>
- Sugden, B. D., & Woods, S. W. (2007). Sediment Production From Forest Roads in Western Montana. *JAWRA Journal of the American Water Resources Association*, 43(1), 193–206. <https://doi.org/10.1111/j.1752-1688.2007.00016.x>
- Thompson, C. J., Takken, I., & Croke, J. (2008). Hydrological and sedimentological connectivity of unsealed roads. In *Sediment Dynamics in Changing Environments* (pp. 524–531). Christchurch, New Zealand: International Association of Hydrological Sciences, IAHS Publ. 325, 2008.
- Trevisani, S., & Cavalli, M. (2016). Topography-based flow-directional roughness: Potential and challenges. *Earth Surface Dynamics*, 4(2), 343–358. <https://doi.org/10.5194/esurf-4-343-2016>
- Trevisani, S., & Rocca, M. (2015). MAD: Robust image texture analysis for applications in high-resolution geomorphometry. *Computers and Geosciences*, 81, 78–92. <https://doi.org/10.1016/j.cageo.2015.04.003>
- van Meerveld, H. J., Baird, E. J., & Floyd, W. C. (2014). Controls on sediment production from an unpaved resource road in a Pacific maritime watershed. *Water Resources Research*, 50(6), 4803–4820. <https://doi.org/10.1002/2013WR014605>
- Wemple, B. C., Jones, J. a, & Grant, G. E. (1996). Channel network extension by logging roads in two basins, western Cascades, Oregon. *Water Resources Bulletin*, 32(6), 1195–1207. <https://doi.org/10.1029/2002WR001744>
- White, R. A., Dietterick, B. C., Mastin, T., & Strohman, R. (2010). forest roads mapped using LiDAR in steep forested terrain. *Remote Sensing*, 2(4), 1120–1141. <https://doi.org/10.3390/rs2041120>

Chapter 2. Road-Stream Sediment Connectivity Prediction

2.1 Introduction

Roads provide easy accessibility for many activities in the forest; however, they are a large source of sediment supply that negatively affects aquatic ecosystems. Changes in land use to establish access not only for fire management, logging activities, timber transportation, oil and gas, and forest management but also for recreational activities can increase surface erosion on unpaved forest roads (Ramos-Scharrón and MacDonald, 2005; Sugden et al., 2007; van Meerveld et al., 2014; Al-Chokhachy et al., 2016). Sediment generation through surface erosion is considered to occur by larger orders of magnitude in high-active forest roads (Ramos-Scharrón and MacDonald, 2005; Thompson et al., 2008). Unpaved roads with high levels of surface erosion can greatly facilitate the generation of fine-grained 62.5 µm and greater (Baird et al., 2012) material and its movement downstream (Reid and Dunne, 1984) creating a negative impact on aquatic ecosystems (Miller, 2014). It is of particular concern that sediment contamination from high-use unpaved roads impacts the native salmonid habitats. The Alberta's east slopes have been considered as critical habitats for native Bull trout and Cutthroat trout due to the reduction of their population attributed primarily to the existence of roads (Hurkett, 2009; Oldman Watershed Council, 2010). The increase in water turbidity, the obstacle to fish passage and the reduction of spawning areas can be some of the main off-site effects caused by fine sediments input into streams (Lisle, 1989; McCaffery et al., 2007; Alder et al., 2015).

To help managers understand sediment impact on streams, studies have been done that report linkages between road-related sediment sources (e.g. landslides and debris) and stream quality. Assessing the factors for sediment generation and the potential for sediment to move and reach the streams (Table 2-1) have been fundamental for modeling sediment dynamics. Most of the models incorporate elements that have been commonly used to estimate sediment production rates such as contributing area and slope (Anderson and Anderson, 1987; Anderson and MacDonald, 1998; Marchi and Dalla Fontana, 2005; Borselli et al., 2008). Some studies have also considered distance to streams and vegetation as important factors influencing upslope sediment production (Wischmeier and Smith, 1978; Luce and Black, 1999; Borselli et al., 2008;

Al-Chokhachy et al., 2016). Similarly, there are models formulated to assess the sediment downslope movement (Table 2-2); they have focused on analyzing variables such as distance to streams, differences in elevation, and topographic roughness as factors influencing the sediment plume flow, and thus sediment input into streams (Beven and Kirkby, 1979; Marchi and Dalla Fontana, 2005; Miller and Burnett, 2007; Borselli et al., 2008).

Furthermore, the use of digital elevation models (DEM) and geographic information systems (GIS) platforms have greatly assisted in the understanding of watershed management (Benda et al., 2007). In large areas with diverse geomorphology, DEMs can allow a rapid assessment of factors influencing sediment generation and transport, as well as identify areas with potential for sediment connectivity (White et al., 2010; Baartman et al., 2013; Cantreul et al., 2017). Such is the case of SedInconnect, developed by Crema and Cavalli (2018), which evaluates an index of connectivity IC (Borselli et al., 2008; Cavalli et al., 2013; Trevisani and Cavalli, 2016) with wide applicability to geomorphic processes in alpine areas. Another example combines DEM predictions with field data, as is the case of the Road Erosion and Delivery Index (READI) which has been used in the evaluation of erosion and sediment delivery from unpaved road networks to streams (Benda et al., 2007; Benda et al. 2019)

According to the literature, at the site scale, a wide number of studies have focused on evaluating road sediment connectivity by combining field and DEM data. On the other hand, to compensate for the lack of field data for extensive areas, studies have considered the use of DEM metrics (e.g., landslide connectivity). Therefore, in this research, the overall goal was to generate a model to predict the road-stream sediment connectivity through the applicability of metrics extracted from a high-resolution DEM data only. The objectives for this chapter are 1) to adapt the methods of landslide connectivity to predict the connectivity of sediment generated from road surface erosion, and 2) to use field data to contrast the predicted connectivity against the estimated connectivity in the field.

2.2 Methods and Materials

2.2.1 Study Area

The study area (Figure 2-7) is located in south-west Alberta in the north part of the Oldman watershed headwaters region along the eastern slopes of the Canadian Rocky Mountains and

foothills. The vegetation is characterized by a combination of coniferous and deciduous trees populating the high elevations. Among the most important conifers that can be found in the high elevations are douglas fir (*Pseudotsuga menziesii*), englemann spruce (*Picea engelmannii*), and white spruce, (*Picea glauca*); the lower elevation is commonly populated by lodgepole pine (*Pinus contorta*) and douglas fir (*Pseudotsuga menziesii*) trees, as well as mixed Aspen forests (Oldman Watershed Council, 2010). The Oldman watershed comprises an area of approximately 23000 km² on the Canadian side (Oldman Watershed Council, 2010). The study area comprises approximately 1354 km² involving eight sub-watersheds (Table 2-3), which are considered important habitats for Alberta's native fish species, which include two species at risk: Bull trout (*Salvelinus confluentus*) and Cutthroat trout (*Oncorhynchus clarkii lewisi*) (Hurkett, 2009; Sawatzky, 2016).

Approximately 2% of the Oldman watershed headwaters region is covered by road infrastructure (Oldman Watershed Council, 2010), of which Off-road vehicles (OHVs) trails 0.7% are recognized as being disturbing streams more than roads 0.6% and pipelines 0.3% (Table 2-4) (Oldman Watershed Council, 2010). Additionally, the density of all linear footprints in the upper part of the Oldman watershed ranges from 1.2 to >3 km/km² exceeding the standard of 0.6 km/km² (Fiera, 2014) which gives an overview of the number of existing road infrastructure in the area.

2.2.2 Data Overview

The input data used in the present study were the following:

- 1) **Wet Areas Mapping (WAM).** A 1-meter hydrologically corrected raster dataset from a LiDAR-based point cloud data was used in the present study. WAM was developed by the Alberta Agriculture and Forestry, University of New Brunswick, and the Forest Watershed Research Centre (White et al., 2012). For this research, the dataset was provided by the Government of Alberta through the Alberta Environment and Parks – Informatics Branch under the DMR# 1704M08 (GOA, 2018).
- 2) **WAM derived Stream Features.** The dataset was provided by the Government of Alberta, Environment and Parks – Informatics Branch, through the Alberta Environment and Parks

– Informatics Branch under the DMR# 1704M08 (GOA, 2018). The dataset contained stream features derived from a 1-meter WAM in a shapefile format -.shp- (Esri, 2018).

3) **Road Network.** The road lines dataset was obtained from the Government of Alberta, Alberta Environment and Parks in a shapefile format -.shp- (Esri, 2018). The dataset contained a spatial representation of cutlines, truck trails, graveled road (one and two lanes), and unimproved roads in the Province of Alberta (GOA, 2018). It should be noted that due to the purpose of this study, paved or improved roads were not included

All the input dataset was managed and processed employing ArcGIS platform (Esri, 2018), stored in a Universal Transverse Mercator’s projection (UTM) Zone 12, North American Datum (NAD) 1983 datum.

2.2.3 Modeling Framework

Sediment Production Overview

Sediment production from upslope sediment sources has been widely studied from a geomorphic and gravitational perspective. Miller and Burnett (2007) reported that topographic irregularities across landscapes can greatly influence upslope sediment production. In a study carried out in the Oregon Coast Range, Miller and Burnett (2007) estimated the sediment production from landslide runout through the following expression:

$$P = P_0 \times W_T \times a_p \quad (Eq. 1)$$

Where:

P, Sediment Production

P₀, Landslide density

W_T, Topographic weighting term

a_p, Area of a single pixel

Another approach to assess upslope sediment production is that suggested by Borselli et al. (2008). The model incorporates the contributing area and slope as key variables as well as a weighting factor based on the crop/vegetation management C-factor. The C-factor is the same

as that used in Wischmeier and Smith (1978) and Renard et al. (1991), which represents the effects of plants, soil cover, and disturbance activities on soil erosion in agricultural areas.

$$D_{up} = \bar{W} \times \bar{S} \times \sqrt{A} \quad (Eq. 2)$$

Where:

D_{up} , Upslope component for sediment production

\bar{W} , Average weighting factor of the upslope contributing area (dimensionless)

\bar{S} , Average slope gradient of the upslope contributing area (m/m)

A , Upslope contributing area (m²)

Forest roads surfaces have high erodibility potential and sediment production can vary by large orders of magnitude (Thompson et al., 2008). Anderson and Anderson (1987) highlighted that the sediment production potential, for example, at stream crossings can be influenced by slope gradient, slope length, disturbed area, and vegetation cover. Similarly, Benda et al. (2016) in a study carried out in the Simonette Watershed in Alberta, noted that road-surface area, slope, surfacing material, traffic, and rainfall intensity can greatly influence road sediment production. By considering the physical components of road drainages, Benda et al. (2016) presented the following equation to estimate sediment production from road surfaces:

$$P_{SED} = A \times S_R^n \times y(t, l) \quad (Eq. 3)$$

Where:

P_{SED} , Total sediment flux calculated as the integral of sediment production over time.

A , Road-segment surface area contributing sediment to a drain.

S_R^n , Average slope of the road segment, the exponent n refers to an empirical constant, and

$y(t, l)$, Sediment yield based on time and rainfall intensity.

Sediment Production Modeling Procedure

To predict the sediment production from the road surface, I investigated the road drainage attributes as well as the role each one plays in the production dynamics (Figure 2-1). Similarly, I explored the structure of various models related to sediment production (Table 2-1) including

the models proposed by Miller and Burnett (2007), Borselli et al. (2008), Cavalli et al. (2013), and Benda et al. (2016).

Therefore, for any road segment as depicted in Figure 2-4, the production potential was calculated for each DEM cell of 1-meter resolution. It was assumed that each 1 m² of the road has the potential to produce sediment. From the total sediment produced from points P1 and P2 and headed to point Px, part of the sediment could be either delivered along the ditches, on the roadsides, taken off the road or else arrive at the Px point without any interference. The road drainage structure characteristics are very important; for example, the existence of a steep road gradient and a high contributing area might generate high sediment volumes. As shown in Figure 2-4, the slope of the road which goes from less steep as in P1-Px to steeper as in P2-Px may influence the sediment flow direction towards the sink in Px. Similarly, in terms of contribution area, the width and length of the road surface can highly affect the amount of sediment generated at P1 and P2 and their potential contribution to the outlet Px, as long as the path is not affected by impediments. If there is a lack of impedance across the road surface and steep road gradient, as is the case in the upper parts of the Star, Livingstone, Upper Oldman, and Trout sub-basins, sediment particles have the potential to reach the nearby stream from any point on the road surface.

In this context, I used the following formulation to calculate the road sediment production based on the DEM data as the only input source.

$$P_r = R_r \times SL_r \times A_r \quad (\text{Eq. 4})$$

Where:

P_r , Road sediment production potential computed based on the following aspects.

R_r , Road surface roughness weighting factor considered as an impedance factor including topographic changes across the road network such as concavity and convexity, structural failures such as holes due to water in the underlying soil structure and traffic passing over the affected area, and the presence of deep gullies on the surface.

SL_r , Slope of the road and the flow length in a steepness surface where each DEM cell belongs only to the road surface.

A_r , Road contributing area. The road flow accumulation represents the drainage area, indicating where the sediment comes from and where it gets accumulated. At a starting point, several cells send the sediment they have previously received from neighboring cells to others defined by DEM derived flow direction.

With this in view, the sediment production prediction from the DEM involved the following steps:

Slope of the road

I proceeded to calculate the slope of the road based on the following considerations: the slope α was not considered in the calculation because α corresponds to the "vertical gradient" of the landscape, which is based on the vertical distance as a function of the difference between the maximum and minimum elevation of the entire area (Figure 2-2B). Rather, the slope of the road θ refers to the "horizontal gradient", where the horizontal distance intersects the vertical distance mentioned above (Figure 2-2A). Therefore, I calculated the horizontal gradient in terms of the difference between the maximum and minimum elevations of the road line.

Based on the above considerations, I used the following procedure to calculate the slope of the road in ArcGIS version 10.6.1 (Esri, 2018):

- From the road coverage (Esri shapefile format .shp), I converted the road lines to points using the Generate Points Along Lines tool in ArcGIS (Esri, 2018). For truck trails and cutlines, the spacing distance between points was set up to 4 and 2 meters, respectively.
- From the DEM, I extracted and allocated the elevation values to the corresponding points previously generated. However, in order to make these values represent the elevation with respect to the road surface as a baseline, I calculated the difference between the maximum and minimum elevations of the points adjacent to the points of interest.

- Subsequently, the slope of the road becomes the result of the calculation between the points spacing distance (established in the previous step) and the corresponding elevation.
- With the purpose of facilitating the data processing and management, slope points were buffered and converted to raster. For the buffer, I have used the Alberta recreation corridor and trails classification manual (GOA, 2009). Generally, truck trails have approximately an average width of 5 m and cutlines around 3 m. Therefore, buffers were applied at an average of 4 m. The raster conversion (slope raster) maintained the same DEM spatial resolution of 1 meter.
- Furthermore, in order to avoid Null generation cells in future geoprocessing steps, I applied a threshold of 0.001 to the slope cells containing zero values.

Flow length

Procedure included:

- The road coverage (shapefile format .shp), I converted the lines to polygons using the same buffer size previously applied to the slope points (4 m); in this way, same 4 m was considered for the road width.
- Utilizing this polygon layer as a mask, the road network raster was extracted from the original DEM to further calculate the flow direction for each road DEM cell.
- Moreover, the D-infinite algorithm was applied as a flow method for flow direction computation. I used the D-infinity flow direction method because it identifies the most likely direction that flow would take from among the multiple direction possibilities under slope influence (Tarboton, 1997). Thus, the flow direction raster was the main input to calculate the flow length downstream.

Contributing Area

Procedure included:

- Flow accumulation is a raster of accumulated flow (Figure 2-3) which was calculated for the road segments based on the previous flow direction raster. I used the D-infinity flow direction method (Tarboton, 1997) to calculate the flow accumulation; therefore, each

accumulated cell flows into each downslope cell according to its direction downslope (Esri, 2018). This way, high flow accumulation values can be linked to high sediment accumulation areas on the road surface, which allows identification of concave areas, stream crossings, and culverts along the road network.

Sediment Plume Length Overview

Scoured material delivery from unpaved roads to streams can be considered the main off-site effect in forested lands (Alder et al., 2015). Generally, the sediment is deposited along watercourses and waterbodies altering the functioning of the hydrologic system, including changes in the morphology, with increasing turbidity and a reduction in spawning areas (Alder et al., 2015).

A number of models have been performed to evaluate sediment transportation capacity (Table 2-2). La Marche and Lettenmaier (2001) in a study carried out in the Deschutes River in Washington State, have noted that road-stream sediment transfer capacity can be influenced primarily by hillslope topographic characteristics and the distance to the channels. The downslope component equation D_{dn} developed initially by Borselli et al. (2008) has also considered that sediment delivery is governed by downslope characteristics such as distance to streams and slope. Besides, Cavalli et al. (2013) suggested that surface roughness conditions the flow path for sediment movement downslope.

$$D_{dn} = \sum_i \frac{d_i}{W_i \times S_i} \quad (Eq. 5)$$

Where:

D_{dn} , Downslope delivery component

W_i , Average weighting factor,

S_i , Average slope gradient (m/m),

d_i , Flow length along the i^{th} cell according to the steepest downslope direction (m).

Sediment Plume Length Modeling Procedure

I investigated the hillslope characteristics to estimate the sediment plume length based on the DEM metrics and the equations suggested by Borselli et al. (2008) and Cavalli et al. (2013). Similarly, I evaluated the topographic roughness for downslope conditions based on the topographic roughness method suggested by Trevisani et al. (2016).

From the potential sediment production sites P1 and P2 as seen in Figure 2-5, the sediment particles “X” contact either a stream crossing or a culvert Px. Otherwise “X” moves off the road surface downwards becoming a sediment plume headed to the targets (streams). Sediment plume traveling distance downhills can be controlled by the presence of cooperating factors such as the hillslope gradient and erosion features. The steepest surfaces are more vulnerable to erosion and erosion features can facilitate the particle movement creating channels. On the other hand, impediment factors such as vegetation and topographic roughness create a barrier which can reduce sediment transportation. In general, it is believed that the sediment plume traveling process is mainly controlled by surface irregularities. Therefore, the sediment delivery process varies from the sediment being deposited along the traveling path or directly in the channel. Within this framework, the sediment plume length and delivery potential are examined in terms of topographic roughness as the main factor conditioning sediment movement downhills.

Therefore, within the previous framework, I used the following equation to estimate the sediment plume traveling distance downslope:

$$D_p = C_{sr} \times D_r \quad (Eq. 6)$$

Where:

D_p , Sediment plume traveling potential downhills

C_{sr} , Least-cost corridor path based on slope and roughness

D_r , Distance ratio to the nearest stream

With this in view, the sediment plume length prediction from DEM involved the following steps:

- I computed the flow direction for the whole sub-watershed by using the DEM as input data. Because overland flow may take various directions downhills, I also applied the D-

infinite flow direction method to determine the direction of the sediment plume downhill (Tarboton, 1997).

- Then, I computed the flow length (FL_w) based on the previous flow direction and the stream lines as input data. This way, the FL_w describes the flow traveling distance from any initiation point within the watershed to the streams.
- Using the sediment production and the streams data, I calculated the nearest distance (ND_r) from the road to the stream. This ND_r describes the sediment plume traveling distance from any initiation point on the road surface to the nearest stream. But, the ND_r does not take into account the irregularities of the surface, it is rather based on the Euclidean distance.
- From operating the ND_r and FL_w , I determined the distance ratio (D_r).
- The slope α (Figure 2-2B) was calculated considering this time the vertical vector, and in percentage.
- From the DEM, I calculated the slope of the watershed which is (α) in Figure 2-2B, the "vertical gradient" of the landscape. The slope was set up in percentage.
- By using the slope, I estimated the least-cost distance for the road sediment cells to the streams (S_{cd}).
- By using the roughness data (R_{ri} as noted in lines later), I estimated the least-cost distance for the road sediment cell to the streams (R_{cd}).
- With S_{cd} and R_{cd} , I assessed the least-cost corridor path from road source to streams (C_{sr}).

Topographic Roughness Overview

There can be a variety of factors reducing or increasing the sediment motion downhill. Among them can be cited the presence of barriers, sinks, or dense vegetation cover. Therefore, non-connection can occur due to infiltration and depositional processes along the sediment plume pathway (Bracken and Croke, 2007; Baartman et al., 2013).

Based on *Eq. 6*, Cavalli et al. (2013) point out that a topographic roughness-based weighting factor works better when topography appears to be the leading factor for sediment production and transportation in very steep landscapes rather than the C-factor from RUSLE. In fact, the

weighting factor can define the level of importance of the factors that have the most influenceable position on upslope production.

Cavalli et al. (2013), states that the topographic Roughness Index (RI) corresponds to the standard deviation of the residual topography which is calculated by subtracting an averaged DEM from the original DEM (Grohmann et al., 2011) and applying a 5×5 cell moving-window.

$$RI = \sqrt{\frac{\sum_{i=1}^{25} (X_i - X_m)^2}{25}} \quad (Eq. 7)$$

Where:

RI , Roughness index

25, Number of the processing cells within the 5×5 cells moving window,

X_i , Value of one specific cell of the residual topography within the moving window,

X_m , Mean of the 25 cells values.

Due to the possibility of generating high distortion values of roughness in steep areas and very small roughness variations in flat areas. In order to avoid that spatial roughness variability, Trevisani and Cavalli (2016) suggest normalizing the natural logarithm of the roughness index to calculate the roughness-based weighting factor. This roughness index normalization is an alternative to that indicated by Cavalli et al. (2013) where the roughness index is divided between the maximum roughness values to obtain a roughness-based weighting factor.

$$W = 1 - \frac{\ln(R) - \ln(R_{min})}{\ln(R_{max}) - \ln(R_{min})} \quad (Eq. 8)$$

Where:

W, Roughness-based weighting factor

R_{max} is the maximum and **R_{min}** is the minimum value of roughness in the area of interest.

However, by using a high-resolution DEM data, the intention is to maximize the extraction of useful fine-scale morphological information as stated by Trevisani and Cavalli (2016). Besides, it is important to note that in terms of sediment transportation, the topographic irregularities or

the anisotropy in surface morphology (Trevisani and Cavalli, 2016) can constrain sediment plume flow where roughness has low values and can increase the sediment plume movement otherwise.

Consequently, for highly-irregular landscape surfaces, the topographic roughness combined with a surface gravity-driven flow direction happens to be meaningful in terms of modeling sediment connectivity and strengthening the capability to analyze landscape features (Trevisani and Rocca, 2015; Trevisani and Cavalli, 2016)

Topographic Roughness Modeling Procedure

I evaluated both upslope and downslope components under the influence of impediment factors. The impediment factor uses the median of absolute directional differences (MAD) algorithm to estimate the topographic flow-directional roughness values (Cavalli et al., 2013; Trevisani and Rocca, 2015; Trevisani and Cavalli, 2016) This method, developed originally by Trevisani and Rocca (2015) for alpine environments where mostly geomorphic processes such as landslides occur and later improved by Trevisani and Cavalli (2016), measures the roughness index considering the potential direction taken by the sediment plume downhill under the influence of gravity. For its computation, MAD flow-directional roughness requires the residual DEM data which as stated by Grohmann et al. (2011), Cavalli et al. (2013), Trevisani and Rocca (2015), and Trevisani and Cavalli (2016) can be estimated by extracting all topographic differences from the original DEM (Eq. 10).

- *Calculate an averaged DEM.* Because landscapes contain vast morphological variation, a multi-pass mean roving window is applied to the original DEM. In addition, as the degree of smoothing controls the total signal exposed by the residual DEM, it appears to be a key factor on the analysis of fine-scale morphology; therefore, using a low degree of smoothing can be ideal (Trevisani and Rocca, 2015).
- *Subtract the averaged DEM from the original DEM.*

$$R_t = DEM_0 - DEM_{mean} \quad (Eq. 9)$$

Where:

R_t , Residual topography

DEM_0 , Original DEM

DEM_{mean} , Smoothed DEM using an X cell by cell moving window.

With this in view, the topographic roughness calculation from DEM involved the following steps:

I calculated the weighting factor for upslope and downslope components by applying the MAD flow-directional roughness (Trevisani and Rocca, 2015; Trevisani and Cavalli, 2016). The MAD flow-directional roughness bases its calculation on the residual topography as the main input. Therefore, its computation involved the following procedure:

- First, I obtained an averaged DEM from the DEM by applying a moving window of 3 by 3. The averaged DEM can let to distinguish the landscape morphology variation.
- I subtracted the averaged DEM from the original pit-filled DEM as in Eq. 9. The next step was to obtain the residual topography raster.
- As in Trevisani and Rocca (2015) and Trevisani and Cavalli (2016), the residual topography serves to estimate the MAD roughness flow-directional. Using the MAD tool in Trevisani and Rocca (2015), it was selected the output raster which characterizes the surface as anisotropy in surface morphology where low values indicate heterogeneous surface and high values homogeneity. The resulting roughness values were applied to the upslope and downslope components.

Sediment Connectivity Overview

Generally, connectivity refers to the degree of linkage between two points. Sediment transportation capacity plays an important role in connectivity (Hooke, 2003; Borselli et al., 2008; Bracken et al., 2015) with the sediment plume traveling a distance from its initiation point and its arrival to the destination point would define how well these two points are connected across the landscape.

Connectivity to streams can happen in different ways and be controlled by surface roughness (Croke et al., 2005; Croke and Hairsine, 2006; Borselli et al., 2008). For example, road sediment can reach the stream by (1) direct linkage to a stream channel, (2) indirect linkage on hillslope area due to gully occurrence, and (3) diffuse linkage because of infiltration, fences, vegetation making the pathway dispersed. The presence of incisive gullies on hillslope can turn a sediment plume into a continuous and (i) direct discharge to the stream or they can lead to (ii) a disperse flow path. Figure 2-1, adapted from Wemple et al. (1996), illustrates the road drainage structure and sediment delivery dynamics.

The Index of Connectivity IC (Borselli et al., 2008; Cavalli et al., 2013) has been widely applied to different studies (Borselli et al., 2008 ; Cavalli et al., 2013; Gay et al., 2016; Rainato et al., 2017; Cantreul et al., 2017; López-Vicente and Álvarez, 2018; Grauso et al., 2018; Crema and Cavalli, 2018).

The IC addresses sediment connectivity in terms of the potential that each downslope DEM cell has to receive sediments from other upslope cells, is controlled by surface characteristics, slope, and type of land use within a watershed.

$$IC = \log_{10} \left(\frac{D_{up}}{D_{dn}} \right) \quad (Eq. 10)$$

Where:

D_{up} and D_{dn} are the upslope and downslope components of connectivity.

Sediment Connectivity Modeling Procedure

The sediment connectivity calculation from DEM involved the usage of the following equation:

$$SC = \frac{P_r}{D_p} \quad (Eq. 11)$$

Where

SC , Sediment connectivity from the road to streams

P_r , Road sediment production (upslope)

D_p , Sediment plume traveling distance potential downhill (downslope)

2.1.1 Field Survey Location Selection

Field studies can play an important role in supporting modeling performances (Al-Chokhachy et al., 2016). Therefore, sediment connectivity modeling approaches integrating a field component help prove whether the DEM-based connectivity represents the reality (Borselli et al., 2008). To make the modeling approach consistent, the field-based connectivity can be characterized in the same manner as DEM-based connectivity. In this regard, adapted from the Protocol for Evaluating the Potential Impact of Forestry and Range Use on Water Quality in British Columbia, CA, designed by Carson et al. (2009), the field connectivity assessment involves the following aspects:

- **Contributing area.** It involves the identification of the road component from which its area is calculated based on its width and length (Carson et al., 2009):

$$A_o = L \times W \quad (Eq. 12)$$

Where:

A_o , Area of the identified element (m²)

L , Length of the identified element (m)

W , Width of the identified element (m)

The sediment contributing area can be estimated by weighting the total area of the identified component by its portion of the area under potential erosion.

$$A = A_o \times E \quad (Eq. 13)$$

Where:

A , Sediment contributing area (m²)

E , Portion of the rea under erosion (%)

- **Sediment plume Length.** Based on the direct measurement of the plume traveling distance (m) on the direction of the flow.

- ***Impediment factors.*** Data describing natural (slope, vegetation, erosion features) and human-made barriers such as water bars, stone and sand fences, culverts as part of the soil and water management activities.
- ***Field connectivity estimation.*** Visual observation can be carried out for connectivity assessment in the field to establish the level of connectivity as per indicated by Carson et al. (2009) in Table 2-10.

Field Component Design

The field component for connectivity estimation was intended to better understand the performance of the DEM-based sediment connectivity prediction. Therefore, a field study was carried out in a selected sampling area located within the Oldman River watershed during the summer of 2018 (Figure 2-8). Only were road surface and ditches considered as sources of sediment production, cutslope and hillslopes were excluded.

Field experiment objective

The purpose of this fieldwork was to collect data regarding erosion and sediment plume characteristics at the sampling sites to evaluate the following considerations:

- Whether the high erosion potential roads from the DEM were related to high erodible areas in the field
- Whether the connectivity from the DEM was correlated with field data
- Whether the plume length (traveling distance) measured in the field could serve to improve connectivity index predicted from DEM.

Sampling Area Characteristics

Sampling Area

From the eight sub-watersheds conforming the total study area in the Oldman River Watershed (Table 2-5 and Figure 2-8), the sampling area spans approximately 601.4 km² and includes approximately 1459.8 km of cutlines and 498.0 km of truck trails. This sampling area was selected considering the watersheds' remarkable variability in topography across the Canadian

Rocky Mountains and Foothills valleys; thus, the sampling area is believed to be the most representative portion of the total study area (Figure 2-8).

Sampling Sites

Focusing on the sediment connectivity, sediment production, and plume length high values (spots), it was performed a validation of the predicted values with field data. A number of 135 sites with high values and distributed across the road network within the sampling area were selected for this study (Table 2-5). Even though their random selection, the sites were believed to represent the road connectivity situation in each sampled watershed as per the predicted results from the DEM. Therefore, by using the field form (Appendix B), road drainage characteristic, sediment plume length, and connectivity were planned to collect at each site (Tables 2-6, 2-7, and 2-8).

2.1.2 Field Connectivity Estimation

Once in the field, due to the accessibility conditions, from the 135 sites expected to be studied, only were a total of 103 sites characterized as per the field form. For each of them, locations (X, Y coordinates in meters) were recorded using Etrex Garmin GPS (~ above meter accuracy). Additionally, from previous fieldwork carried out by the Government of Alberta (GOA) with the purpose of assessing connectivity in Race Horse, Livingstone, and Dutch creeks, a dataset containing several sites and located within the sampling area were used to reinforce the previous field dataset. However, from the GOA dataset, there were extracted the variables of interest matching the field form. Therefore, the final number of sites considered in this study reached 196.

Field Sediment Production

Sediment production was assessed for each sampling site based on the attributes indicated in Table 2-8. The procedure was as follows:

- First, the length (m) and width (m) of the road and ditch were measured at the site, and then, calculated the road surface and ditch area (m²).
- At each site, from visual observation, it was estimated the percentage of the erodible area from the total are estimated from the road surface and ditch. This portion of the erodible

area refers to the percentage of the eroded area or susceptible to erosion at the time the field observation was carried out. Moreover, the erodible area can be used to determine the area that potentially generates sediment.

- Therefore, the road surface and ditch contributing areas were calculated by multiplying their original areas (m^2) by their portion of erodible areas.
- Using the equation formulated by (Marchi and Dalla Fontana, 2005) (Table 2-2), the sediment production (upslope) from the road surface and from the ditch were calculated based on their contributing areas (m^2) and their slopes (m/m). The slope of the road surface and ditch were measured in percentage at the site. Furthermore, since the roughness factor was used for the DEM sediment production prediction, similarly, a field roughness was also considered for field production. Then, from Table 2-6, the closest components fitting such surface characteristic at the site were the “Soil & Water Management” and the “Erosion Features”. Therefore, both components were taken into account as weighting factors to estimate the final sediment production from the road surface and ditch.
- Finally, both final production values (road surface and ditch) were added representing the total sediment produced at the site.

Field Sediment Plume Length

Plume length was measured following the path and the direction of flow from the road to downhill (m). For small sediment plumes, the length was measured until its maximum arrival off the road surface. For long sediment plumes, the length was split into small sections in order to facilitate the measurement. And, for distant sediment plumes or non-accessible ones, the length was measured until certain distance and the rest was estimated. In addition, slope (m/m) was measured for each sediment plume and represented in percentage. Likewise, barriers (vegetation, fences, and other structures) reducing sediment plume movement were found at the sites. In this context, from Table 2-7, the slope and the components of the barrier were utilized as weighting factors.

Field Connectivity

The connectivity from the field was based on whether the road, the ditch, and the sediment plume had some degree of connection to the nearest stream either by means of culverts (engineered drainage), ford/stream crossings (natural drainage), or gullies. Consequently, as indicated in Table 2-8, the observed connectivity assigned to the site ranged from 0 to 1, non-connected to fully connected, respectively.

2.3 *Statistical Analysis*

The final dataset consists of data, sediment production, sediment plume length, connectivity, and delivery. In turn, each of them has estimates from the field, from DEM (no roughness), and from DEM (with roughness).

Initially a total of 248 sites were sampled in the field; however, only 196 sites had road surface and ditches information. Therefore, sediment production was evaluated for N=196 from the field and their corresponding in the DEM. Because there were few sites with sediment plume information and the desire to avoid loss of information, from the 258 sites, 51 sites referred to sediment plume length. There were no restrictions for their selection; however, most of them corresponded to road surfaces and a minority to cutslopes and hillslopes. Finally, for connectivity and delivery, the number of samples was 44. In this case, the selection was limited to only road surfaces and ditches. In order to effectuate the analysis Field-DEM, the same number of sites were selected from the DEM.

Connectivity was the main dependent variable (dimensionless). It was assumed that there is approximately a linear relationship between DEM predicted values and the Field estimates (Sediment production m^3 , Sediment plume Length m , and Sediment Delivery m^3). Thus, regression lines were performed in order to confirm whether the DEM values fit the Field estimates. The analysis was conducted in R (RStudio, 2018) where the relationship consisted of relating $Y \sim X$.

Furthermore, to evaluate the extent up to which the DEM values fit the Field residuals were calculated by operating *Field estimates – DEM Predicted values*, and fitting accuracy was tested by utilizing the coefficient of determination r^2 at a selection criterion of $\alpha=0.05$.

All data analyses were computed using R statistical software RStudio, Version 1.1.423 (RStudio, 2018).

2.4 Results

2.4.1 DEM vs Field Sediment Production

The data analysis was conducted based on DEM-based and Field-based sediment production estimates. The maximum and minimum sediment estimated from the field were respectively 196.86 and 1.80 m³, with an average of 43.76 m³ and standard deviation (SD) of 38.85 m³ (Table 2-10). For DEM sediment production (*No roughness*), the maximum and minimum production predicted were respectively 292.39 and 3.01 m³, with an average of 68.29 m³ and SD of 57.88 m³. Whereas for DEM sediment production (*MAD roughness*), the maximum and minimum production predicted were 202.31 m³ and 2.95 m³ with 56.97 m³ on average and 44.04 m³ variance from the average (Table 2-10).

An analysis of residual has been also carried out to diagnose the fitting. From DEM sediment production (*No roughness*) ~ Field sediment production relationship (DFsp) the residuals showed a minimum of -45.80 m³ and a maximum of 235.91 m³ while the DEM sediment production (*MAD roughness*) ~ Field sediment production relationship (DFsp-r) residuals presented a minimum of -42.985 m³ and a maximum of 81.519 m³ (Table 2-11). From this performance, it can be noted that the distribution of the DFsp residuals appeared to be a bit more symmetrical across the mean value zero (0) compared to the DFsp-r residuals (Table 2-11). As in Figure 2-18A and 18B, it can be seen that a good number of points fall near the mean zero between -50 and +50 reflecting that the fitting guess was acceptable. Likewise, some residuals with high positive values (on the y-axis) showed that the fitting was too low whereas negative residuals reflected that the fitting was high making them non-acceptable. To confirm this situation, the standard error SE (noted as *std.error*) showing the points around the DFsp linear function presented a SE equal to 3.71 while for the DFsp-r its SE was 2.24 (Table 2-11).

As the DFsp intercept equals to 15.86, it seems to reflect that when the Field sediment production is zero m³, it can be expected the DEM production be 15.86 m³ (Table 2-11). However, if considering a scenario with a baseline of 10 units of magnitude, for every 10 m³ increase in the Field sediment production, the average increase in DEM production would be of

12 m³. Similarly, for the DFsp-r intercept, the results show that when Field sediment production equals to zero m³, the sediment production from DEM can reach 13.20 m³. And, for every 10 m³ increase in Field production, the DEM average sediment production can be approximately 10 m³ (Table 2-11).

To verify whether the previous results were statistically significant based on the SE, the DFsp resulted in 1.07 and 1.32 at a 95% confidence interval (Table 2-11). These values assumed that in the case of Field sediment production increases by 10, the DEM production increases by 10.7 – 13.2 m³. Correspondingly, for DFsp-r results indicated that when Field sediment production increases by 10, the DEM production ranges between 9.2 – 10.8 m³.

Additionally, to assess the accuracy of the Field-Dem goodness-of-fit, the DFsp residual standard error (RSE) equaled to 34.48 indicating that it is more likely that the sediment production at all sampling sites (N=196) deviates from the true regression line by approximately 34.48 m³, on average (Table 2-11). Whereas, for DFsp-r, the RSE indicates that the deviation from the true regression line occurs by an average of 20.77 m³. However, in order to know whether these RSE values were significant, the coefficient of correlation (r²) was employed as it lets to assess the portion of the fitting variance ranging between 0 and 1 (Table 2-11).

For the DFsp, the r² showed that 64 % of the DEM predicted results fit the Field sediment estimates. Similarly, for DFsp-r, the r² showed that 77 % of DEM production sediment variances fit the Field production estimations (Table 2-11).

From a visual analysis in Figure 2-14, sediment production from the DEM tends to approximate the field sediment production values when roughness was applied. This assumption was supported by the statistical results given above when DFsp-r presented a strong r² of 0.78. Consequently, the predicted DEM sediment production ranged between 20 and 80 m³ with a maximum of 220 m³, while the sediment production from the field ranged between 20 and 60 m³ with a maximum of 200 m³. On the other hand, when no weighting factor was applied, the DEM sediment production ranged between 30 and 90 m³, with the highest value around 300 m³. From this, in general, the road sediment production ranges estimated from the DEM and the field tended to oscillate between 0 and 100 m³.

2.4.2 DEM vs Field Sediment Plume Length

The maximum sediment plume length measured in the Field was 37.4 m, while the minimum was 0.3 m with 8.42 m on average and 8.75 m of variation (Table 2-10). The predicted lengths varied greatly between length measured in the Field and the length predicted from the DEM (*No roughness*), the maximum and minimum were respectively 10.37 and 0.16 m, with an average of 2.45 and a variation of 2.4 m. Likewise, the values of length from DEM (*MAD roughness*) were highly variable compared to the length from Field but closer to length from DEM (*No roughness*). The maximum and minimum DEM (*MAD roughness*) predicted length were respectively 11.13 and 0.05 m, with an average of 2.22 m and standard deviation (SD) of 2.82 m (Table 2-10). This situation can be explained by the extreme length outlier predictions (Table 2-10).

In this context, to verify this condition, the DEM sediment plume length (*No roughness*) ~ Field sediment plume length relationship (DFpl) showed that the maximum and minimum residuals were between 5.84 and -4.59 m, while the DEM sediment plume length (*MAD roughness*) ~ Field sediment plume length relationship (DFpl-r) ranged from 5.39 and -4.28 m (Table 2-12). As in Figure 2-19A and 19B, a good number of sediment plumes present length values falling between -2 and +2 which can imply their prospective fitting. Additionally, the DFpl and DFpl-r sediment plume length deviations occur both at 2.9% from their corresponding average lengths (Table 2-12). It can be also noted that when the Field sediment plume length is zero m, the DEM plume increases by 0.88 m (Table 2-12). For example, if considering a baseline of 10, for each 10 m length measured in the Field, the DEM sediment plume length predictions increase by approximately 1.9 m on average. Similarly, it is more likely that the DEM sediment plume length equals to 0.1 m when Field sediment plume length is zero m, which means that for every 10 m in the Field sediment plume length increase, DEM sediment plume length averages 2.5 m (Table 2-12).

To verify the significance of the previous results utilizing the SE and at 95% confidence interval, the DFpl values resulted in 0.13 and 0.24, which means that in case of Field sediment plume length increases by 10 m as said it before, the DEM sediment plume length could do it by 1.3 and 2.4 m (Table 2-12). Likewise, the results in lengths based on SE and 95% confidence level,

the DFpl-r indicated that if Field sediment plume length rises by 10 m, the DEM sediment plume length does it by 1.9 and 3.1 m (Table 2-12).

Additionally, to confirm the sediment plume length fitting accuracy, the DFpl and DFpl-r RSE values were 1.78 for both (Table 2-12). The RSE shows the possibility for DFpl and DFpl-r sediment plume length values at all sampling sites (N = 51) get deviated from the true regression line by an approximate average of 1.78 m (Table 2-12). To confirm whether these RSE values were significant, the r-squared (r^2) explained 46.1 % of DFpl sediment plume length data were close to the fitted regression. Similarly, for the DFpl-r, the sediment plume length data was more strongly correlated when normalized by roughness ($r^2=0.61$) (Table 2-12).

2.4.3 DEM vs Field Sediment Connectivity

Considering the connectivity as a function of upslope and downslope interaction, the summary suggests that DEM vs. Field connectivity normalized by roughness (DFc-r) does a better job explaining the variance in connectivity ($r^2=0.52$) (Table 2-13). On the other hand, RSE DFc-r's (Sigma) was lower than the DEM vs Field (DFc) when no weighting factor was applied (Table 2-13). The concern with normality was supported when compared to the Q-Q plots (Figure 2-20A and 20B). Although the far left and right side of the DFc-r has signs of non-normality, most of the connectivity values tried to be near the fitted line.

Values of connectivity when the weighted factor was applied ranged from approximately a little (0.45) to a lot (0.85) whereas the non-weighted connectivity ranged from a half (0.5) to a lot (0.85) for the 44 sites in total. Values of 1 and 0 connectivity were also present in a reduced number of sites (Figure 2-13).

2.4.4 DEM vs Field Sediment Delivery

From the DEM vs. Field delivery relationship (Figure 2-12), it suggests that delivery improves from $r^2= 0.48$ to 0.55 when normalized by roughness (DFd-r), with $p<0.05$ and RSE decreasing from 25.5 to 18 (Table 2-13).

However, when comparing visually the DFd-r with the non-roughness delivery (DFd) (Figure 2-21A and 21B), the normal Q-Q plots showed that the DFd residuals were closer to the fitted line while the DFd-r presented some residuals far from the normal line. Likewise, it can be

noted that the DFd and DFd-r linear assumptions did not support for delivery data less than <60 units. If low residuals were not considered, the prediction would be better represented when over 60 units (Figure 2-12).

2.5 Discussion

2.5.1 Sediment production

Predictions of sediment production from road surface come from a model structured utilizing only DEM metrics. In this study, from a number of models developed by researchers to estimate sediment production (Burnett and Miller, 2007; Borselli et al., 2008; Cavalli et al., 2013; TerrainWorks and fRI, 2018), I executed analysis of the variables that these models use. Therefore, I adapted the models to a model that can fit the conditions of the study area and be able to predict road surface sediment production using only a DEM as input data.

In this study, I considered the slope as one of the key factors for sediment generation. In some circumstance, the slope of the road may be considered non-significant as it might decrease when the road-segment length increases (Reid and Dunne, 1984). Generally, for traffic and safety, the road slope tends to be approximately 10 - 12% (MacDonald and Coe, 2008). However, considering the topography conditions of the Oldman watershed mountainous region, the road surface slope can be higher than the standard, Thus, in the present study, the slope has been computed taking into account the road surface as the horizontal baseline and its differences in elevation.

Another important aspect in the adaptation of the model is the roughness, which has been emphasized by many researchers as a factor that also influences sediment production (Grohmann et al., 2011; Benda et al., 2016; Trevisani and Cavalli, 2016). However, as road surfaces are mainly well compacted, studies rarely mention roughness application for road surface erosion. In this study, I adapted the notions given by Borselli et al. (2008), Cavalli et al. (2013), and Trevisani and Cavalli (2016) about the application of roughness for areas governed by geomorphic processes to areas affected by surface erosion. Additionally, even though the roads are treated as planar surfaces, the study area is characterized by steep gradients making the accessibility difficult even through OHV trails (e.g. Star, Girardi, and Allison creeks). Therefore, in this study, I treated concave, convex, and erosion features on the road as part of

the irregularities on the surface. Researchers have also agreed that roughness has much to do with the rates in sediment production and has been used as a weighting factor (Borselli et al., 2008; Cavalli et al., 2013).

In this sense, it can be noted that without considering the roughness, the maximum sediment generation predicted by the model was 292.39 m³ while with roughness it was 202.31 m³ closely approximating to field estimates (196.86 m³). It is also good to note that when using roughness, the model had a good approximation to the field estimates when the predictions of sediment production ranged from approximately zero to 80 m³ ($r^2 = 0.77$, $a < 0.05$). However, the model overpredicted the high productions (Figure 2-9, 2-18). The possible explanations of why the model does not fit the high values can be the following:

- 1) The number of sampled sites correspond to 196. It was expected to survey more sites. However, because of the inaccessibility to the sites in the sampling area, I was not able to collect more data. Thus, the data was mainly collected from the passable OHV trails (Table 2-5).
- 2) Since roughness was used to predict the sediment production from DEM, a roughness to normalize the field sediment production was also needed. Therefore, in order to match the DEM roughness model, from the field data, I selected the soil and water management and the road erosion features data as the closest variable to represent roughness from the field. However, I believe this notion can be improved by considering other variables such as traffic or precipitation as weighting factors.
- 3) Another limitation can be related to the MAD flow-directional roughness I used as a weighting factor to predicted production from the DEM. The MAD flow-directional roughness performed well (77%) for sediment produced between approximately zero to 80 m³. It remains unclear whether another type of roughness could better predict high values above 80 m³.

2.5.2 Sediment Plume Length

The proposed model focuses on the least cost distance that the flow would have to travel to reach the channel from the road. By making an exploratory look at the data (Figure 2-11), the model predicts sediment plume average traveling distance of 2.45 m without the effects of

impediment and 2.22 m with an impediment, which compared to field sediment plume average length of 8.42 m could mean the model performance is possibly low. The possible source of error can be attributed to a number of sites with sediment plume length data. Most of the sediment plume lengths at the 51 sites were short, and there were few long plumes (37.4 m the longest) which became outliers. I was not able to collect more sediment plume data because of the inaccessibility condition in the sampling area. In addition, the main OHV trails did not have sediment plume occurrences. I think that having a good number of long lengths could have let the model verify the predicted high values more precisely. On the other hand, the model had good performance predicting sediment plume lengths (<12 m) (Figure 2-10). I believe there can be still an improvement on this prediction.

2.5.3 Connectivity

This study only establishes data correlation at the 44 sites extended across the sampling area. The model predicts sediment connectivity average of 0.61 (with roughness) compared to 0.55 from the field. When looking at the connectivity categories (Carson et al., 2009), it means model goes between “half=0.5” connected to “a lot=0.8”, and the field estimation slightly passes the “half”. Because of the absence of sediment plumes in the area and their short length, the validation of the sediment connectivity model with field data explains a variability of $r^2=0.52$ and $\alpha < 0.05$, which is significant.

2.6 Conclusions

The OHVs trails were of particular interest in this study because they are believed to impact negatively the aquatic ecosystem in the Oldman watershed headwaters. Thus, sediment connectivity was studied based on two components: sediment production from road surface (upslope component) and sediment plume traveling distance (downslope component). The model relies on two key variables slope and roughness. The upslope component comprises the slope of the road (focused on the linear horizontal features) while the downslope component applies the slope of at the level of the entire watershed (focused on the linear vertical features). The roughness method based on the mean absolute difference MAD flow-directional served as a weighting factor for both components of the connectivity prediction.

Sediment production model had acceptable performance. Although the model overpredicted high values, it can be concluded that the model performs well when values are around the average. Therefore, from the 196 sites studied in the field, 77% were correlated with the field data. The sediment plume traveling distance to streams was evaluated based on the least cost distance the slope and the roughness factors may signify for the sediment plume. From 51 sites verified, 61% have a good correlation with the field. Based on these two components, the sediment connectivity model predicts by 52% variability compared to the field data.

The topographic roughness, as well as the slope, played an important role in the sediment generation and its transfer downstream suggesting that they should not be undervalued. Additionally, in this study, I focused specifically on road surface and ditches (horizontal features); however, it is suggested that in future studies it would be ideal to include cutslope and hillslope as potential sediment suppliers to streams.

Tables and Figures

Table 2-1. Compilation of sediment production models applied to different research contexts

Author	Purpose	Model	Characteristics	Application
(Marchi and Dalla Fontana, 2005)	Evaluate the topographic control on erosion and overland flow.	$SPI = A^{0.5}S$	SPI = “index of contributing area”(m). A=contributing area (squared root), and S=local slope.	(Marchi and Dalla Fontana, 2005)
(Borselli et al., 2008)	Assess upslope production for connectivity index.	$D_{up} = \bar{W}\bar{S}\sqrt{A}$	W=average weighting factor, S=average slope gradient (m/m), A=upslope contributing area (m ²).	(Borselli et al., 2008; Marco Cavalli et al., 2013)
Anderson and Anderson (1987)	Evaluate road erosion at a stream crossing.	$EPI = A \times LS \times VM$	For Alberta conditions, Erosion Potential Index (EPI). A=panel area, VM=vegetation management, LS=length slope	Anderson & Anderson (1987)
Wischmeier and Smith (1978)	Revised Universal Soil Loss Equation (RUSLE):	$A = R \times K \times L \times S \times C \times P$	A=soil loss, R=rainfall erosivity, K=soil erodibility, LS=hill length/slope, C=vegetation cover, P=Land Use Practice.	(Hartcher and Post, 2005; Demirci and Karaburun, 2012)
(Dube' et al., 2004)	Total soil erosion from roads. Washington Road Surface Erosion Model (WARSEM)	$T_{(t/year)} = (TS + CS)A_f$ $TS = L_r \times W_r \times GE_r \times S_r \times T_f \times G_f \times P_f \times D_f$ $CS = GE_r \times CS_f \times CS_h \times L_r \times D_f$	TS=tread sediment, CS=cut-slope sediment, A _f =road age factor. Sediment Production variability: Road length (L _r) and width (W). Erosion factors: geologic erosion (GE _r), road tread surfacing (S _r), traffic (T _f), road grade (G _f), precipitation (P _f), sediment delivery (D _f), cut-slope (CS _f), cut-slope height (CS _h)	(Aruga et al., 2005; Akay et al., 2008)
(Al-Chokhachy et al., 2016)	Estimate road sediment production (Luce and Black, 1999)	$E = B \times L \times S \times V \times R$	E=Sediment produced, B=average erosion rate (kg/m elevation), L=road length (m), S=slope of the road (m/m), V=vegetation cover, and R=road surfacing factor.	(Al-Chokhachy et al., 2016)
(Luce and Black, 1999)	Road Sediment Production	$EaLS^2$	Road Sediment production proportional to L=road segment length, S ² =the square of the slope.	Various authors
Anderson and MacDonald (1998)	Sediment yield from the road surface	$E = a + b \times A \times S$	E=yearly average sediment yield, A=road contributing area, S=road slope, and a and b=empirical parameters	
(Reid and Dunne, 1984)	Determine average sediment production from road surface	$C = U \times Q \times L \times S$	C=sediment concentration, Q=discharge, L=road segment length, S=gradient, U=dummy variable (represents road type).	(Reid and Dunne, 1984)
(Cissel et al. 2012)	Road sediment production (Luce and Black 1999)	$E = \frac{aLSrv}{2}$	E= road segment erosion, a=annual base erosion rate, L=road segment length, S=slope, r=road surface (type), v=flow path vegetation (density)	(Cissel et al. 2012)

Table 2-2. Compilation of models associated with sediment plume traveling downslope.

Author	Purpose	Model	Characteristics	Application
(O'Loughlin, 1986)	Estimate the relative soil saturation.	$w = \left(\frac{Q_a}{Tbsin\theta} \right)$	W=soil wetness index, a =contributing area (m ²), b =length of the grid size (m), T=soil transmissivity (m ² /day), θ =local ground slope, Q =steady-state rainfall intensity.	Mass movement (Brazil) Cited by (Gomes et al., 2008)
(Montgomery and Dietrich, 1994)	Predict critical rainfall q_{cr} erosivity based on topographic control and landslide.	$q_{cr} = \left[\frac{Tsin\theta \left(\frac{\rho_s}{\rho_w} \right)}{\frac{a}{b}} \right] \left[1 - \frac{tan\theta}{tan\phi} \right]$	T=soil transmissivity, q =ground surface gradient, ρ_s =soil wet bulk density, ρ_w =water density, a =contributing area, b =contour length perpendicular to flow direction, ϕ =friction angle of the soil.	(Miller and Burnett, 2007)
(Miller and Burnett, 2007)	Topographic Index	$I_T = Csin\theta \left(\frac{a}{b} \right)^{-1} (1 - tan\theta)$	Based on the q_{cr} (Montgomery and Dietrich, 1994)	(Miller and Burnett, 2007)
(Marchi and Dalla Fontana, 2005)	Evaluate the topographic control on erosion and overland flow.	$SPI = A^{0.5}S$	SPI=stream power index or "index of contributing area"(m). A =contributing area, S =local slope.	(Marchi and Dalla Fontana, 2005)
(Marchi and Dalla Fontana, 2005)	Compute the index of basin ruggedness by Melton Ruggedness Number (MRN).	$MRN = \frac{(H_{max} - H_{min})}{A^{0.5}}$	H_{max} and H_{min} maximum and minimum elevation within the basin, respectively. A , drainage basin area.	(Marchi and Dalla Fontana, 2005)
(Borselli et al., 2008)	Compute of connectivity index.	$D_{up} = \bar{W}\bar{S}\sqrt{A}$ $D_{dn} = \sum_i \frac{d_i}{W_i \times S_i}$	W/W_i = average weighting factor, S/S_i = average slope gradient (m/m), A = upslope contributing area (m ²), and d_i = length of the flow path along the i th cell (m).	(Borselli et al., 2008; Marco Cavalli et al., 2013)
(Beven and Kirkby, 1979)	Compute the topographic wetness index	$TWI = \ln \left(\frac{a}{tan\beta} \right)$	a =upslope contributing area, β = local slope gradient.	(Qin et al., 2007)

Table 2-3. Sub-watersheds constituting the study area for sediment connectivity assessment

Note 1) The Oldman watershed comprises an area of approximately 23000 km² on the Canadian side. **2)** Trout Creek contains both public and private lands; the present study only takes into account Trout Creek’s public lands.

Main Watersheds	Selected Sub-watersheds	Area Km² Approx.
Willow Creek	Trout Creek	188.3
Upper Oldman River	Livingstone River	358.1
	Upper Oldman River above reservoir	274.2
	Dutch Creek	154.7
	Racehorse Creek	306.7
Crownsnest River	Allison Creek	51.4
	Girardi Creek	10.2
	Star Creek	10.4
Total		1354

Trout Creek public area considered

Selected Sub-watershed	Original Area Km² Approx.	Public Considered Km² Approx.
Trout Creek	444.906	188.3

Table 2-4. Road disturbance in the Oldman watershed

Oldman Watershed Mountain Sub-basins	% of Total Area
OHV	0.7
Roads	0.6
Pipelines	0.3
Abandoned/other linear features	0.4

Source: Fiera (2014) and AWRI (2010)

Table 2-5. Sampling areas selected in relation to the total areas of each sub-basin. The values are approximate. OHV (main trails and cutline trails) approximate length along which the sampling sites are located.

Sampling Sub-basins	Approximate sampling area coverage Km²	Length of OHVs coverage Approx. Km		Number of sampled sites
		Main trails	Cutlines trails	
Trout Creek (only public area)	188.3	24.7	-	15
Livingstone Creek	190.0	40.3	-	13
Upper Oldman River above reservoir	82.0	21.9	-	15
Dutch Creek	51.0	13.5	0.7	15
Racehorse Creek	234.0	88.9	14.7	12
Allison Creek	28.0	9.4	1.8	14
Girardi Creek	10.2	-	3.4	9
Star Creek	10.4	6.6	-	10
Total	793.9	205.3	20.6	103

Table 2-6. Road sediment production - field measurement attributes

Source of erosion	Attributes	Data Type	Process	Values	Units of Measurement
-Road surface	Soil & water management:	Continue	Field observation - assign values	Poor (0), fair (0.2), average (0.5), good (0.8), excellent (1)	Dimensionless
-Ditch	Status	Continue	Field observation - assign values	Inactive (0), temporarily or permanently deactivated (0.5), active (1)	Dimensionless
	Soil type	Discrete	Field Observation – assign type	Silt, Sand, Clay	Dimensionless
	Slope	Continue	Field Direct measurement	--	Percentage
	Quality	Discrete	Field Observation - assign type	Improved, Graveled, Native	Dimensionless
	Erosion features	Continue	Field observation - assign values	None (0) little (0.2) half (0.5) a lot (0.8) all (1)	Dimensionless
	Length	Continue	Field Direct measurement	--	Meters
	Width	Continue	Field Direct measurement	--	Meters
	Estimate portion of erodible area	Continue	Field Direct measurement	--	Percentage
	Total erodible area	Continue	Post Field Calculation	--	Square Meters

Table 2-7. Sediment plume length - field measurement attributes

Source of erosion	Attributes	Data Type	Process	Values	Units of Measurement
-Road surface	Plume presence	Discrete	Field Observation	Yes, No	Dimensionless
	Buffer, barriers	Continue	Field Observation - assign value	None (0), a little (0.2), about half (0.5), a lot (0.8), all (1)	Dimensionless
-Ditch	Plume length	Continue	Field Direct measurement	--	Meters
	Plume width	Continue	Field Direct measurement	--	Meters
	Plume slope	Continue	Field Direct measurement	--	Percentage
	Plum material	Discrete	Field Observation – assign type	Silt, Sand, Clay	Dimensionless

Table 2-8. Road-stream connectivity - field measurement attributes

Source of erosion	Attributes	Data Type	Process	Values	Units of Measurement
-Road surface	Drainage type	Discrete	Field Observation - assign values	Natural, Engineered	Meters
	Drainage Class	Discrete	Field Direct Observation	e.g. Ford, culvert, water bars	Dimensionless
-Ditch	Connectivity to drainage	Continue	Field Observation - assign values	None (0), little (0.2), half (0.5), a lot (0.8), total (1)	Dimensionless

Table 2-9. Connectivity valuation

Adapted from the Protocol for Evaluating the Potential Impact of Forestry and Range Use on Water Quality, (Carson et al. 2009)

Estimated Connectivity	Example	Range	Connectivity Value
None	Ditch-blocked interceptor culvert draining 70 m of road discharging onto long, hummocky forested slope	(<0.1)	0
A little	A 200 m ² road surface collecting storm flow and dropping it onto forest floor within 15 meters of creek	(0.1-0.3)	0.2
About half	A small area of disturbed cutbank (50 m ²) with 2 meters of forest floor separation from stream	(0.3-0.7)	0.5
A lot	Ditch-blocked interceptor culvert draining 200m of road discharging onto a steep forested slope within 4 m of stream	(0.7-0.9)	0.8
All	Ditch drainage running directly into stream or road surface drainage running off road bridge	(>0.9)	1

Table 2-10. Summary for exploratory data analysis: sediment production, sediment plume length, sediment connectivity, and delivery

	Sediment production			Plume Length			Connectivity			Delivery		
	Field Sed.Prod	DEM Sed.Prod (No roughness)	DEM Sed.Prod (MAD roughness)	Field PLength	DEM PLength (No roughness)	DEM PLength (MAD roughness)	Field Connectivity	DEM Connectivity (No roughness)	DEM Connectivity (MAD roughness)	Field Delivery	DEM Delivery (No roughness)	DEM Delivery (MAD roughness)
Stand deviation	38.85	57.88	44.04	8.75	2.40	2.82	0.30	0.30	0.31	33.73	44.67	36.65
Mean	43.76	68.29	56.97	8.42	2.45	2.22	0.50	0.61	0.61	27.85	45.03	37.74
n	196.00	196.00	196.00	51.00	51.00	51.00	44.00	44.00	44.00	44.00	44.00	44.00
Median	32.58	52.44	46.32	4.70	1.64	0.98	0.50	0.63	0.64	15.38	25.74	23.17
Coeff. of Variation	0.89	0.85	0.77	1.04	0.98	1.27	0.60	0.50	0.51	1.21	0.99	0.97
Upper Quantile.100%	196.86	292.39	202.31	37.40	10.37	11.13	1.00	1.00	1.00	124.06	163.42	149.72
LowerQuartile.0%	1.80	3.01	2.95	0.30	0.16	0.05	0.00	0.00	0.00	0.00	0.00	0.00

Table 2-11. DEM ~ Field sediment production fitting assessment

DEM Sed.Prod (No roughness) ~ Field Sed.Prod					DEM Sed.Prod (MAD roughness) ~ Field Sed.Prod						
Residuals:					Residuals:						
	<u>Min</u>	<u>1Q</u>	<u>Median</u>	<u>3Q</u>	<u>Max</u>		<u>Min</u>	<u>1Q</u>	<u>Median</u>	<u>3Q</u>	<u>Max</u>
	-45.80	-19.00	-11.22	11.34	235.91		-42.985	-13.423	-7.443	5.055	81.519
Coefficients:					Coefficients:						
	<u>Estimate</u>	<u>Std. Error</u>	<u>t-statistic</u>	<u>Pr(> t)</u>		<u>Estimate</u>	<u>Std. Error</u>	<u>t-statistic</u>	<u>Pr(> t)</u>		
(Intercept)	15.85595	3.71467	4.268	3.08e-05 ***	(Intercept)	13.20128	2.23822	5.898	1.61e-08 ***		
Field Sed.Prod	1.19819	0.06355	18.854	< 2e-16 ***	Field Sed.Prod	1.00021	0.03829	26.120	< 2e-16 ***		
<i>Signif. codes: 0 '***' 0.001 '**' 0.01 '*' 0.05 '.' 0.1 ' ' 1</i>					<i>Signif. codes: 0 '***' 0.001 '**' 0.01 '*' 0.05 '.' 0.1 ' ' 1</i>						
Residual standard error: 34.48 on 196 degrees of freedom					Residual standard error: 20.77 on 196 degrees of freedom						
Multiple R-squared: 0.640,					Multiple R-squared: 0.770,						
Adjusted R-squared: 0.6451					Adjusted R-squared: 0.7775						
F-statistic: 355.5 on 1 and 194 DF					F-statistic: 682.3 on 1 and 194 DF						
p-value: < 2.2e-16					p-value: < 2.2e-16						
Confidence Interval (level = 0.95)					Confidence Interval (level = 0.95)						
	<u>2.5 %</u>	<u>97.5 %</u>				<u>2.5 %</u>	<u>97.5 %</u>				
(Intercept)	8.529622	23.182280			(Intercept)	8.7869132	17.615653				
Field Sed.Prod	1.072852	1.323536			Field Sed.Prod	0.9246874	1.075733				

Table 2-12. DEM ~ Field sediment plume length fitting assessment

DEM PLength (No roughness) ~ Field PLength					DEM PLength(MAD roughness) ~ Field PLength						
Residuals:					Residuals:						
	<u>Min</u>	<u>1Q</u>	<u>Median</u>	<u>3Q</u>	<u>Max</u>		<u>Min</u>	<u>1Q</u>	<u>Median</u>	<u>3Q</u>	<u>Max</u>
	-4.5938	-0.8204	-0.5488	0.7204	5.8375		-4.2808	-0.4521	-0.2755	0.4615	5.3871
Coefficients:					Coefficients:						
	<u>Estimate</u>	<u>Std. Error</u>	<u>t-statistic</u>	<u>Pr(> t)</u>		<u>Estimate</u>	<u>Std. Error</u>	<u>t-statistic</u>	<u>Pr(> t)</u>		
(Intercept)	0.88350	0.34750	2.542	0.0142 *	(Intercept)	0.09936	0.34777	0.286	0.776		
Field PLength	0.18632	0.02877	6.477	4.29e-08 ***	Field PLength	0.25231	0.02879	8.764	1.33e-11 ***		
<i>Signif. codes: 0 '***' 0.001 '**' 0.01 '*' 0.05 '.' 0.1 ' ' 1</i>					<i>Signif. codes: 0 '***' 0.001 '**' 0.01 '*' 0.05 '.' 0.1 ' ' 1</i>						
Residual standard error: 1.779 on 49 degrees of freedom					Residual standard error: 1.78 on 49 degrees of freedom						
Multiple R-squared: 0.4612,					Multiple R-squared: 0.6105,						
Adjusted R-squared: 0.4502					Adjusted R-squared: 0.6026						
F-statistic: 41.95 on 1 and 49 DF,					F-statistic: 76.8 on 1 and 49 DF,						
p-value: 4.295e-08					p-value: 1.33e-11						
Confidence Interval (level = 0.95)					Confidence Interval (level = 0.95)						
	<u>2.5 %</u>	<u>97.5 %</u>				<u>2.5 %</u>	<u>97.5 %</u>				
(Intercept)	0.1851642	1.5818383			(Intercept)	-0.5995043	0.7982179				
Field PLength	0.1285081	0.2441341			Field Sed.Prod	0.1944565	0.3101693				

Table 2-13. DEM ~ Field sediment connectivity and delivery fitting assessment summary

	r.squared	adj.r.squared	sigma	statistic	p.value	df	logLik	AIC	BIC	deviance	df.residual
DEM Connectivity (No roughness) ~ Field Connectivity	0.456	0.443	0.227	35.2	4.93 E-07	2	3.76	-1.52	3.83	2.17	42
DEM Connectivity (Mad-roughness) ~ Field Connectivity	0.518	0.509	0.194	68.1	2.50E-10	2	10.8	-15.7	-10.3	1.57	42
DEM Delivery (No roughness) ~ Field Delivery	0.482	0.424	25.5	89.8	5.49E-12	2	-204	414	419	27356	42
DEM Delivery (Mad-roughness) ~ Field Delivery	0.546	0.508	18	136	9.82E-5	2	-189	383	389	13655	42

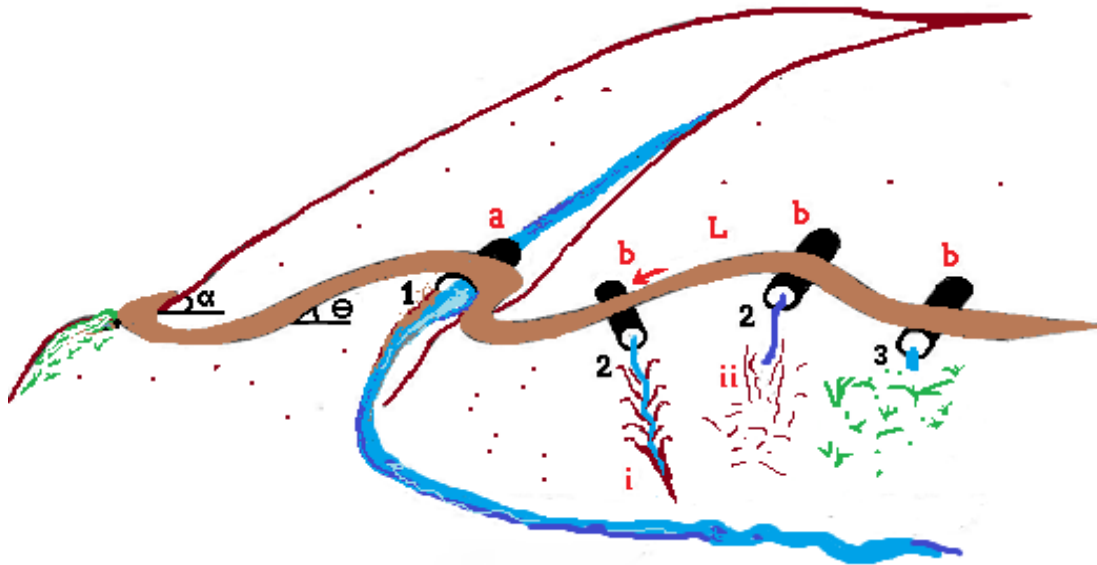


Figure 2-1. Road drainage structure on forest roads. Length (L), road gradient (Θ), hillslope gradient (α), stream crossings (a), culverts (b). The sediment delivery dynamic: directly to a stream channel (1), through gullies (2), soil re-infiltration (3). The way of traveling: through incisive gullies (i), diffusive path (ii). Adapted from Wemple et al. (1996).

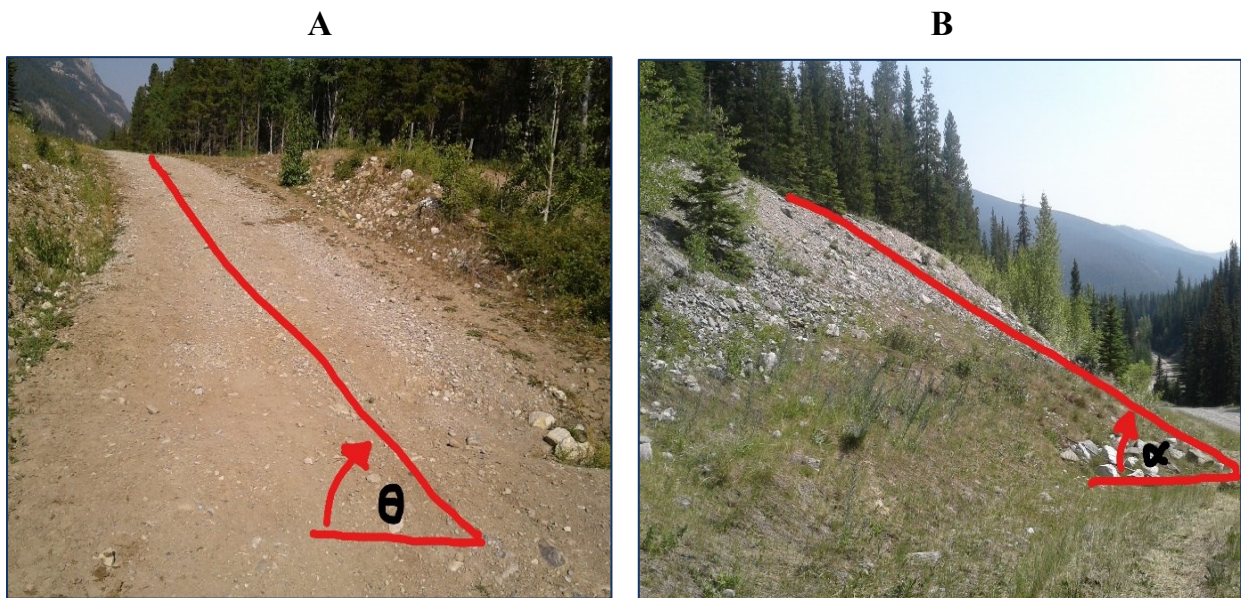


Figure 2-2. Slope characterization for the model: the slope of the road and slope of the watershed area. The slope of the road based on horizontal vector utilized for sediment production computation (A). Slope based on vertical vector utilized to characterize the downslope condition gradient (B).

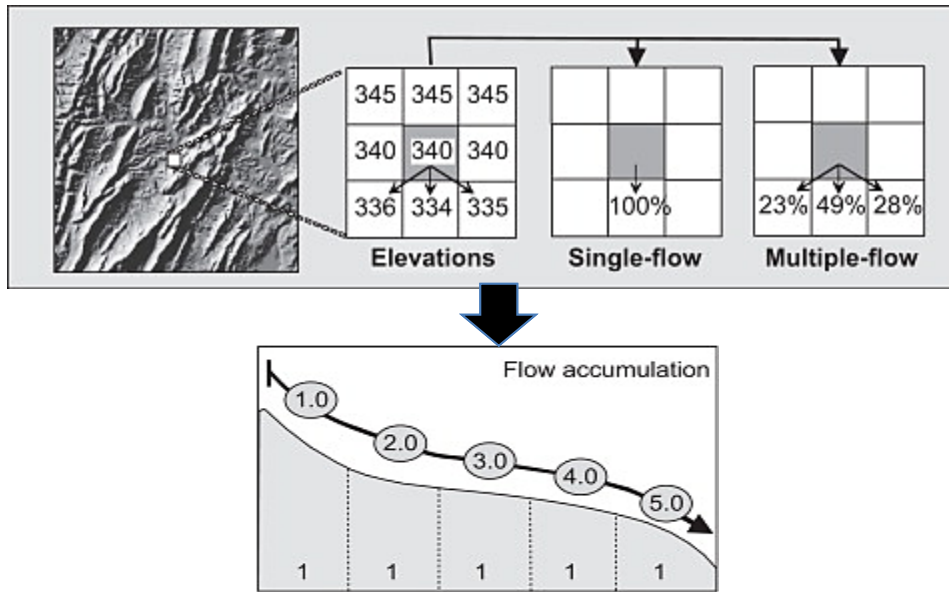


Figure 2-3. Representation of the method for flow accumulation calculation from DEM cells. Adapted from Schäuble et al. (2008).

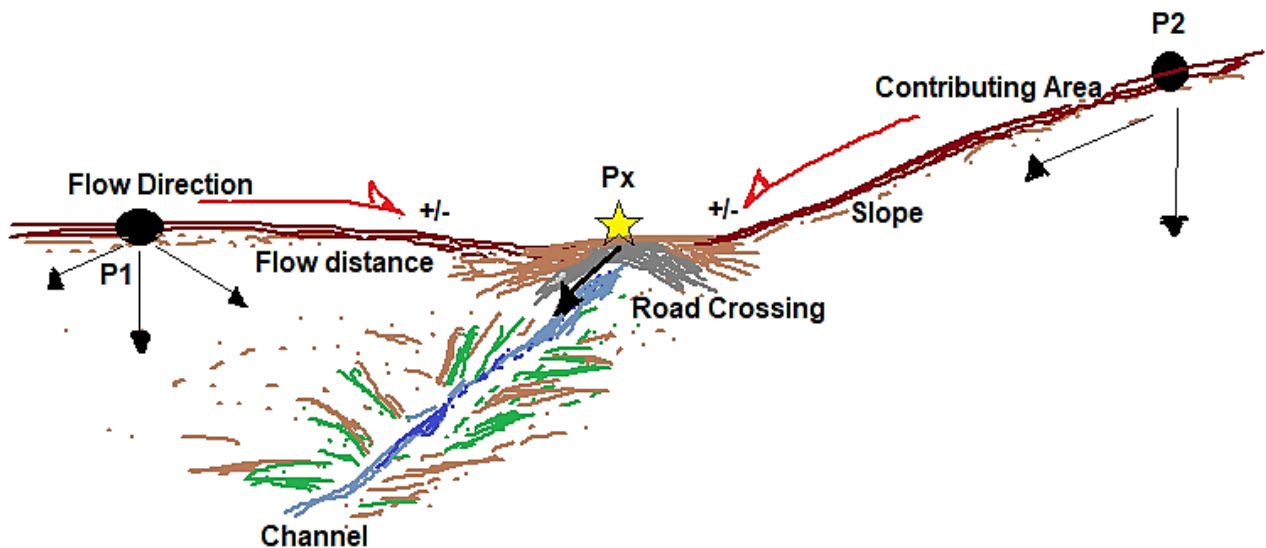


Figure 2-4. Schematic portraying the upslope components for road sediment production estimation. From erosion points P1 and P2: road crossings, culverts, concave areas, and stream channels are denoted by Px point. The sediment generation from the road surface represented by the contributing area and the slope of the road and influenced by the erosive forms on the surface as well as the road maintenance status.

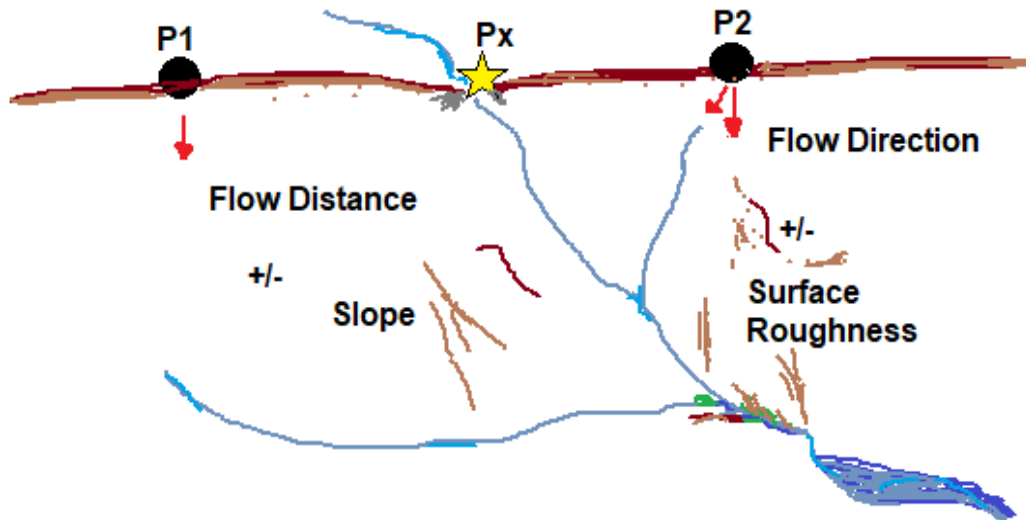


Figure 2-5. Schematic describing the components for sediment transportation from erosion initiation points P1 and P2 to Px point. Sediment plume travels directly to the nearest stream (Px) or travels downhill challenged by surface conditions leading to loss or gain of material.

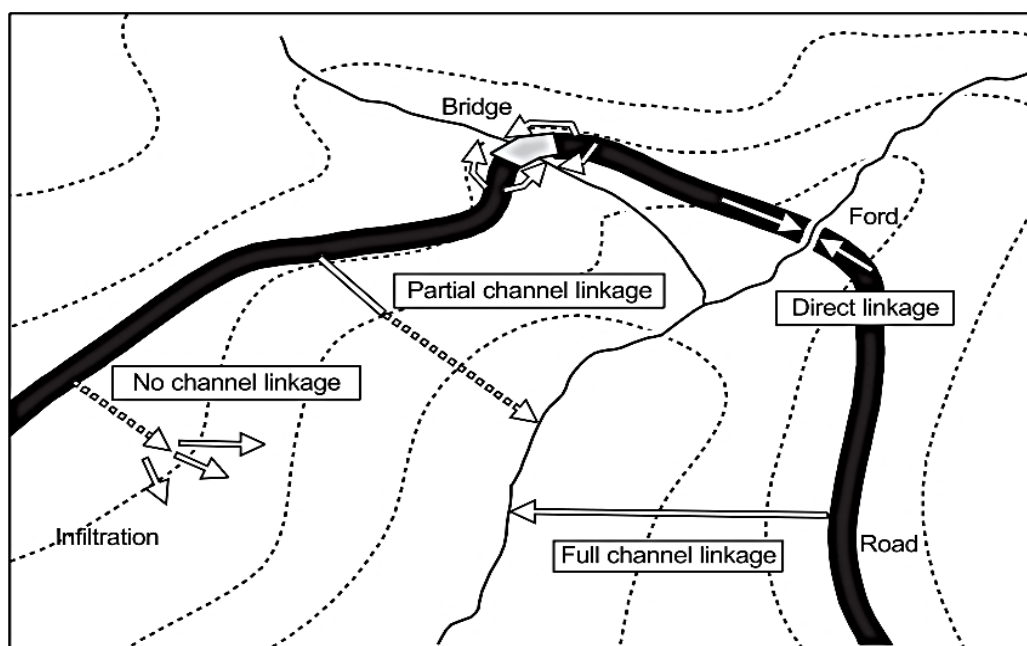


Figure 2-6. Sediment plume flowing directions for potential connectivity to streams affected by downhill topographic conditions. Adapted from Croke and Hairsine (2006).

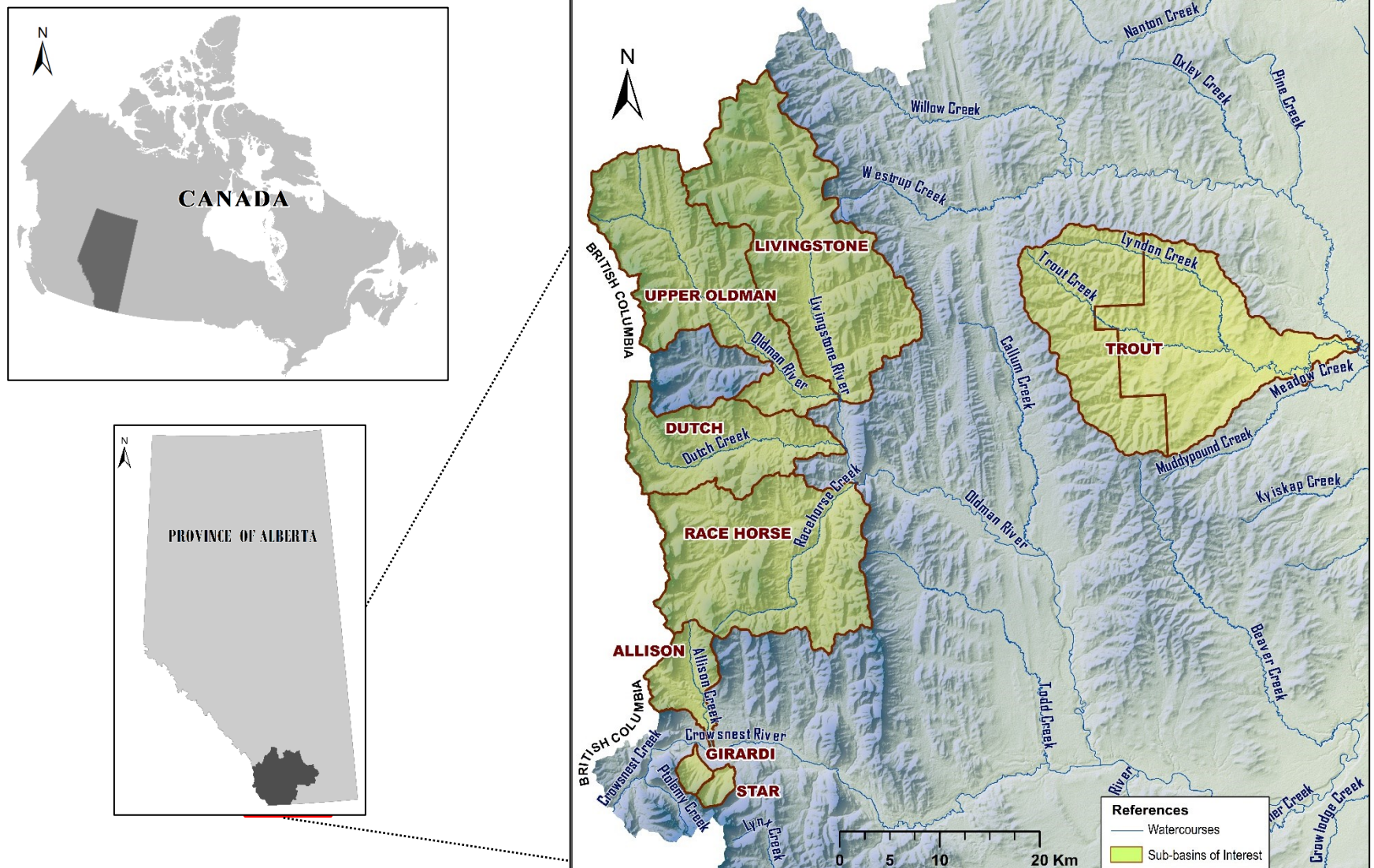


Figure 2-7. Location of the study area. Data Source: Government of Alberta (GOA, 2018)

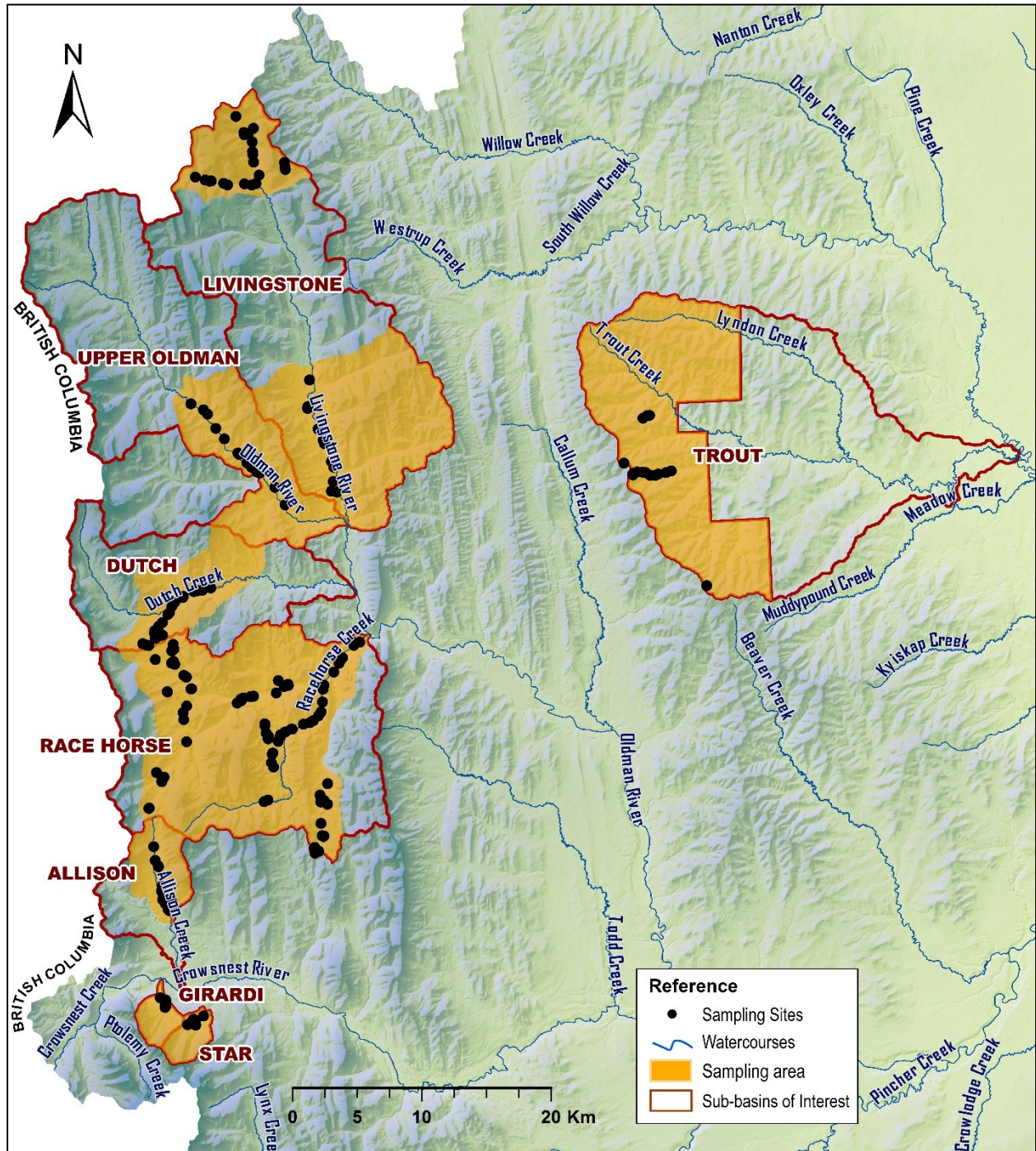


Figure 2-8. Location of the sampling area. Data Source: Government of Alberta (GOA,2018)

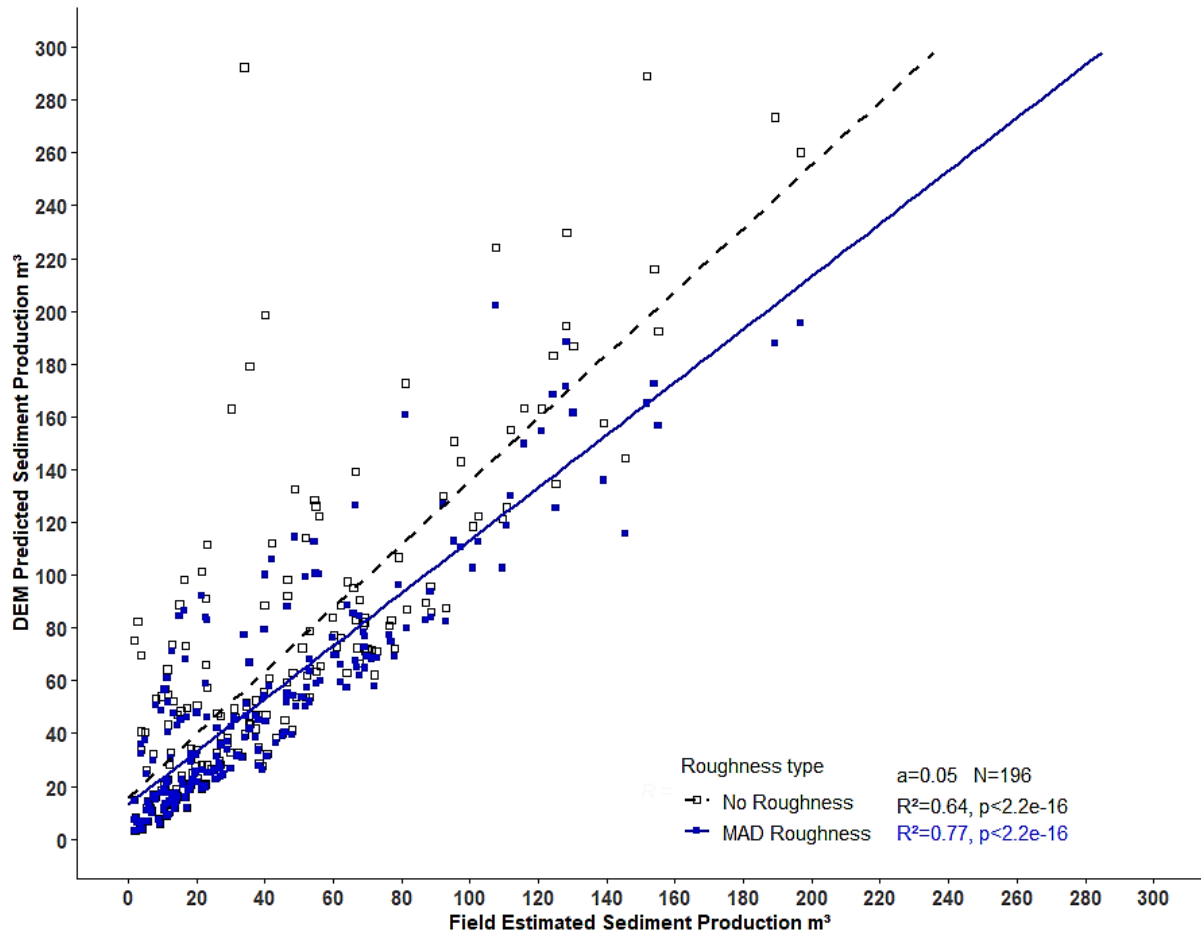


Figure 2-9. The volume of sediment production (m^3) predicted from DEM versus the sediment production (m^3) estimated from the field at the corresponding site ($N=196$). No topographic roughness was applied for the predicted production values from the DEM.

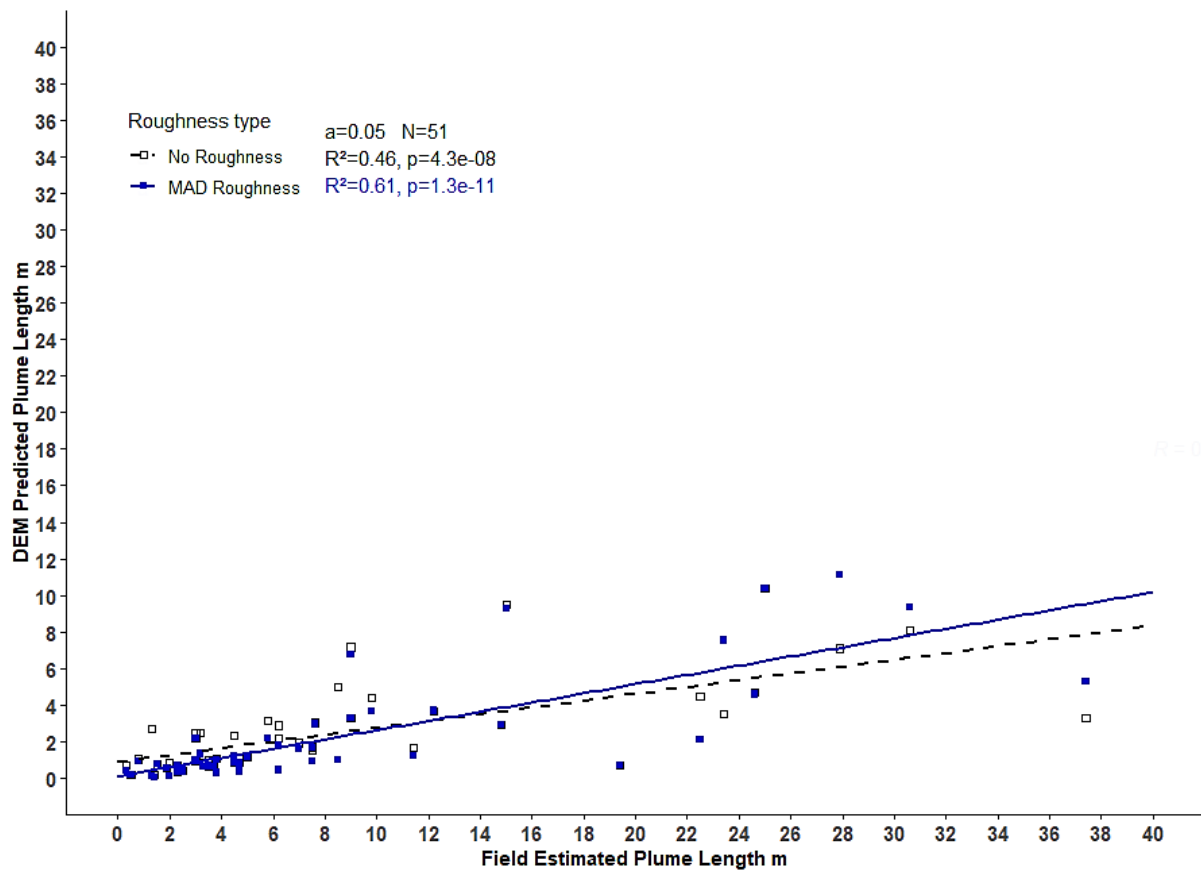


Figure 2-10. Sediment plume travel distance (m) predicted from the DEM versus the plume length estimated from the field at the corresponding sites (N=51).

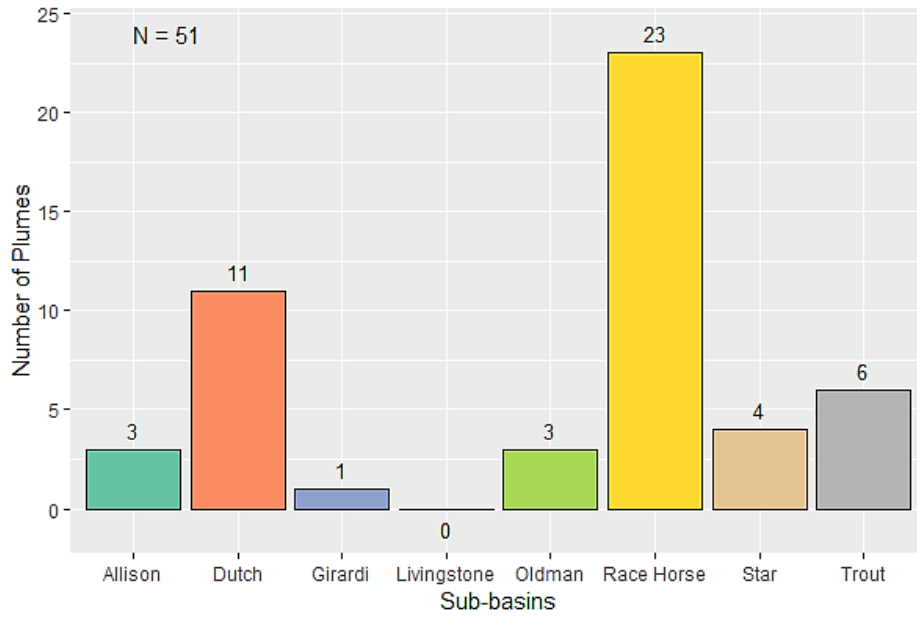


Figure 2-11. Number of sediment plumes found in each sub-basin.

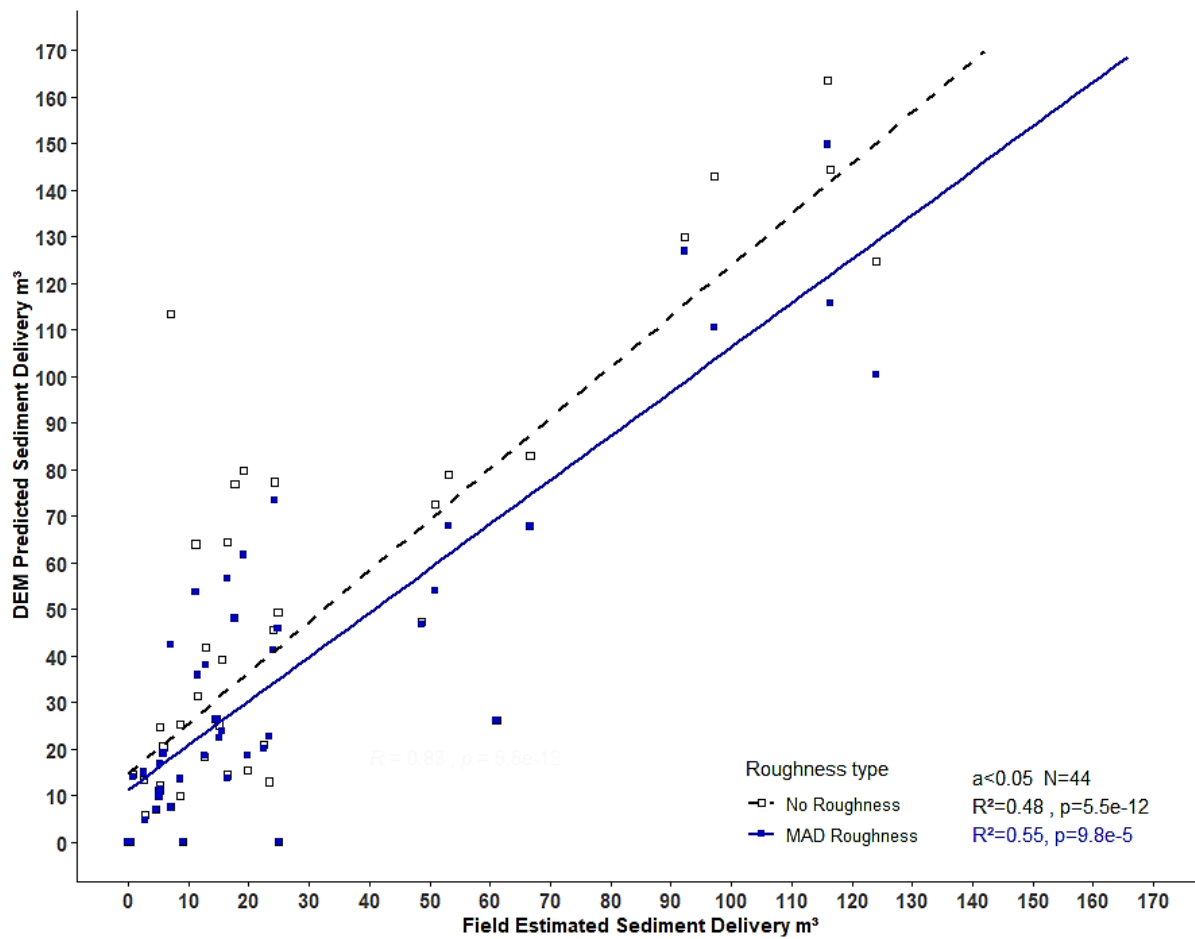


Figure 2-12. The volume of sediment delivery estimated from DEM versus Field sediment delivery at the sites (N= 44).

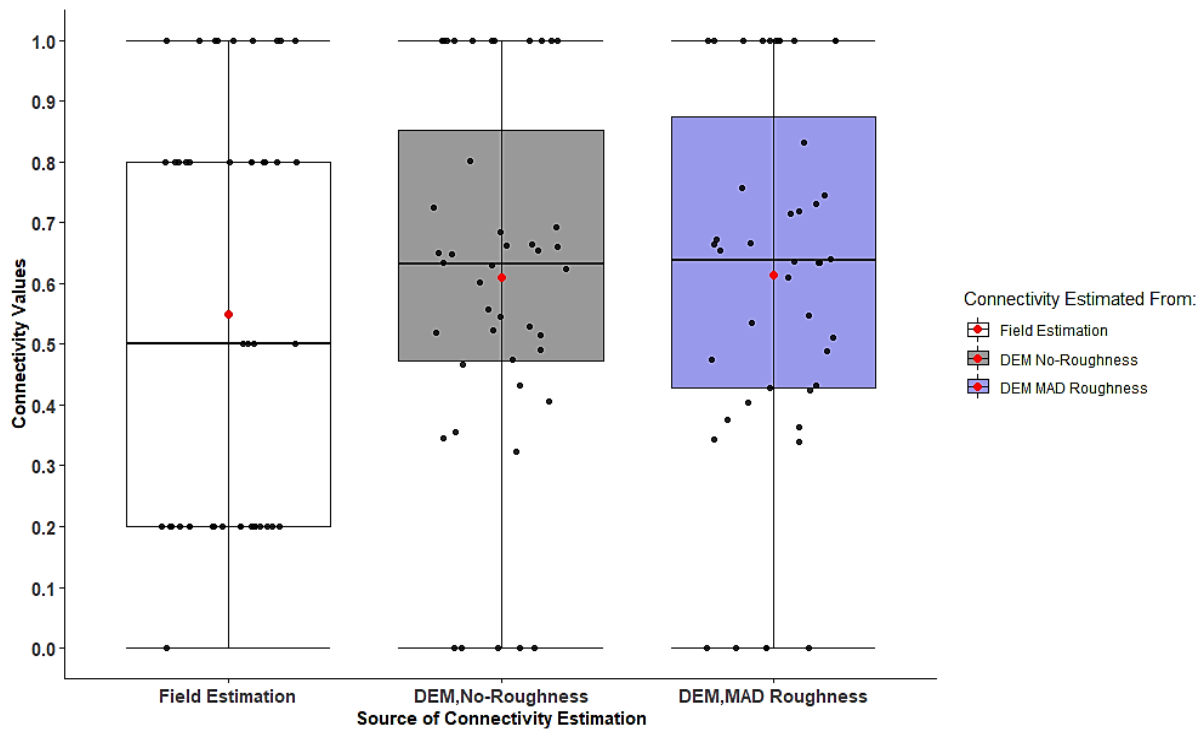


Figure 2-13. Connectivity estimated from Field and Connectivity predicted from the DEM with no roughness (no weighting factor applied) and with roughness (weighted factor applied) (N= 44). Field connectivity corresponds to connectivity categories assigned directly in the field at the evaluated sites according to the connectivity classification in Carson et al. (2009) which varies from 0 = none to 1= all connected (Table 2-9).

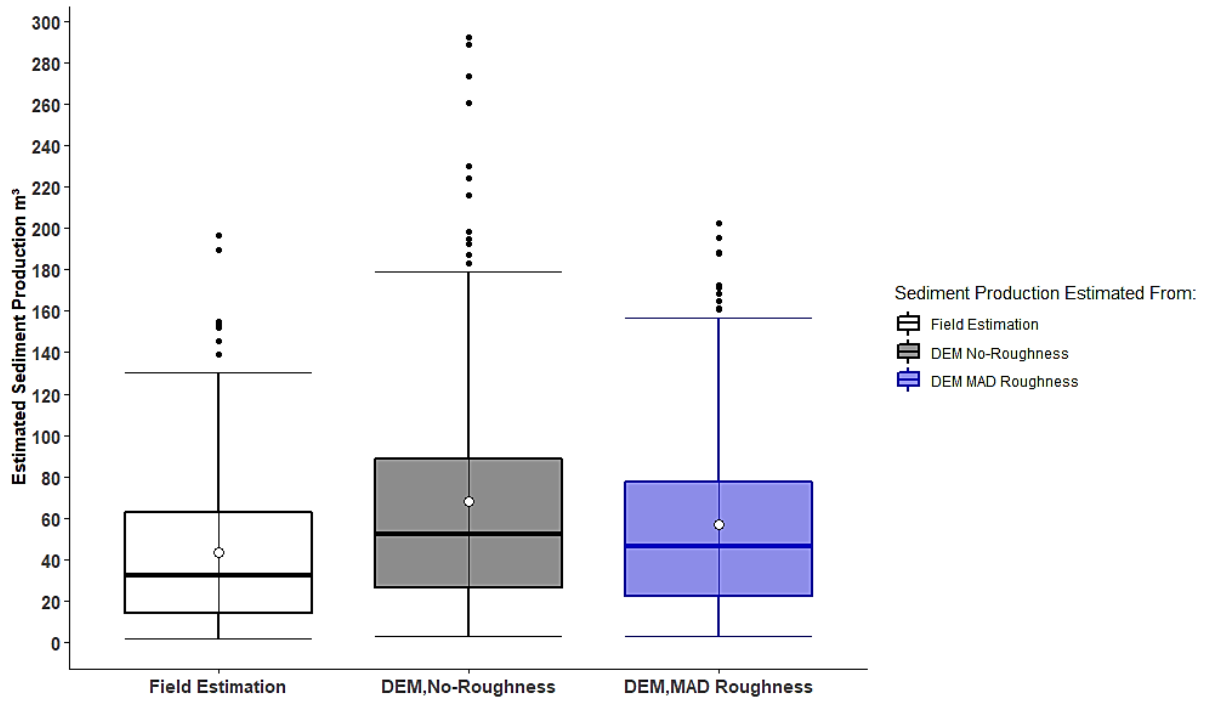


Figure 2-14. Sediment production predicted from roads (m³) based on the DEM and field (N=196).

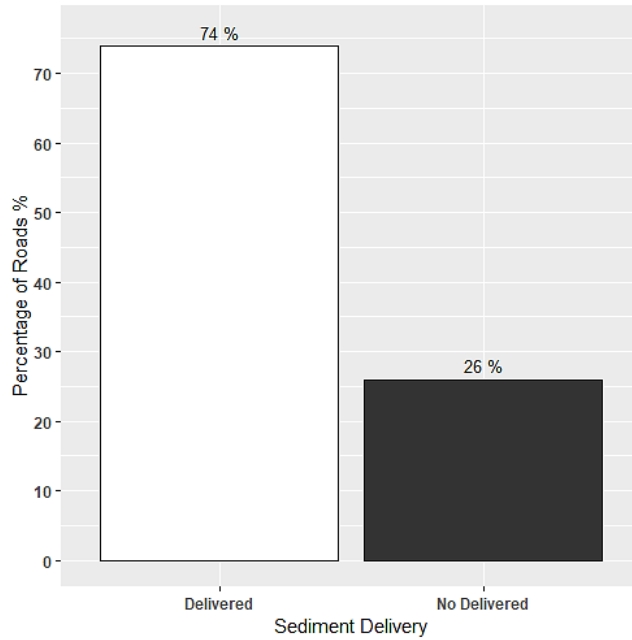


Figure 2-15. DEM predicted the percentage of roads classified by their sediment delivery status: delivered and non-delivered.

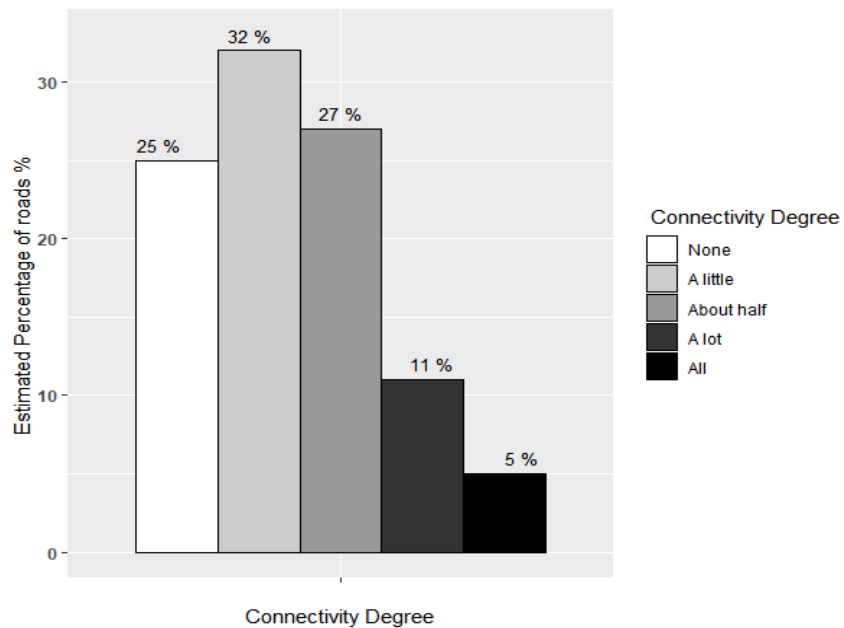


Figure 2-16. DEM predicted the percentage of roads classified by their connectivity level.

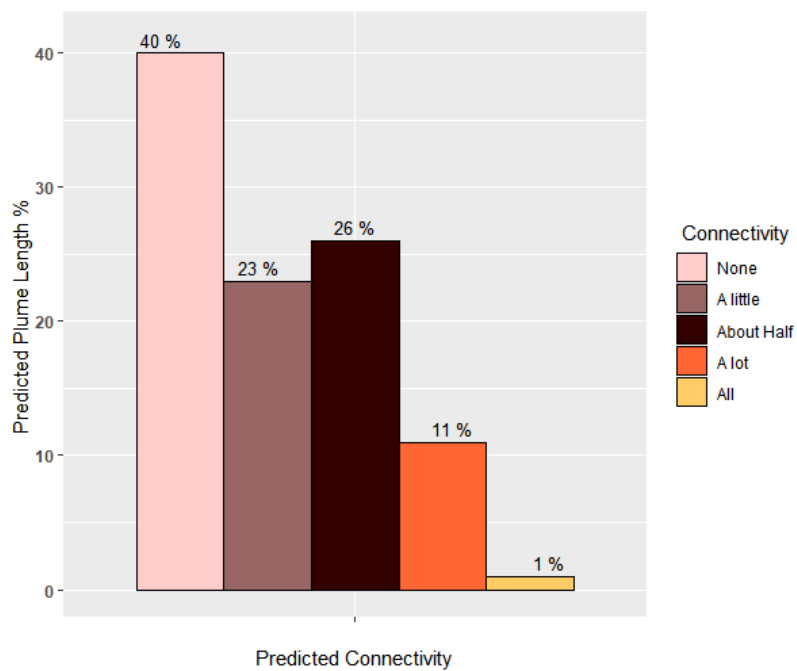
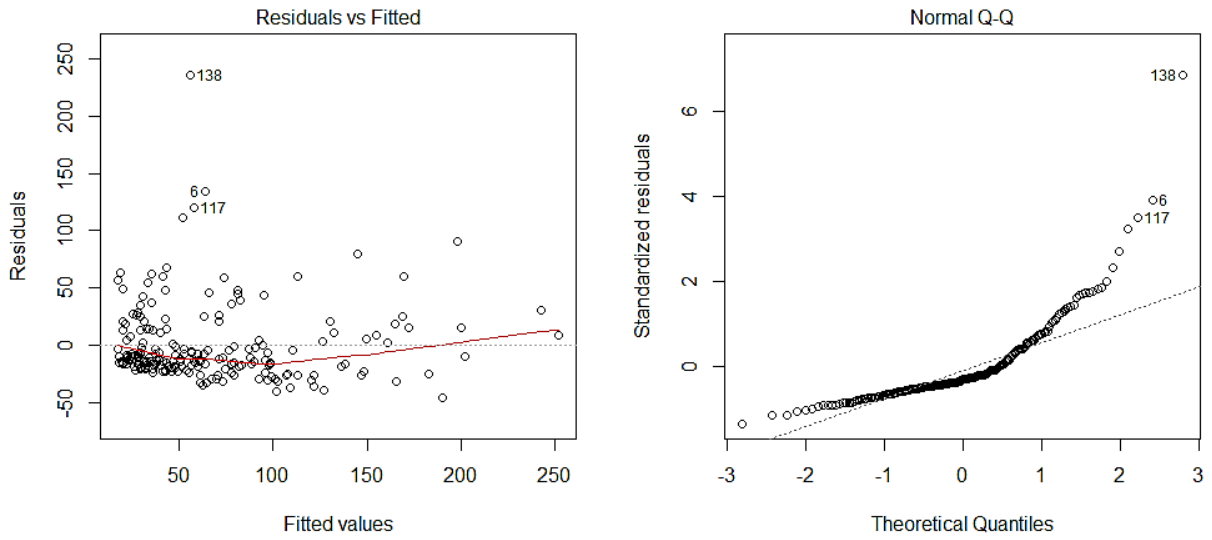


Figure 2-17. Roads classified by their estimated percentage of sediment plumes length versus their connectivity class.

A. DFsp---Sediment generation (no roughness used)



B. DFsp-r---Sediment generation (MAD flow-directional roughness used)

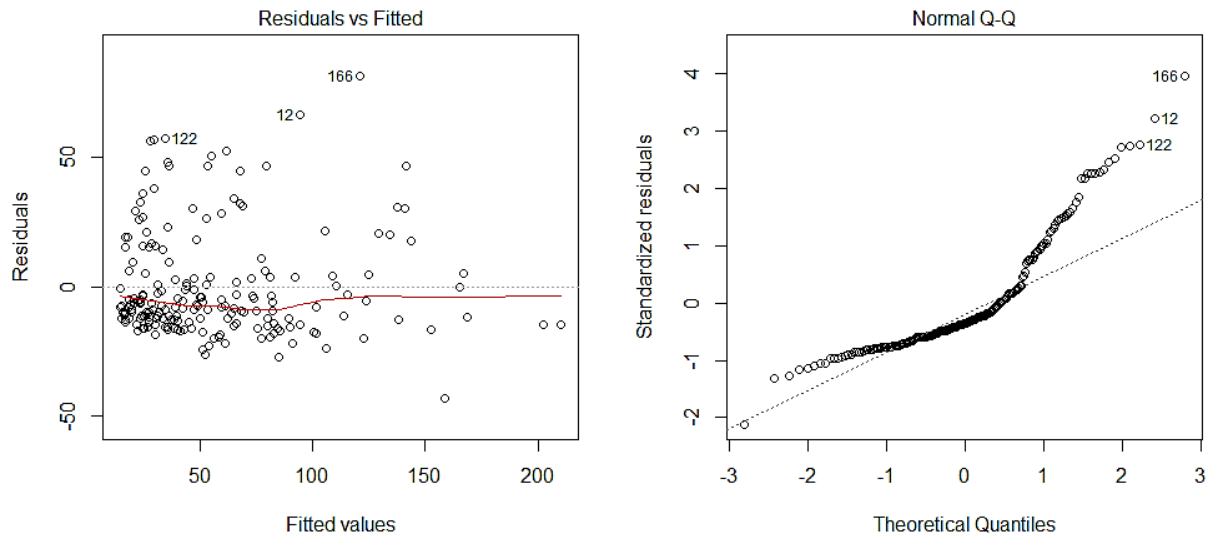
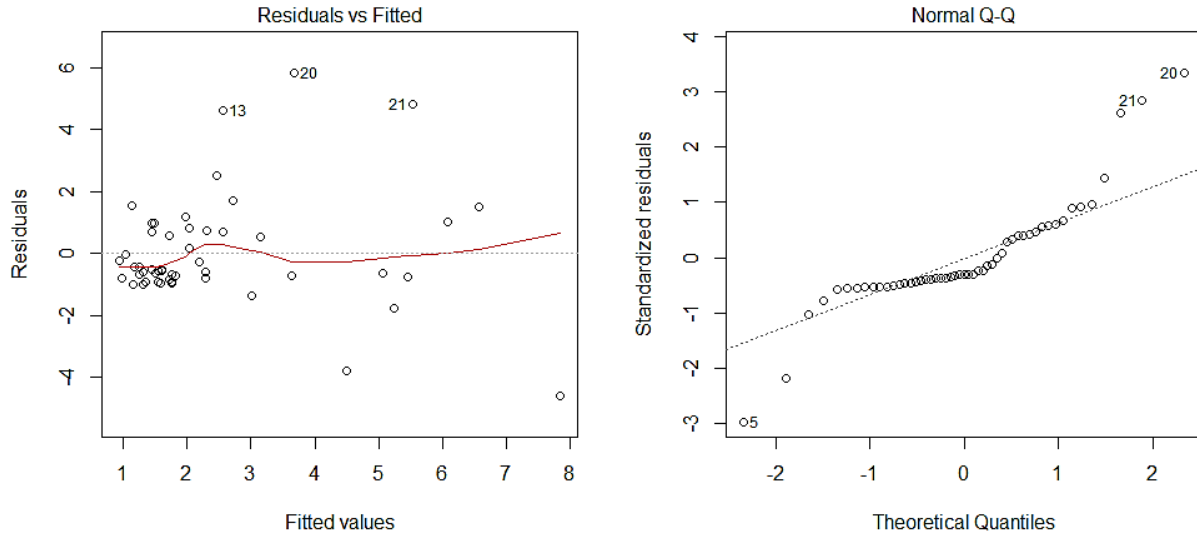


Figure 2-18. DEM vs. Field sediment production fitting results

A. DFpl --- Sediment plume length (no roughness used)



B. DFpl-r ---Sediment plume length (MAD flow-directional roughness used)

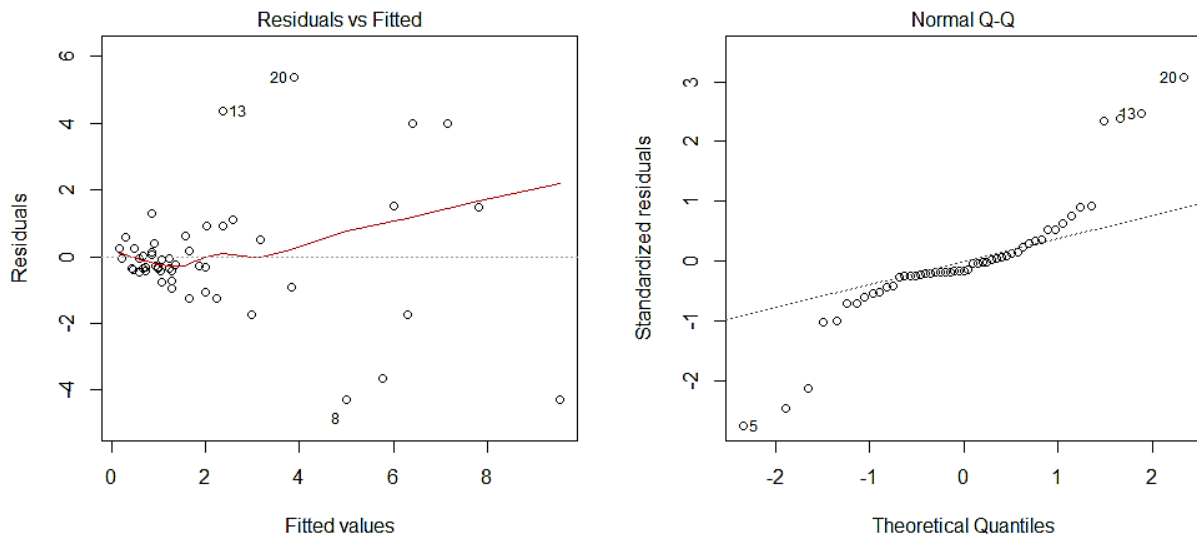
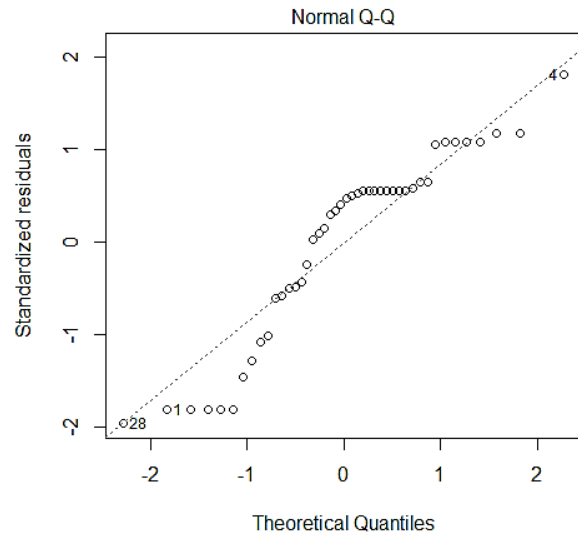
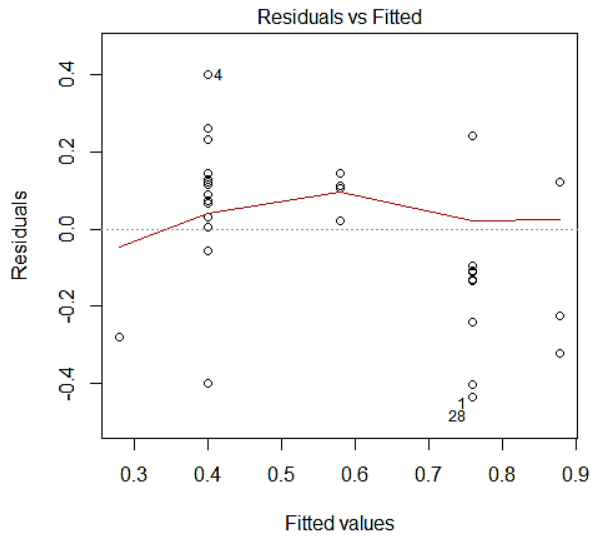


Figure 2-19. DEM vs. Field sediment plume length fitting results

A. DFC---Connectivity (no roughness used)



B. DFC-r---Connectivity (MAD flow-directional roughness used)

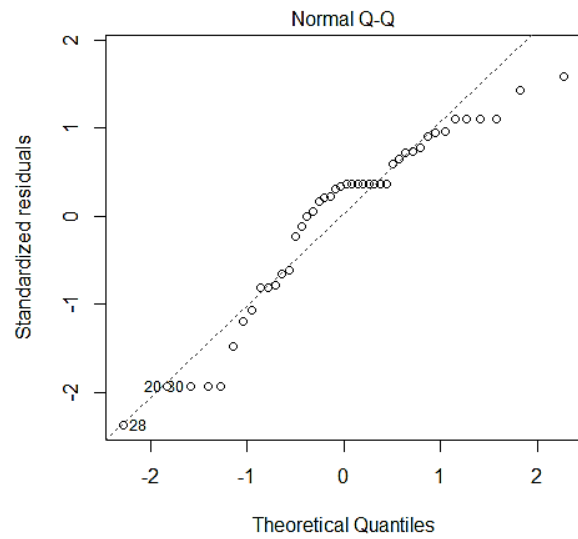
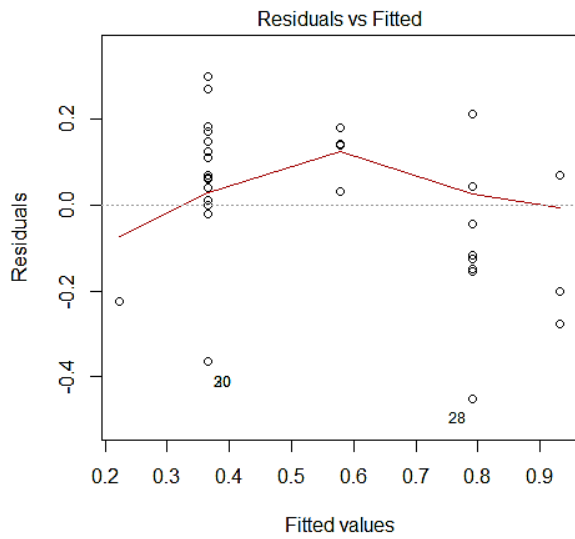
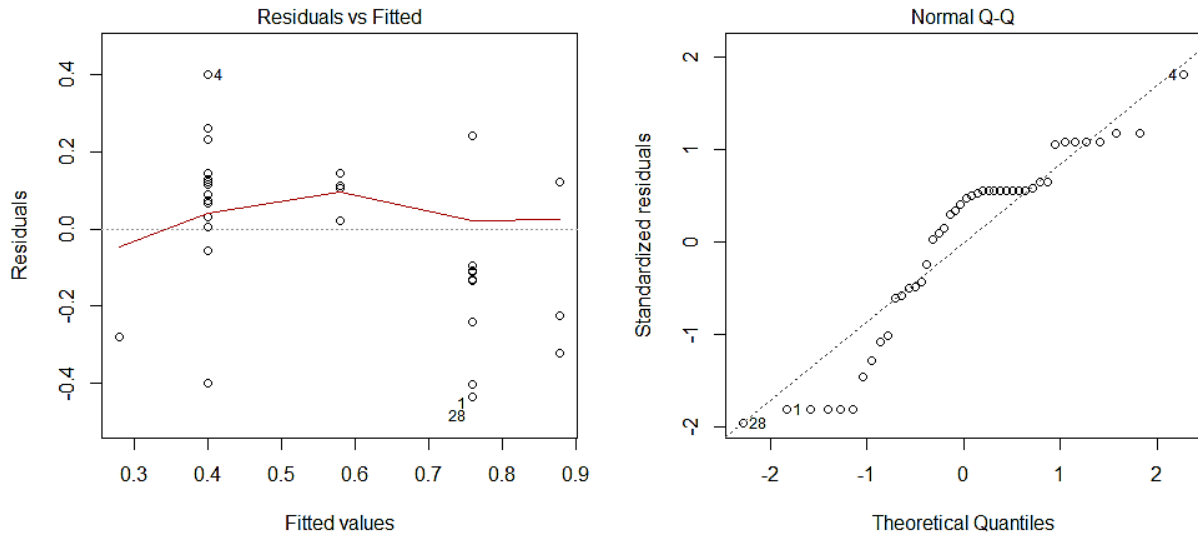


Figure 2-20. DEM vs. Field connectivity fitting results.

A. DFd---Delivery (no roughness used)



B. DFd-r---Delivery (MAD flow-directional roughness used)

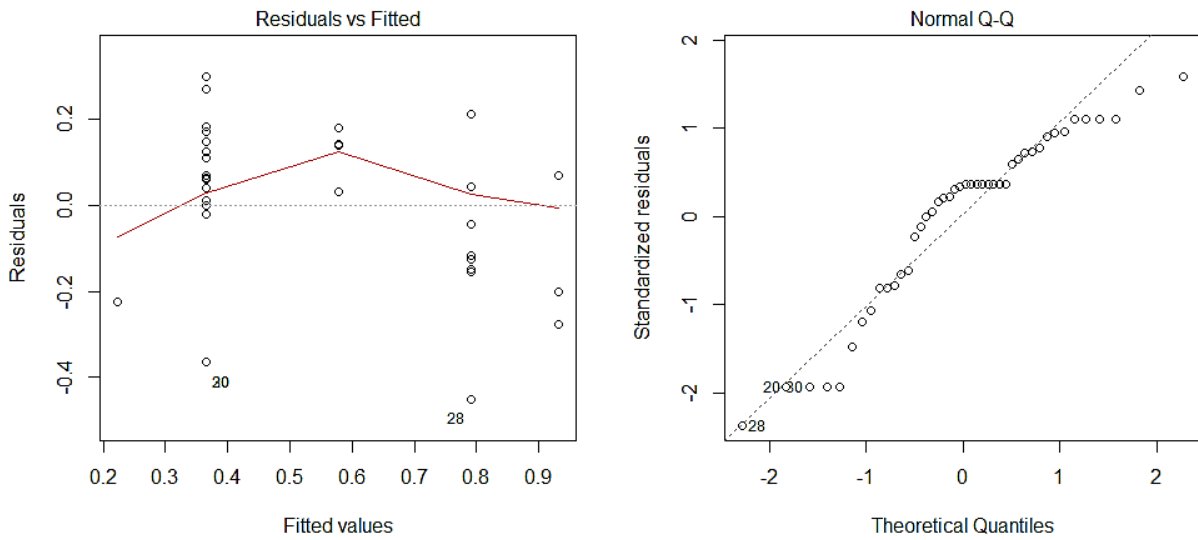


Figure 2-21. DEM vs. Field delivery fitting results.

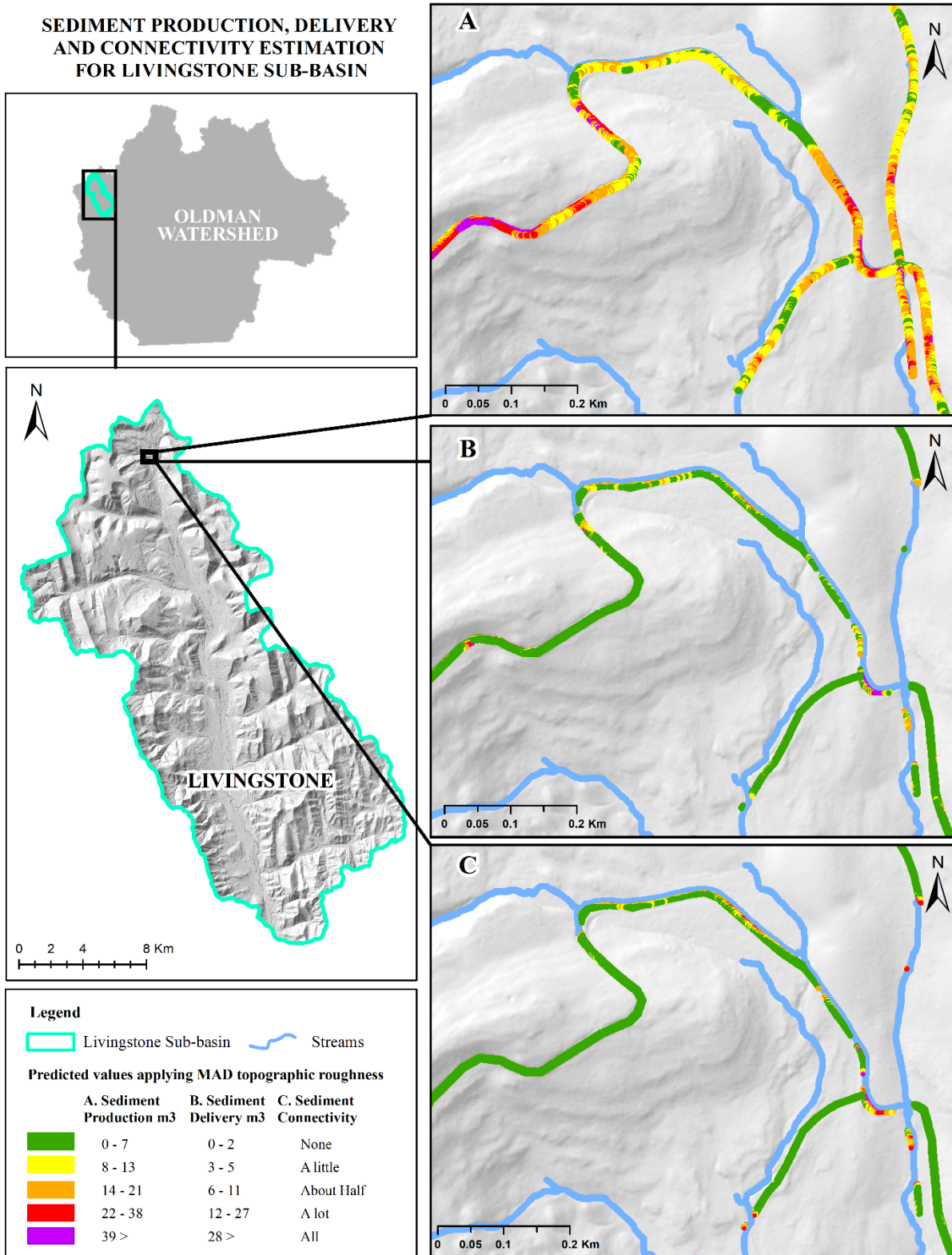


Figure 2-22. Sediment production, delivery, and connectivity for Livingstone sub-basin.

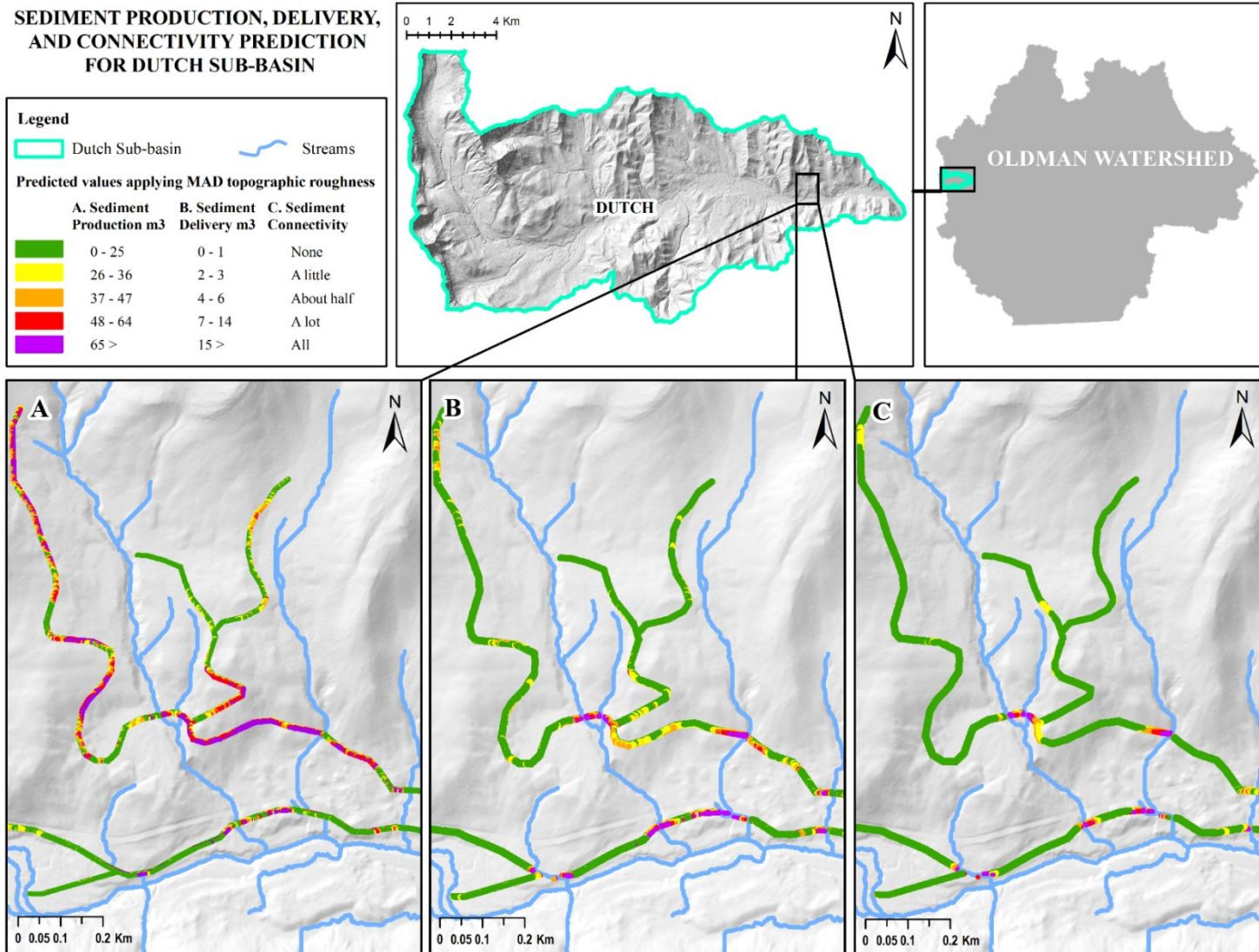


Figure 2-23. Sediment production, delivery, and connectivity for Dutch sub-basin.

References

- Akay, A. E., Erdas, O., Reis, M., & Yuksel, A. (2008). Estimating sediment yield from a forest road network by using a sediment prediction model and GIS techniques. *Building and Environment*, *43*(5), 687–695. <https://doi.org/10.1016/j.buildenv.2007.01.047>
- Alberta Agriculture and Forestry, University of New Brunswick, Forest Watershed Research Centre (2018) WAM-wet areas mapping of Alberta. Edmonton, AB: Alberta Environment and Parks – Informatics Branch. Data access through DMR# 1704M08, Project: Testing Erosion Prediction Tools in Alberta Road Networks.
- Al-Chokhachy, R., Black, T. A., Thomas, C., Luce, C. H., Rieman, B., Cissel, R., ... Kershner, J. L. (2016). Linkages between unpaved forest roads and streambed sediment: why context matters in directing road restoration. *Restoration Ecology*, *24*(5), 589–598. <https://doi.org/10.1111/rec.12365>
- Alder, S., Prasuhn, V., Liniger, H., Herweg, K., Hurni, H., Candinas, A., & Gujer, H. U. (2015). A high-resolution map of direct and indirect connectivity of erosion risk areas to surface waters in Switzerland—A risk assessment tool for planning and policy-making. *Land Use Policy*, *48*, 236–249. <https://doi.org/10.1016/j.landusepol.2015.06.001>
- Anderson, D. M., & MacDonald, L. H. (1998). Modeling road surface sediment production using a vector geographic information system. *Earth Surface Processes and Landforms*, *23*, 95–107. <https://doi.org/doi.org/10.1002>
- Anderson, P., & Anderson, R. (1987). Erosion potential index : a method for evaluating sheet erosion at stream crossings. Edmonton : Alberta Forestry, Lands and Wildlife. <https://doi.org/10.5962/bhl.title.110391>
- Aruga, K., Sessions, J., & Miyata, E. S. (2005). Forest road design with soil sediment evaluation using a high-resolution DEM. *Journal of Forest Research*, *10*(6), 471–479. <https://doi.org/10.1007/s10310-005-0174-7>
- Baartman, J. E. M., Masselink, R., Keesstra, S. D., & Temme, A. J. A. M. (2013). Linking landscape morphological complexity and sediment connectivity. *Earth Surface Processes and Landforms*, *38*(12), 1457–1471. <https://doi.org/10.1002/esp.3434>
- Benda, L., Andras, K., Miller, D., Netmap, T., & Shasta, M. (2016). *Road Cumulative Effects Analysis in the Simonette River Watershed*. Retrieved from www.terrainworks.com
- Benda, L., James, C., Miller, D., & Andras, K. (2019). Road Erosion and Delivery Index (READI): A Model for Evaluating Unpaved Road Erosion and Stream Sediment Delivery. *Journal of the American Water Resources Association*. <https://doi.org/10.1111/1752-1688.12729>
- Benda, L., Miller, D., Andras, K., Bigelow, P., Reeves, G., & Michael, D. (2007). NetMap: A new tool in support of watershed science and resource management. *Forest Science*, *53*(2), 206–219. <https://doi.org/doi.org/10.1093/forestscience/53.2.206>
- Beven, K. J., & Kirkby, M. J. (1979). A physically based, variable contributing area model of

- basin hydrology. *Hydrological Sciences Bulletin*, 24(1), 43–69.
<https://doi.org/10.1080/02626667909491834>
- Borselli, L., Cassi, P., & Torri, D. (2008). Prolegomena to sediment and flow connectivity in the landscape: A GIS and field numerical assessment. *Catena*, 75(3), 268–277.
<https://doi.org/10.1016/j.catena.2008.07.006>
- Bracken, Louise J., and Croke, J. (2007). The concept of hydrological connectivity and its contribution to understanding runoff-dominated geomorphic systems, 21, 2267–2274.
<https://doi.org/10.1002/hyp.6313>
- Bracken, L. J., Turnbull, L., Wainwright, J., & Bogaart, P. (2015). Sediment connectivity: A framework for understanding sediment transfer at multiple scales. *Earth Surface Processes and Landforms*, 40(2), 177–188. <https://doi.org/10.1002/esp.3635>
- Burnett, K. M., & Miller, D. J. (2007). Streamside policies for headwater channels: An example considering debris flows in the Oregon coastal province. *Forest Science*, 53(2), 239–253. <https://doi.org/doi.org/10.1093/forestscience/53.2.239>
- Cantreul, V., Bièlders, C., Calsamiglia, A., & Degré, A. (2017). How pixel size affects a sediment connectivity index in central Belgium. *Earth Surface Processes and Landforms*.
<https://doi.org/10.1002/esp.4295>
- Carson, B., Maloney, D., Chatwin, S., Carver, M., & Beaudry, P. (2009). Protocol for Evaluating the Potential Impact of Forestry and Range Use on Water Quality (Water Quality Routine Effectiveness Evaluation). Victoria, BC. Retrieved from <http://www.publications.gov.bc.ca>
- Cavalli, M., Goldin, B., Comiti, F., Brardinoni, F., & Marchi, L. (2017). Assessment of erosion and deposition in steep mountain basins by differencing sequential digital terrain models. *Geomorphology*, 291, 4–16. <https://doi.org/10.1016/j.geomorph.2016.04.009>
- Cavalli, M., Trevisani, S., Comiti, F., & Marchi, L. (2013). Geomorphometric assessment of spatial sediment connectivity in small Alpine catchments. *Geomorphology*, 188, 31–41.
<https://doi.org/10.1016/j.geomorph.2012.05.007>
- Crema, S., & Cavalli, M. (2018). SedInConnect: a stand-alone, free and open source tool for the assessment of sediment connectivity. *Computers and Geosciences*, 111(December 2016), 39–45. <https://doi.org/10.1016/j.cageo.2017.10.009>
- Croke, J. C., & Hairsine, P. B. (2006). Sediment delivery in managed forests: a review. *Environmental Reviews*, 14(1), 59–87. <https://doi.org/10.1139/a05-016>
- Croke, J., Mockler, S., Fogarty, P., & Takken, I. (2005). Sediment concentration changes in runoff pathways from a forest road network and the resultant spatial pattern of catchment connectivity. *Geomorphology*, 68(3–4), 257–268.
<https://doi.org/10.1016/j.geomorph.2004.11.020>
- Demirci, A., & Karaburun, A. (2012). Estimation of soil erosion using RUSLE in a GIS framework: A case study in the Buyukcekmece Lake watershed, northwest Turkey. *Environmental Earth Sciences*, 66(3), 903–913. <https://doi.org/10.1007/s12665-011->

- Esri (2018). ArcMap Release 10.6.1. Computer software. Redlands, CA: Environmental Systems Research Institute.
- Fiera Biological Consulting Ltd (Fiera). (2014). Oldman Watershed Headwaters Indicator Project - Final Report (Version 2014.1). Edmonton, Alberta. Fiera Biological Consulting Report #1346. Retrieved from <https://oldmanwatershed-council.squarespace.com/s/HeadwatersIndicatorsProject.pdf>
- Gay, A., Cerdan, O., Mardhel, V., & Desmet, M. (2016). Application of an index of sediment connectivity in a lowland area. *Journal of Soils and Sediments*, 16(1), 280–293. <https://doi.org/10.1007/s11368-015-1235-y>
- Gomes, R. A. T., Guimarães, R. F., Carvalho, O. A., Fernandes, N. F., Vargas, E. A., & Martins, É. S. (2008). Identification of the affected areas by mass movement through a physically based model of landslide hazard combined with an empirical model of debris flow. *Natural Hazards*, 45(2), 197–209. <https://doi.org/10.1007/s11069-007-9160-z>
- Government of Alberta. (2009). Alberta Recreation Corridor and Trails Classification System. Alberta Tourism, Parks and Recreation. Retrieved from www.tpr.gov.alberta.ca
- Government of Alberta (2018) WAM derived Stream Features (vector digital data). Edmonton, AB: Alberta Environment and Parks – Informatics Branch. Data access through DMR# 1704M08, Project: Testing Erosion Prediction Tools in Alberta Road Networks.
- Government of Alberta (2018) Cutlines and Trails of Alberta (vector digital data). Cited 2017. Edmonton, AB: Alberta Environment and Parks. Retrieved from: <https://maps.alberta.ca/genesis/rest/services/Access/Latest/MapServer>
- Government of Alberta (2014) Watersheds of Alberta (vector digital data). Cited 2018. Edmonton, AB: Alberta Environment and Parks. Retrieved from: https://maps.alberta.ca/genesis/rest/services/Watersheds_of_Alberta/Latest/MapServer
- Grauso, S., Pasanisi, F., & Tebano, C. (2018). Assessment of a Simplified Connectivity Index and Specific Sediment Potential in River Basins by Means of Geomorphometric Tools. *Geosciences*, 8(2), 48. <https://doi.org/10.3390/geosciences8020048>
- Grohmann, C. H., Smith, M. J., & Riccomini, C. (2011). Multiscale analysis of topographic surface roughness in the Midland Valley, Scotland. *IEEE Transactions on Geoscience and Remote Sensing*, 49(4), 1200–1213. <https://doi.org/10.1109/TGRS.2010.2053546>
- Hartcher, M. G., & Post, D. A. (2005). Reducing Uncertainty in Sediment Yield Through Improved Representation of Land Cover: Application to Two Sub-catchments of the Mae Chaem, Thailand. In *International Congress on Modelling and Simulation: Advances and Applications for Management and Decision Making* (pp. 1147–1153). Melbourne, VIC; Australia; 12 Dec-15 Dec: MODSIM05. Retrieved from <https://pdfs.semanticscholar.org/0659/fa09533a249be75b59b119c0c977a783b9bd.pdf>

- Hooke, J. (2003). Coarse sediment connectivity in river channel systems: A conceptual framework and methodology. *Geomorphology*, 56(1–2), 79–94. [https://doi.org/10.1016/S0169-555X\(03\)00047-3](https://doi.org/10.1016/S0169-555X(03)00047-3)
- Hurkett, B. (2009). Bull Trout Population Assessment in the Upper Oldman River Drainage. Lethbridge, Alberta. Retrieved from <https://www.ab-conservation.com/publications/report-series/bull-trout-population-assessment-in-the-upper-oldman-river-drainage-2009/>
- La Marche, J. L., & Lettenmaier, D. P. (2001). Effects of forest roads on flood flows in the Deschutes River, Washington. *Earth Surface Processes and Landforms*, 26(2), 115–134. [https://doi.org/10.1002/1096-9837\(200102\)26:2<115::AID-ESP166>3.0.CO;2-O](https://doi.org/10.1002/1096-9837(200102)26:2<115::AID-ESP166>3.0.CO;2-O)
- Lisle, T. E. (1989). Sediment transport and resulting deposition in spawning gravels, north coastal California. *Water Resources Research*, 25(6), 1303–1319. <https://doi.org/10.1029/WR025i006p01303>
- López-Vicente, M., & Álvarez, S. (2018). Influence of DEM resolution on modeling hydrological connectivity in a complex agricultural catchment with woody crops. *Earth Surface Processes and Landforms*, 43(7), 1403–1415. <https://doi.org/10.1002/esp.4321>
- Luce, C. H., & Black, T. a. (1999). Sediment production from forest roads in western Oregon. *Water Resources Research*, 35(8), 2561. <https://doi.org/10.1029/1999WR900135>
- MacDonald, L. H., & Coe, D. B. R. (2008). Road Sediment Production and Delivery: Processes and Management. In *First World Landslide Forum* (pp. 381–384). 18-21 November. Tokyo, Japan: United Nations University. Retrieved from <https://ucanr.edu/sites/forestry/files/138028.pdf>
- Marchi, L., & Dalla Fontana, G. (2005). GIS morphometric indicators for the analysis of sediment dynamics in mountain basins. *Environmental Geology*, 48(2), 218–228. <https://doi.org/10.1007/s00254-005-1292-4>
- McCaffery, M., Switalski, T. A., & Eby, L. (2007). Effects of Road Decommissioning on Stream Habitat Characteristics in the South Fork Flathead River, Montana. *Transactions of the American Fisheries Society*, 136(3), 553–561. <https://doi.org/10.1577/T06-134.1>
- Miller, D. J., & Burnett, K. M. (2007). Effects of forest cover, topography, and sampling extent on the measured density of shallow, translational landslides. *Water Resources Research*, 43(3), 1–23. <https://doi.org/10.1029/2005WR004807>
- Miller, D. J., & Burnett, K. M. (2008). A probabilistic model of debris-flow delivery to stream channels demonstrated for the Coast Range of Oregon, USA. *Geomorphology*, 94(1–2), 184–205. <https://doi.org/10.1016/j.geomorph.2007.05.009>
- Miller, R. H. (2014). Influence of log truck traffic and road hydrology on sediment yield in western Oregon. Oregon State University in. Retrieved from <http://ir.library.oregonstate.edu/xmlui/handle/1957/49899>
- Montgomery, D. R., & Dietrich, W. E. (1994). A physically based model for the topographical control on shallow landsliding. *Water Resources Research*, 30(4), 1153–1171.

<https://doi.org/10.1029/93WR02979>

- O'Loughlin, E. M. (1986). Prediction of Surface Saturation Zones in Natural Catchments by Topographic Analysis. *Water Resources Research*, 22(5), 794–804.
<https://doi.org/10.1029/WR022i005p00794>
- Oldman Watershed Council. (2010). Oldman River State of the Watershed Report 2010. Lethbridge, Alberta. Retrieved from www.oldmanbasin.org
- Qin, C., Zhu, A. X., Pei, T., Li, B., Zhou, C., & Yang, L. (2007). An adaptive approach to selecting a flow-partition exponent for a multiple-flow-direction algorithm. *International Journal of Geographical Information Science*, 21(4), 443–458.
<https://doi.org/10.1080/13658810601073240>
- Rainato, R., Picco, L., Cavalli, M., Mao, L., Neverman, A. J., & Tarolli, P. (2017). Coupling Climate Conditions, Sediment Sources and Sediment Transport in an Alpine Basin. *Land Degradation and Development*. <https://doi.org/10.1002/ldr.2813>
- Ramos-Scharrón, C. E., & MacDonald, L. H. (2005). Measurement and prediction of sediment production from unpaved roads, St John, US Virgin Islands. *Earth Surface Processes and Landforms*, 30(10), 1283–1304. <https://doi.org/10.1002/esp.1201>
- Reid, L. M., & Dunne, T. (1984). Sediment production from forest road surfaces. *Water Resources Research*, 20(11), 1753–1761. <https://doi.org/10.1029/WR020i011p01753>
- Renard, K. G., Foster, G. R., Weesies, G. a., & Porter, J. P. (1991). RUSLE: Revised universal soil loss equation. *Journal of Soil and Water Conservation*, 46(1), 30–33. Retrieved from <http://www.jswconline.org/content/46/1/30.short>
- RStudio Team (2018). RStudio: Integrated Development for R. RStudio, Inc., Boston, MA URL <http://www.rstudio.com/>.
- Sawatzky, C. D. (2016). Information in support of a recovery potential assessment of Bull Trout (*Salvelinus confluentus*) (Saskatchewan – Nelson rivers populations) in Alberta. *DFO Can. Sci. Advis. Sec. Res. Doc.*, 2016/113(December).
- Schäuble, H., Marinoni, O., & Hinderer, M. (2008). A GIS-based method to calculate flow accumulation by considering dams and their specific operation time. *Computers and Geosciences*, 34(6), 635–646. <https://doi.org/10.1016/j.cageo.2007.05.023>
- Sugden, B. D., & Woods, S. W. (2007). Sediment Production From Forest Roads in Western Montana1. *JAWRA Journal of the American Water Resources Association*, 43(1), 193–206. <https://doi.org/10.1111/j.1752-1688.2007.00016.x>
- Tarboton, D. G. (1997). A new method for the determination of flow directions and upslope areas in grid digital elevation models. *Water Resources Research*, 33(2), 309–319.
<https://doi.org/10.1029/96WR03137>
- TerrainWorks Inc., & fRI, F. R. I. (2018). Identifying Unpaved Road Sediment Delivery to Critical Fish Habitats for Strategic Prioritization of Mitigation Actions in Alberta. Retrieved from www.terrainworks.com

- Thompson, C. J., Takken, I., & Croke, J. (2008). Hydrological and sedimentological connectivity of unsealed roads. In *Sediment Dynamics in Changing Environments* (pp. 524–531). Christchurch, New Zealand: International Association of Hydrological Sciences, IAHS Publ. 325, 2008.
- Trevisani, S., & Cavalli, M. (2016). Topography-based flow-directional roughness: Potential and challenges. *Earth Surface Dynamics*, 4(2), 343–358. <https://doi.org/10.5194/esurf-4-343-2016>
- Trevisani, S., & Rocca, M. (2015). MAD: Robust image texture analysis for applications in high-resolution geomorphometry. *Computers and Geosciences*, 81, 78–92. <https://doi.org/10.1016/j.cageo.2015.04.003>
- van Meerveld, H. J., Baird, E. J., & Floyd, W. C. (2014). Controls on sediment production from an unpaved resource road in a Pacific maritime watershed. *Water Resources Research*, 50(6), 4803–4820. <https://doi.org/10.1002/2013WR014605>
- Wemple, B. C., Jones, J. a, & Grant, G. E. (1996). Channel network extension by logging roads in two basins, western Cascades, Oregon. *Water Resources Bulletin*, 32(6), 1195–1207. <https://doi.org/10.1029/2002WR001744>
- White, B., Ogilvie, J., Campbell, D. M. H., Hiltz, D., Gauthier, B., Chisholm, H. K. H., ... Arp, P. A. A. (2012). Using the Cartographic Depth-to-Water Index to Locate Small Streams and Associated Wet Areas across Landscapes. *Canadian Water Resources Journal / Revue Canadienne Des Ressources Hydriques*, 37(4), 333–347. <https://doi.org/10.4296/cwrj2011-909>
- White, R. A., Dietterick, B. C., Mastin, T., & Strohman, R. (2010). forest roads mapped using LiDAR in steep forested terrain. *Remote Sensing*, 2(4), 1120–1141. <https://doi.org/10.3390/rs2041120>
- Wischmeier, W. H., & Smith, D. D. (1978). Predicting rainfall erosion losses. *Agriculture Handbook No. 537*, (537), 285–291. <https://doi.org/10.1029/TR039i002p00285>

Chapter 3. Sediment Connectivity Adjustment Based on LiDAR-derived DEM Terrain Roughness

3.1 Introduction

The heterogeneity in landscape morphology is recognized as being the most important factor controlling many processes on the landscape (Lane et al., 2009) and, in particular, it is the key variable for sediment dynamic assessments (Ahmad Fadzil et al., 2012; Brubaker et al., 2013; Trevisani and Cavalli, 2016). Landscape heterogeneity evaluation can be carried directly in the field and by image interpretation, however, field data collection can be costly and time-consuming, and image interpretation can lead to uncertainties in forested areas. Thus, Light Detection and Ranging (LiDAR) as a remote sensing method collects data using a pulsed laser to calculate distance ranges to the earth surface. The LiDAR data stored as cloud points provides landscape three-dimensional information shape and surface characteristics; this data can significantly improve the accuracy to distinguish features on the landscape and the topographic roughness measurement. The results can be better than in the traditional remote sensing data (White et al., 2010). The use of high-resolution LiDAR-derived DEMs has become a consistent approach in modeling sediment dynamics controlled by topography at the site and regional scales (Trevisani and Cavalli, 2016; Thomas et al., 2017). For example, the identification of sediment source and depositional areas, the evaluation of flow path conditions for sediment transportation downslope, and most importantly its connection to the stream network under the influence of topographic variables are remarkably important in watershed management (Bracken et al., 2007; Reid et al., 2007; Borselli et al., 2008; Foerster et al., 2014).

Topographic roughness can be defined as the surface subjected to differences in elevation and regulated by the slope (Whelley et al., 2014). Studies have suggested many methods to estimate topographic roughness. Examples of them are via residual topography (Cavalli et al., 2013), multiscale analysis (Ahmad Fadzil et al., 2011, 2012), fractal dimensions (Roy and Robert, 1990), semivariograms (Trevisani and Rocca, 2015), Likewise, other methods measure the standard deviation of elevation, variation of the slope, and curvature (Grohmann et al., 2011;

Brubaker et al., 2013), stream gradient variations (Benda et al., 2007), as well as the use of Manning's roughness coefficient (TerrainWorks and fRI, 2018).

Given the existence of a diverse variety of roughness methods, it can be problematic to calculate topographic roughness focusing on only one method since sediment dynamic is influenced by different topographic related variables. Therefore, taking into account the road supplies sediment to the streams, the problem lies in selecting the roughness method that is more adequate than others to improve road sediment production and road-stream sediment transportation. As far as it is known, an analysis of roughness methods has not been applied to the connectivity of the sediments generated from road surface erosion. The aim of this study is therefore to examine the following objectives: 1) Evaluate roughness methods from high-resolution LiDAR DEM applicable to road-stream sediment connectivity 2) Examine whether roughness methods optimize the performance of road-stream sediment connectivity predictions.

3.2 Overview of Topographic Roughness Modeling

3.2.1 Cell Size

Landforms can vary in size and shape (Berti et al., 2013). Therefore, the variation in cell size can greatly influence the estimates from a LiDAR-derived DEM compared to the field data. Changes in cell size, even if they are minimal, may underestimate or overestimate the results (Grohmann and Sawakuchi, 2013). For example, slope-based roughness that uses a DEM spatial resolution of 50 m may vary substantially from that with a cell size of 2 m (Brubaker et al., 2013).

3.2.2 Optimal Cell Size

Level of spatial resolution (cell size) in a raster is fundamental to capture the required detail of landform shapes and variations in the surface. Small cell size from a raster can display surface specific characteristics while large cell size can generalize the information. Thomas et al. (2017) and Cavalli et al. (2017) suggest that DEMs with 1 to 2 meters resolutions are optimal for estimating topographic roughness influence on sediment movement. Conversely, DEMs with spatial resolutions greater than 2 meters are considered inadequate when, for example, evaluating runoff generation areas, flow pathways, or hillslope conditions (Thomas et al., 2017).

High-resolution DEMs also have disadvantages. Small cell size and the highly detailed surface can interfere with the evaluation of certain topographic variables such as slope (Thomas et al., 2017). For example, a cell size of 0.25-meters may require to be resampled to a larger size to see major trends in slope differences at large extents.

3.2.3 Moving Window

The analysis of landscape morphology is generally linked to the use of cell neighborhood analysis for roughness estimates. By means of neighborhood analysis, a new value is estimated for the cell of interest based on the values of its neighbors (Grohmann and Riccomini, 2009). The new value of the cell depends very much on the statistical function and the neighborhood size applied to it (Grohmann and Riccomini, 2009). The mean, the standard deviation, and the range are the statistical functions commonly used for neighbor operations.

According to the literature, there is no optimal window size; it depends on the object size. Thus, some sizes for the neighborhood can include 3 m x 3 m, 5 m x 5 m (Cavalli et al., 2013), and in some cases up to 10 m x 10 m when it is required to highlight in much more detail the surface variability.

3.3 Methods and Materials

3.3.1 Study Area

For the evaluation of the influence of roughness on sediment connectivity components (upslope and downslope), I have considered the same study area detailed in the previous chapter which consists of eight sub-basins located on the eastern slopes of the Rocky Mountain foothills in the Oldman Basin (Figure 2 -7). For the comparative analysis between the field values and the roughness-weighted values, I have considered the 196 sampling sites (Table 2-5) located throughout the sampling area (Figure 2-8).

3.3.2 Data Source

For this research, I utilized cloud points LiDAR data in log ASCII standard format (.LAS). The dataset was provided by the Government of Alberta through the Alberta Environment and Parks – Informatics Branch under the DMR# 1704M08 (GOA, 2018). From the cloud points dataset, I extracted only those points representing ground (2) and low vegetation (3) classification codes.

The LiDAR point density ranged between 0.95 - 1.51 for ground and between 2.12 - 7.80 for low vegetation (Table 3-1). All the data has been processed and managed to operate the ArcGIS Desktop platform v10.6.1 (Esri, 2018). All data were stored as raster datasets using the Universal Transverse Mercator's projection (UTM) Zone 12, North American Datum (NAD) 1983. The classification codes 2 and 3 served as the input data to create the DEM and DSM (digital surface model) surfaces.

To create the corresponding DEM and DSM raster datasets, I performed the following procedure employing ArcMap v10.6.1 (Esri, 2018):

- *For the DEM*, I executed the process of converting the discrete elevation data points from LiDAR to a continuous dataset. Therefore, using a minimum cell assignment based on the point dataset attributes (Table 3-1), the ground (2) points were the input to create a surface using a triangulated irregular network (TIN) interpolation method. I utilized a sampling cell size of a 1-meter to create the DEM (Table 3-1).
- *For the DSM*, the operation focused on the ground (2) and low vegetation (3) classification codes. Due to the particularities of the present study, coded points (3) were filtered by a maximum of 1 meter in elevation. Subsequently, applying the average cell assignment as per the attributes of the point dataset (Table 3-1) points coded (2) and (3) were interpolated at a sampling interval of 1 meter. Points were interpolated using the TIN model.

I used the TIN model to generate the DEM and DSM because the TIN model bases the creation of a topographic surface on a network of triangles from unstructured points (Esri, 2018). To conform to the triangles representing the surface morphology as close as possible to reality, researchers have used breaklines (linear features) and exclusion boundaries to intensify and improve the TIN interpolation (Tsai, 1993). Commonly, the Delaunay method is widely used to create connected and a non-overlapping triangles from non-ordered points (Tsai, 1993; Hill et al., 2002; Hoja et al., 2005; Alexander, 2009; Esri, 2018); therefore, I used this method as a constraint when executing the TIN interpolation model in ArcGIS.

3.3.3 Modeling

Roughness has been defined in a variety of manners, some researchers based roughness on the variabilities in elevation values (Haneberg et al., 2005; Cavalli and Marchi, 2008; Grohmann et al., 2011) and others on the slope variations (Frankel and Dolan, 2007). Therefore, there have been employed a variety of methods for quantifying the amount of terrain variation and most of them have applied the standard deviation (SD) function (Shepard et al., 2001; Mitasova and Iversonf, 1996; Grohmann et al., 2011). Commonly, the well-known importance of SD lies in the fact that it represents the degree of dispersion of the values from the mean. In terms of DEM cells, this dispersion can be measured within a certain size of neighboring cells.

I based the roughness modeling methods on the variability of the terrain cell values and the vegetation component using 1-meter DEM and DSM, respectively. In this study, I evaluated three methods to compute topographic roughness considering the differences in elevation, slope, and aspect and used the SD as a statistical function. Additionally, in order to examine the vegetation effects on sediment movement, I included a fourth method which corresponds to the SD of vegetation height for above ground roughness estimation. The roughness resulting values were used as weighting factors to evaluate the possible fluctuations in the production of road surface sediment and its transfer downslope in relation to field values.

The roughness resulting values were used as weighting factors to evaluate the possible fluctuations in the production of road surface sediment and its transfer downslope in relation to field values. In this sense, the procedure I performed to calculate the SD-roughness types by using LiDAR DEM is presented below.

Standard Deviation of the Elevation

To estimate the SD of elevation-based roughness, I used the focal statistics tool in ArcMap. A moving window of 3 by 3 cell was applied to a pit-filled DEM using the SD function. I selected the 3 by 3 relative window size because a small windows size can difficult to see the variabilities in elevation while a large size would generalize the details.

Standard Deviation of the Residual Topography

As it was intended to compare the findings with other roughness methods; I considered adequate to use the same window size as in the previous calculation. The procedure involved, first, in averaging the pit-filled DEM by using a 3 by 3 moving window. To calculate the residuals in elevation, the smoothed DEM was subtracted from the original DEM (Haneberg et al., 2005; Trevisani and Cavalli, 2016). By employing the focal statistics tool in ArcMap, I applied a 3 x 3 moving window to the new raster and used the SD function to calculate the SD of the residual topography.

Standard Deviation of the Slope & Aspect

This roughness method was based on the directional statistics distribution of slope and aspect. Mitasova and Iversonf (1996) suggested the use of the directional derivative to evaluate changes in the flow direction for sediment transport. By using this method, it is calculated the directional mean angle between the slope and aspect. I selected this method to calculate the topographic roughness because slope and aspect can potentially influence the flow direction and therefore its movement downhill (Mitasova and Iversonf, 1996).

The SD of slope & aspect roughness was computed employing a previous pit-filled DEM, the procedure involved the following steps:

1. I used the method for directional distribution data analysis in (Marr, 2014) and adapted it to be applicable to a DEM. The direction can be described as the mean vector between x and y . Where φ represents the mean direction angle (Figure 3-1).

$$r = (x, y) = (\cos \varphi, \sin \varphi) \quad (Eq. 1)$$

From the pit-filled DEM, I calculated the $\cos \varphi$ and $\sin \varphi$ by the means of the aspect and slope, respectively (Figure 3-1).

$$X = \frac{\sum_{i=1}^n \cos \varphi}{n}, Y = \frac{\sum_{i=1}^n \sin \varphi}{n} \quad (Eq. 2)$$

$$r = \sqrt{X^2 + Y^2} \quad (Eq. 3)$$

2. After calculating the slope and aspect rasters. I computed $\cos \theta$ for the aspect and the $\sin \theta$ for the slope.

$$\cos \theta = \frac{X}{r} \quad , \quad \sin \theta = \frac{Y}{r} \quad (Eq. 4)$$

3. Thus, to obtain the directional mean angles θ , the angles between the mean vector r and the aspects were normalizing by the slope using the method in (Mitasova and Iversonf, 1996).

$$r = -aspect \times \cos \theta - slope \times \sin \theta = -1 \quad (Eq. 4)$$

A negative value is assigned to r when it concurs the aspect indicating downslope direction. Thus, the slope values are negative increasing the sediment movement capacity (Mitasova and Iversonf, 1996). However, when r opposes the aspect, it assumes negative values indicating upslope direction. Thus, the slope values are positively reducing the sediment movement capacity $r = \cos^2 \theta + \sin^2 \theta = 1$ (Mitasova and Iversonf, 1996).

4. Using the previous slope and aspect derivative raster, it was generated the SD of the slope and aspect by applying 3 by 3 moving window (Purves, 2016).

Standard Deviation of the Vegetation Height

Approaches to evaluating the surface roughness have based on the aerodynamic length (Z_0) of the vegetated surfaces, where Z_0 is assessed as a function of the height, shape, and density of the vegetation (Menenti and Ritchie, 1994; Hammond et al., 2012). Nield et al. (2013) in their work highlights that the height of surface roughness has good performance ($r^2 > 0.79$) compared to other complex roughness metrics. However, due to the vegetation heterogeneity, its estimation means a challenge (Raupach, 1994; Hammond et al., 2012). The standard deviation of the distribution height of the surface is considered to be as one of the simplest ways to characterize vegetation roughness (Nield et al., 2013; Faivre et al., 2017).

Studies have suggested that vegetation height can be obtained by subtracting the DTM from the DSM (Hammond et al., 2012; Chen et al., 2015; Faivre et al., 2017). In this study, I used the codes 2 (ground) and 3 (low vegetation) to represent the DSM from the cloud points. In the study area, grass plants, grass-like plants, forbs, shrubs can be commonly found along the roads and hillslopes (Government of Alberta, 2016). Therefore, from the cloud points, I selected low vegetation up to a maximum of 1 meter in height. Using the resulting raster, I employed the SD function to obtain the variation in height by applying the same moving window of 3 x 3 cell as in the previous roughness methods.

3.4 Results

3.4.1 Sediment production

Sediment production was normalized by using different roughness methods. (Table 3-2). To evaluate the results, I also included the MAD flow-directional roughness calculated in the previous chapter (Table 3-2). When applying the roughness factor, the average sediment production ranged from approximately 51.84 m³ (SD-Elev. roughness) to 57.58 m³ (SD-ResTop roughness). If it is compared to the non-roughness of 68.29 m³ and field production estimates of 43.76 m³, the average production, when weighed by roughness, were, in general, ranging approximately from 50 to 60 m³ (Table 3-2). When looking at the minimum sediment production weighted by roughness, values ranged from 2 to approximately 3 m³ at the sites, while the maximum production did not surplus the 260 m³ (SD-Slope&Aspect roughness). In general, the predicted sediment production can be explained by an average deviation of 44% respect to their corresponding average production estimates (Table 3-2). At a 95% confidence interval, the weighed sediment production and field estimates correlation ranged from 66 to 77% whereas the none-weighted production had a 64%. It can suggest that predicted values are closely around the fitting line which can be confirmed visually in Figure 3-2. Even though the presence of some outliers approximately above 150 m³, sediment production model populated better below 100 m³ when using the different roughness models (Figure 3-2 and 3-3). From this, it can be noted that the MAD flow-directional roughness had a good performance in relation to the other roughness models, which explains that about 77% of the predicted sediment production values were close to their field counterparts (Figure 3-2).

3.4.2 Sediment plume length

Plume traveling distance from the road was estimated based on the application of the different roughness (Table 3-4). In this section, I considered the vegetation roughness as part of the plume length modeling (downslope component). It can be noted that vegetation roughness was not used as a weighting factor for sediment production (upslope component) as vegetation are generally removed from roads surfaces. From field observation, hillslopes were generally populated by shrubs, grass and some aspen trees bordering the roadways. Therefore, as mention in the methods section, I considered a threshold of 1-meter of vegetation height as a potential impediment for sediment plume traveling rather than tree species. Additionally, in the field, there were found that most of the sites either did not have evidence of sediment plumes or they were short in length. Therefore, I used N=51 considering sediment plumes from the road surface and a few numbers of sediment plumes from cutslope (n=7) to compare them against the DEM predicted plume lengths. Results showed that sediment plume average length weighed by roughness ranged from 2.10 m (SD-Veg.Height roughness) to 5.68 m (SD Slope&Aspect roughness) compared to the average of 8.42 m from the field (Table 3-4). It suggests, for example, that 55.3 m³ of average sediment production using SD Slope&Aspect roughness (Table 3-2) can travel an approximate average of 5.68 m downslope (Table 3-4). Given the fact that sediment plumes in the field were short in length (Figure 3-4), at the site scale, it can be assumed that under the influence of slope and aspect a good amount of the 55.3 m³ (large particles) was probably stored along the way and only fines had the possibility to travel 5.68 m. Additionally, in this study, I did not consider sediment particle size as all the predictions based only on the DEM metrics.

The fitting statistics showed that sediment plume length normalized by the SD-Slope&Aspect roughness has the highest correlation of 64% with field sediment plume length (Figure 3-4). For the rest of sediment plume length models, there was an average of approximately 60% of correlation with field data. However, the lowest correlation with field data happened when DEM sediment plume length was not pondered by impedance factor (no-roughness) with 46% (Table 3-5). Therefore, the results on sediment plume length indicated that roughness factor played an important role in determining either the sediment plume traveling distance increase or decrease from the road surface.

3.4.3 Sediment Connectivity

Sediment connectivity represents the fraction between the upslope and downslope components (Borselli et al., 2008; Cavalli et al., 2013). In the present study, that is, the amount of sediment that has been produced from the road surface and its traveling distance from the road becoming a sediment plume. For the purpose of comparison between the connectivity data from the field and DEM, I used N=44 sites from the field (road surface) and their corresponding counterparts from the DEM.

Exploring the results obtained from the roughness performance, sediment connectivity values mostly populate the range between the first and third quartile, that is, from approximately between 0.45 and 0.85 units (Figure 3-5). Among the group of roughness that has been considered for road-stream sediment connectivity estimation, the DEM SD-Slope&Aspect roughness-based connectivity spans a wider interval between the first and third quartile, approximately 0.35 and 0.90 units, respectively. From this exploration, when relating those approximations to the connectivity classification in Carson et al. (2009), it can be assumed that in the sampling area, road sediment is between “a half” and “a lot” connected to streams. Likewise, by exploring the data, the roughness models predicted an average connectivity of 0.6 units (Table 3-4 and Figure 3-5). Consequently, it indicates that roads in the sampling area go on average from “a half” to potentially “a lot” connected (Carson et al., 2009).

On the other hand, by exploring the results in more detail, when it was believed the path has no surface irregularities (DEM No-roughness), the sediment connectivity values presented the lowest capacity to fit the field data ($r^2=0.46$). In Figure 3-5, that is, approximately near the second quartile 46 - 50%. On the other hand, the sediment connectivity predicted by using the DEM SD-Slope&Aspect roughness had more capabilities of fitting the field connectivity by approximately 66% (Figure 3-5) which can be confirmed in Table 3-3.

From these results, it can be noted that roughness certainly plays an important role in the estimation of sediment production, transportation, and connection to streams. Supporting this view, in the Appendix section of the present chapter, the results of the application of two roughness: the DEM SD-Slope&Aspect and the MAD flow-directional roughness can be visualized and compared on the maps.

3.5 Discussion

As in Borselli et al. (2008) and Cavalli et al. (2013), sediment connectivity is computed by the means of the sediment production and the transportation capacity weighed by a roughness factor. In this study, I evaluated different roughness and examined whether they improve the performance of the predictions of the sediment production from road surface (upslope) and sediment plume length downhill (downslope) (Figure 3-5). A same type of roughness was applied both the upslope and a downslope component of connectivity as in Borselli et al. (2008) and Cavalli et al. (2013). To the best of my knowledge, no other authors have specifically applied roughness to predict sediment generation from road surfaces. However, as per the statistics I obtained for the different roughness applications, I believe that there can be still an improvement on the results by applying different roughness to the connectivity components rather than only one. In this sense, in my view, there are important aspects that I consider important to support this idea:

- 1) For the sediment production, when applying the DEM SD-Slope&Aspect roughness as a weighting factor, it provided a low correlation ($r^2=0.66$) in relation to others as can be noted in Figure 3-2 and Table 3-3. On the contrary, by applying the MAD flow-directional roughness, the sediment production values were significant ($r^2=0.77$) (Figure 3-2 and Table 3-3). Although the MAD flow-directional roughness (Trevisani and Rocca, 2015) was meant to evaluate the upslope component in alpine environments, it performed well when applied to OHV trail surfaces in the Oldman watershed study area. The roads studied have characteristics of steep gradients and remarkable topographic variabilities because of its location in the mountainous part of the Oldman watershed (Rocky Mountains).
- 2) For the sediment plume length, the DEM SD-Slope&Aspect roughness had the highest performance predicting the sediment plume traveling distance ($r^2=0.64$) in relation to other roughness models such as the MAD flow-directional roughness (Figure 3-4 and Table 3-5). MAD flow-directional bases its computation on the differences in elevation (topographic flow-directional) which is closely related to slope; however, by using the standard deviation on the slope and aspect gave also good approximations. Grohmann et al. (2011) also noted that roughness based on the standard deviation of the slope has

good capabilities to differentiate fine scale and regional relief at different scales. From the results I obtained for the downslope component, it can be implied that sediment transportation in the area is likely a slope flow-directional driven process.

Consequently, these aspects were the reason why I applied a combination of roughness to sediment connectivity. In this study, this combination was called MSA (proposed) roughness. The sediment connectivity based on the MSA roughness represents the sediment production weighed by MAD flow-directional roughness and the sediment plume length weighed by the DEM SD-Slope&Aspect.

By using MSA roughness, I obtained an improvement in the estimation of sediment connectivity in approximately 0.1 to 0.05 units with respect to the sole application of DEM SD-Slope. Moreover, the statistics supporting the combined roughness indicated that the sediment connectivity model fits the correlation line by 73% considering an $\alpha < 0.05$ (Figure 3-6 and 3-7) and deviates from the average by 30% (Table 3-4).

3.6 Conclusion

In this chapter, considering the sampling area located within the Oldman watershed, road-stream connectivity refers to the ratio between the sediment production from the road and the potential for the sediment to travel a certain distance downslope under the influence of impediment factors. Constraining factors values were evaluated by means of DEM metrics. Thus, MAD flow-directional roughness (Trevisani & Rocca, 2015) was used as a weighting factor to predict sediment production while the SD-Slope&Aspect roughness was employed for the sediment plume distance predictions. The topographic roughness estimation should be considered as a careful procedure in terms of the raster cell size, the moving window size, and type of statistic function utilized (mean or deviation standard). Additionally, the variables that are being considered to calculate the roughness values based on such as the slope, elevation, and flow direction also matters.

Therefore, I believe the procedure I present in this study can help calculate roughness values for sediment connectivity assessments in different study areas.

Tables and Figures

Table 3-1. LAS point characteristics for ground and low vegetation. Ground points correspond to class=2 and low vegetation to class=3; they were used to create the DEM and DSM raster datasets, respectively, for each of the sub-basins.

Sub-Basin	Class	Pt Count	Pt Spacing (Pt/m)	Pt Density (Pt/m ²)	Z Min (m)	Z Max (m)
Allison	2	9759197	1.51	0.44	1519.15	1895.07
	3	4514046	2.22	0.2	1519.31	3083.81
Dutch	2	19158791	1.33	0.57	1635.81	2005.48
	3	5409495	3.02	0.11	1636.38	3049.35
Girardi	2	3232880	1.31	0.58	1346.47	1970.32
	3	1242469	2.12	0.22	1346.74	2702.41
Livingstone	2	72136884	1.14	0.77	1729.62	2176.64
	3	3292526	5.45	0.03	1730.29	2175.66
Race Horse	2	76497429	1.45	0.48	1598.02	1991.04
	3	30227332	2.37	0.18	1598.36	2977.45
Star	2	8960052	1.37	0.53	1408.64	1858.12
	3	3387393	2.24	0.2	1409.03	3644.26
Trout	2	37598212	0.95	1.11	1388.15	1704.41
	3	565445	7.8	0.02	1389.09	1704.71
Upper Oldman	2	36406599	1.06	0.89	1578.22	2051.6
	3	1374083	5.5	0.03	1578.99	2051.39

Table 3-2. Summary of exploratory data analysis for sediment production weighed by roughness.

Statistics	Field Sed.Prod	DEM Sed.Prod (No roughness)	DEM Sed.Prod (MAD roughness)	DEM Sed.Prod (SD Elev. roughness)	DEM Sed.Prod (SD ResTop. roughness)	DEM Sed.Prod (SD Slope&Aspect roughness)
Stand Dev	38.85	57.88	44.04	39.19	43.38	49.56
Mean	43.76	68.29	56.97	51.84	57.58	55.30
n	196.00	196.00	196.00	196.00	196.00	196.00
Median	32.58	52.44	46.32	41.59	48.06	39.46
Coeff of Variation	0.89	0.85	0.77	0.76	0.75	0.90
Minimum	1.80	3.01	2.95	2.93	2.96	2.50
Maximun	196.86	292.39	202.31	185.03	226.58	259.45

Table 3-3. Correlation statistics for sediment production normalized by roughness against the field sediment production estimates.

Relationship	r ²	RSE	F-Statistic	P-Value	Df	Df Residual
DEM Sed.Prod (No roughness) ~ Field Sed.Prod	0.64	34.50	355	9.86E-46	2	194
DEM Sed.Prod (MAD roughness) ~ Field Sed.Prod	0.77	20.80	682	1.96E-65	2	194
DEM Sed.Prod (SD Elev. roughness) ~ Field Sed.Prod	0.70	21.50	456	7.60E-53	2	194
DEM Sed.Prod (SD ResTop. roughness) ~ Field Sed.Prod	0.76	21.10	628	9.68E-63	2	194
DEM Sed.Prod (SD Slope&Aspect roughness) ~ Field Sed.Prod	0.66	29.00	377	2.44E-47	2	194

Table 3-4. Summary of statistics for sediment plume length weighed by roughness.

Statistics	Field PLength	DEM PLength (No roughness)	DEM PLength (MAD roughness)	DEM PLength (SD Elev. roughness)	DEM PLength (SD ResTop. roughness)	DEM PLength (SD Slope&Aspect roughness)	DEM PLength (SD Veg.Height roughness)
Stand Dev	8.75	2.40	2.82	2.89	2.86	6.34	2.92
Mean	8.42	2.45	2.22	2.26	2.24	5.68	2.10
n	51.00	51.00	51.00	51.00	51.00	51.00	51.00
Median	4.70	1.64	0.98	1.00	0.98	2.87	0.87
Coeff of Variation	1.04	0.98	1.27	1.28	1.28	1.12	1.39
Minimum	0.30	0.16	0.05	0.05	0.05	0.24	0.00
Maximun	37.40	10.37	11.13	11.29	11.14	27.40	11.14

Table 3-5. Correlation statistics for sediment plume length normalized by roughness against the field sediment plume length estimates.

Relationship	r²	RSE	F-Statistic	P-Value	Df	Df Residual
DEM PLength(No roughness)~Field PLength	0.46	1.78	41.9	4.29E-08	2	49
DEM PLength (MAD roughness)~Field PLength	0.61	1.78	76.8	1.33E-11	2	49
DEM PLength (SD Elev. roughness)~Field PLength	0.61	1.84	74.1	2.28E-11	2	49
DEM PLength (SD ResTop. roughness)~Field PLength	0.61	1.81	75.2	1.83E-11	2	49
DEM PLength (SD Slope&Aspect roughness)~Field PLength	0.64	3.82	88.9	1.36E-12	2	49
DEM PLength(SD Veg.Height roughness)~Field PLength	0.58	1.93	65.5	1.38E-10	2	49

Table 3-4. Summary of statistics for road-stream sediment connectivity weighed by roughness.

Statistics	Field Connectivity	DEM Connectivity (No roughness)	DEM Connectivity (MAD roughness)	DEM Connectivity (SD Elev. roughness)	DEM Connectivity (SD ResTop. roughness)	DEM Connectivity (SD Slope&Aspect roughness)	DEM Connectivity (SD Veg.Height roughness)	DEM Connectivity (MSA proposed)
Stand Dev	0.30	0.30	0.31	0.31	0.31	0.33	0.32	0.30
Mean	0.50	0.61	0.61	0.61	0.62	0.59	0.61	0.60
n	44.00	44.00	44.00	44.00	44.00	44.00	44.00	44.00
Median	0.50	0.63	0.64	0.63	0.64	0.60	0.66	0.61
CoeffofVariation	0.63	0.50	0.51	0.50	0.49	0.55	0.52	0.51
Minimum	0.00	0.00	0.00	0.00	0.00	0.00	0.00	0.00
Maximun	1.00	1.00	1.00	1.00	1.00	1.00	1.00	1.00

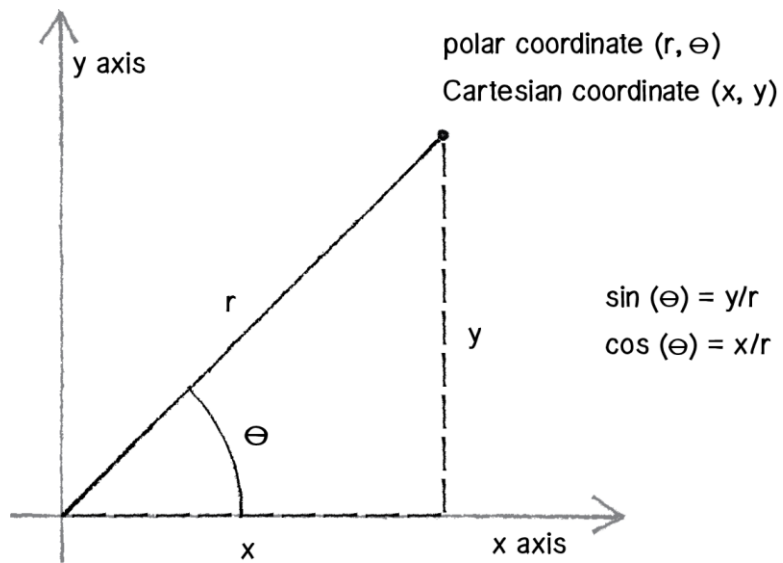


Figure 3-1. Cartesian polar coordinate used to define the angular derivatives to calculate the Slope & Aspect roughness. Figure adapted from <https://cdn.kastatic.org/ka-perseus-images/1559d8785a298fdd0bac0443388b3812c4327ec3.png>

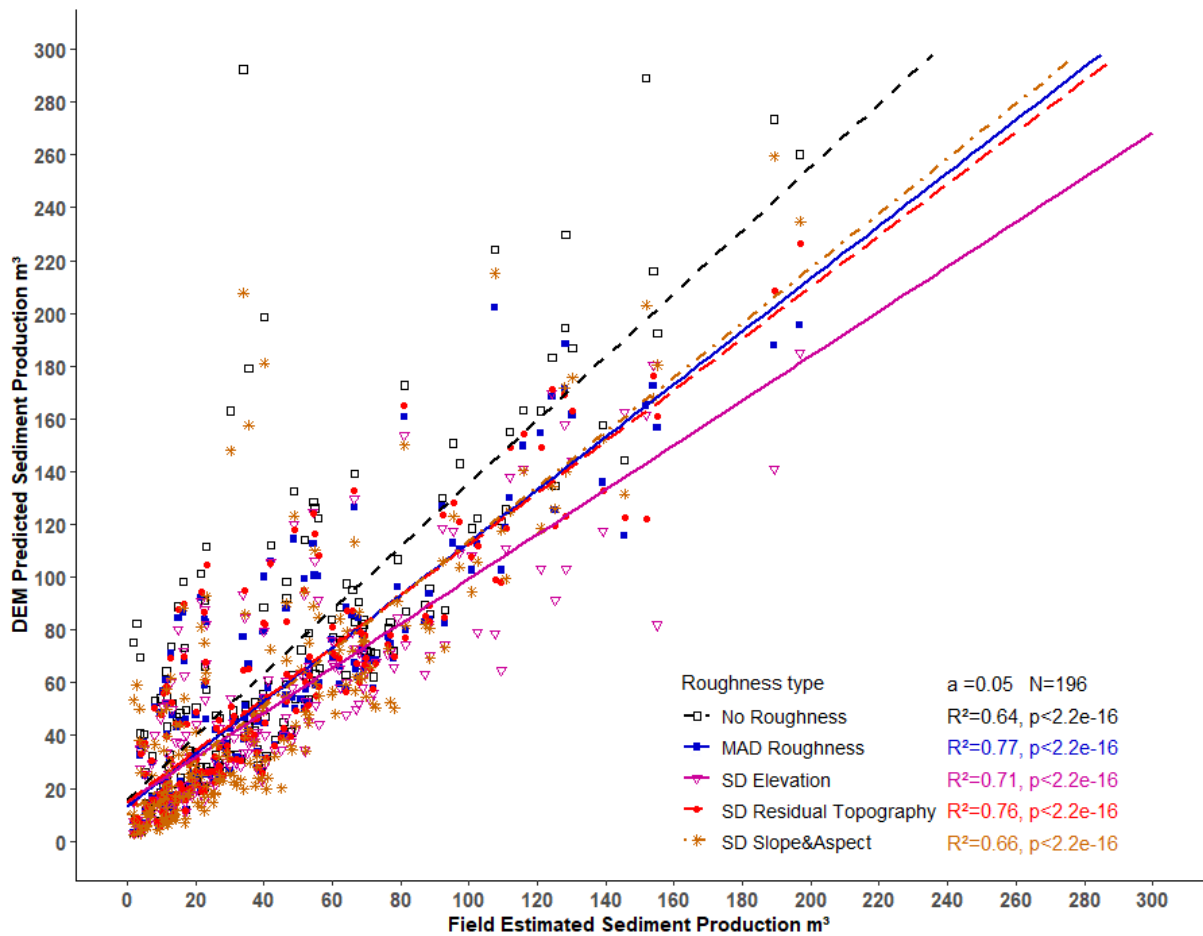


Figure 3-2. Road surface sediment production normalized by using different DEM-derived roughness. The predicted values are contrasted with the field values to evaluate their corresponding statistical correlation within a confidence interval of 0.05 for N = 196.

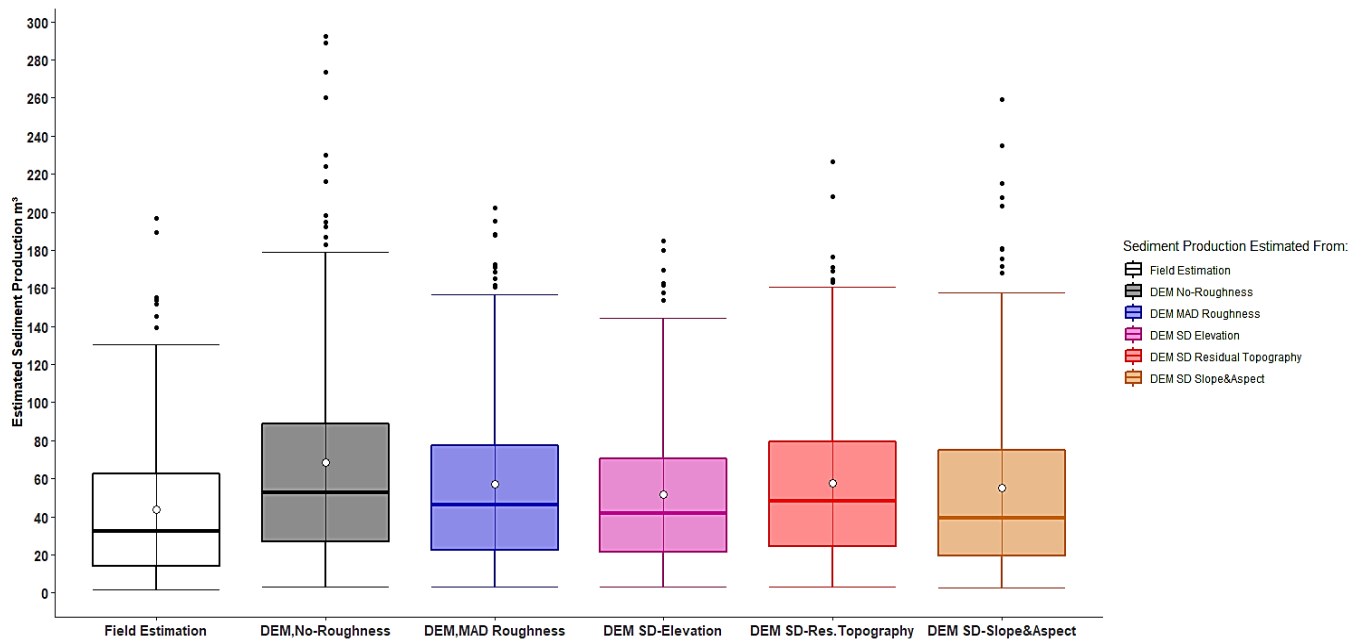


Figure 3-3. Approximate sediment production from road surface (m³) using different DEM-derived terrain roughness, which is compared with the amount of sediment produced in the field (m³).

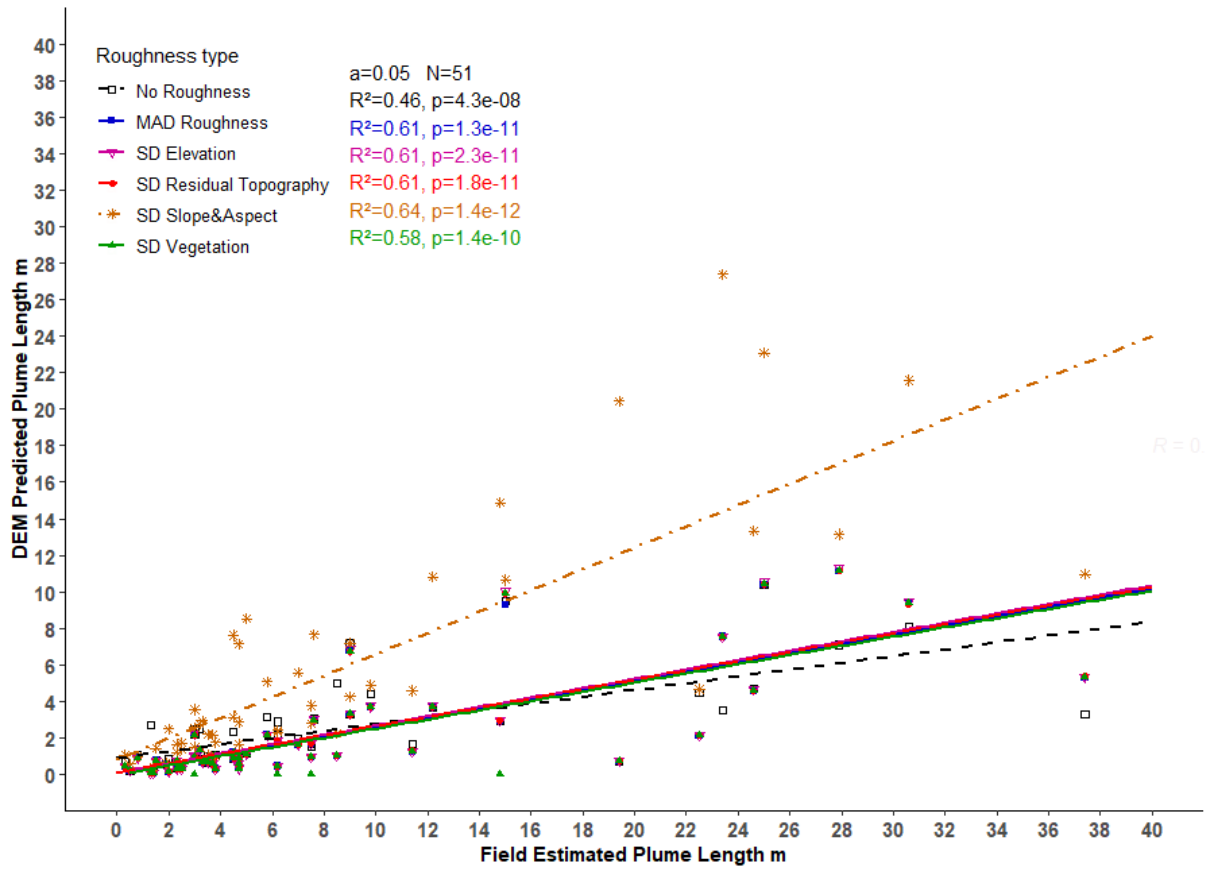


Figure 3-4. Sediment plume traveling distance from road surface normalized by using different roughness. The DEM-derived terrain roughness and the vegetation roughness obtained from DSM are contrasted with the field values to evaluate their corresponding relationship within a confidence interval of 0.05 for N = 51.

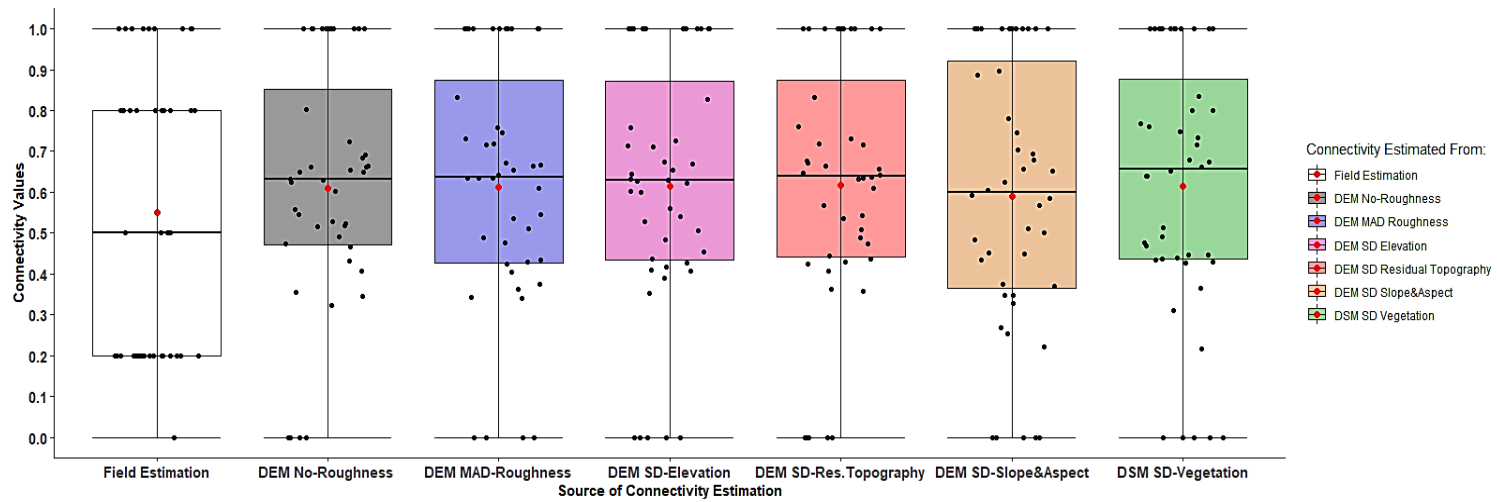


Figure 3-5. Prediction of road-stream sediment connectivity as a result of using DEM terrain and DSM vegetation roughness. Values of connectivity range from 0 (not – connected) to 1 (connected); these values are compared with the field estimated values.

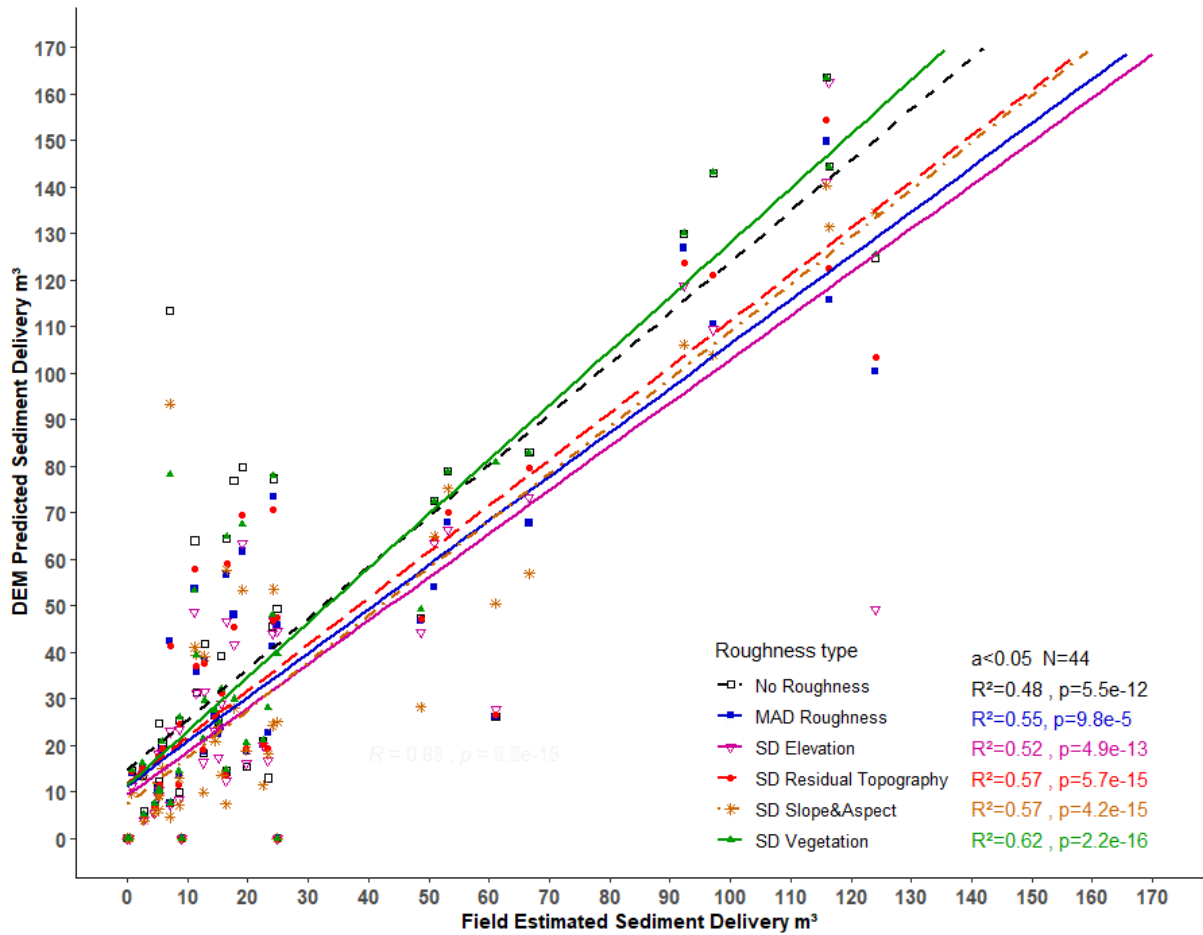


Figure 3-6. Approximates of road surface sediment delivery (m³) by using DEM terrain and DSM vegetation roughness. The predicted values are compared with the field values to assess their correlation within a confidence interval of 0.05.

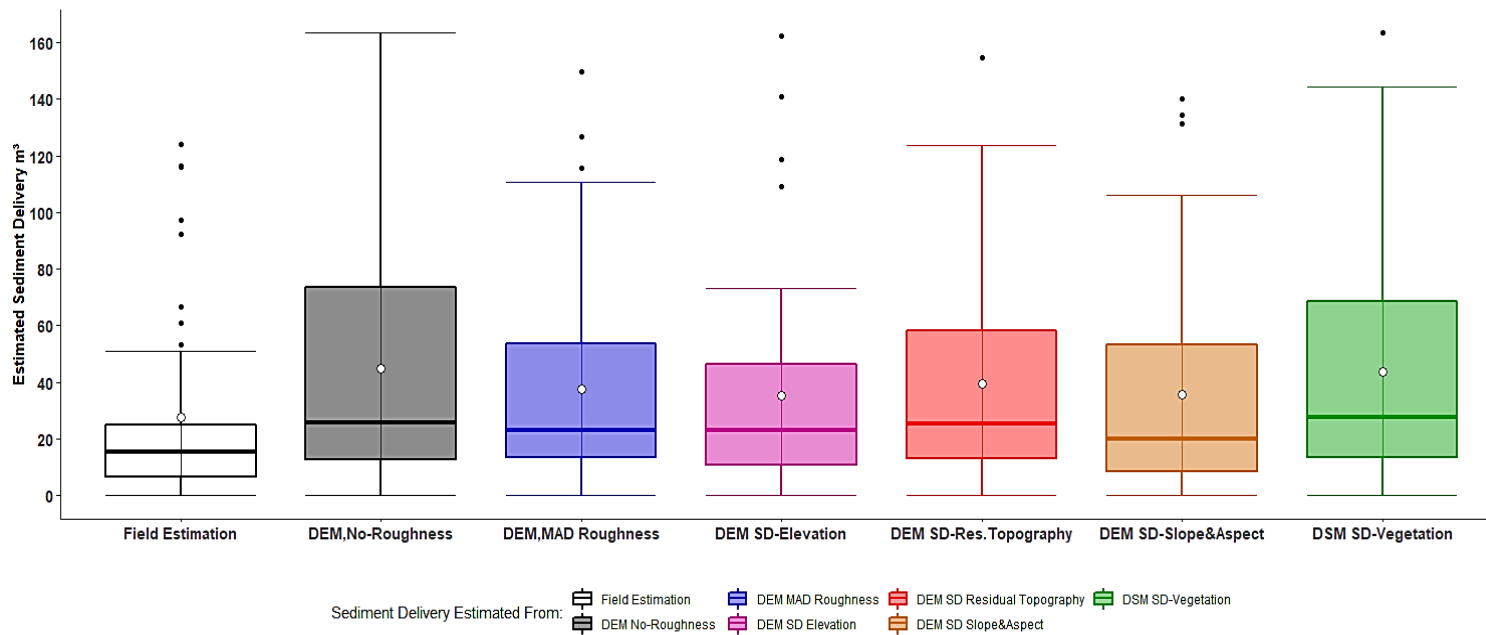


Figure 3-5. Approximate values of road sediment delivery in relation to the delivery from the field by using DEM and DSM roughness.

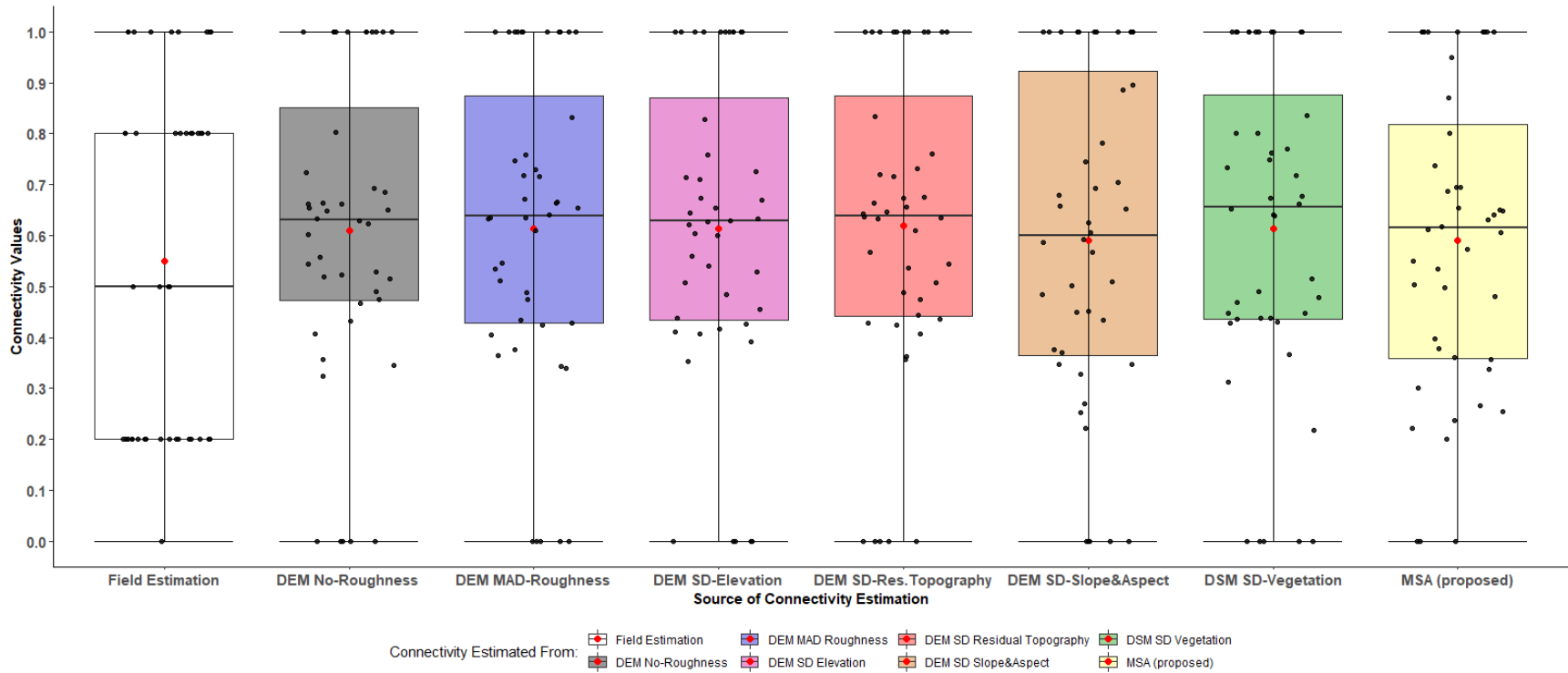


Figure 3-6. Sediment connectivity per type of roughness including the MSA roughness. MSA (proposed) represents the connectivity by combining the DEM MAD-Roughness for upslope component (sediment production) and the DEM SD-Slope&Aspect roughness for downslope component (sediment plume traveling distance).

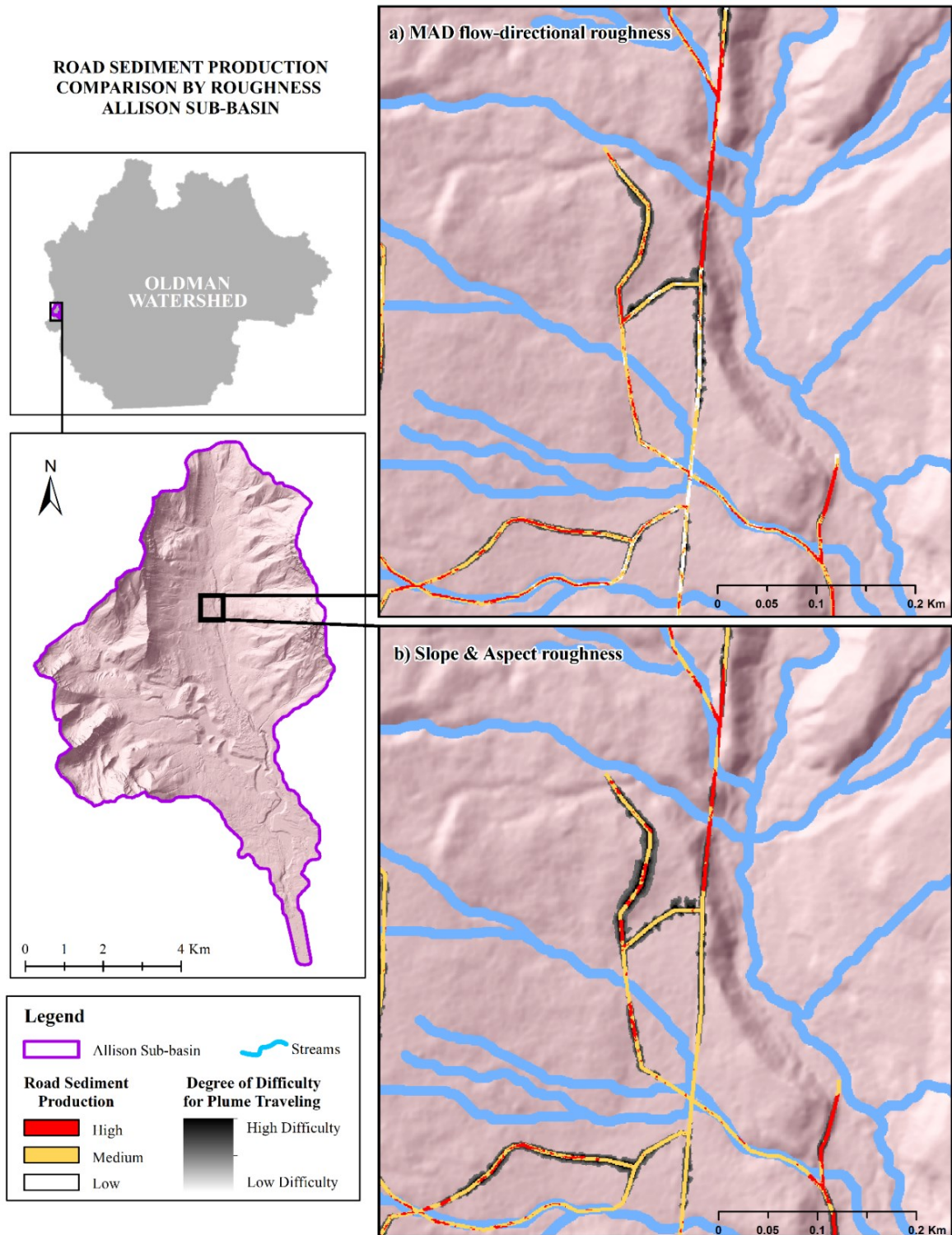


Figure 3-7. Allison Sub-basin. Road sediment production comparison using the Mad flow directional roughness and the Slope & Aspect roughness (directional statistics). For visualization purposes, roughness weighed sediment production was classified in high (red), medium (light orange), and low production (white). Similarly, the sediment plume traveling distance from the road surface is portrayed by a level of difficulty for sediment movement to streams: no movement (black ramp) and potential for movement (gray – or no color).

**ROAD-STREAM SEDIMENT CONNECTIVITY
COMPARISON BY ROUGHNESS
ALLISON SUB-BASIN**

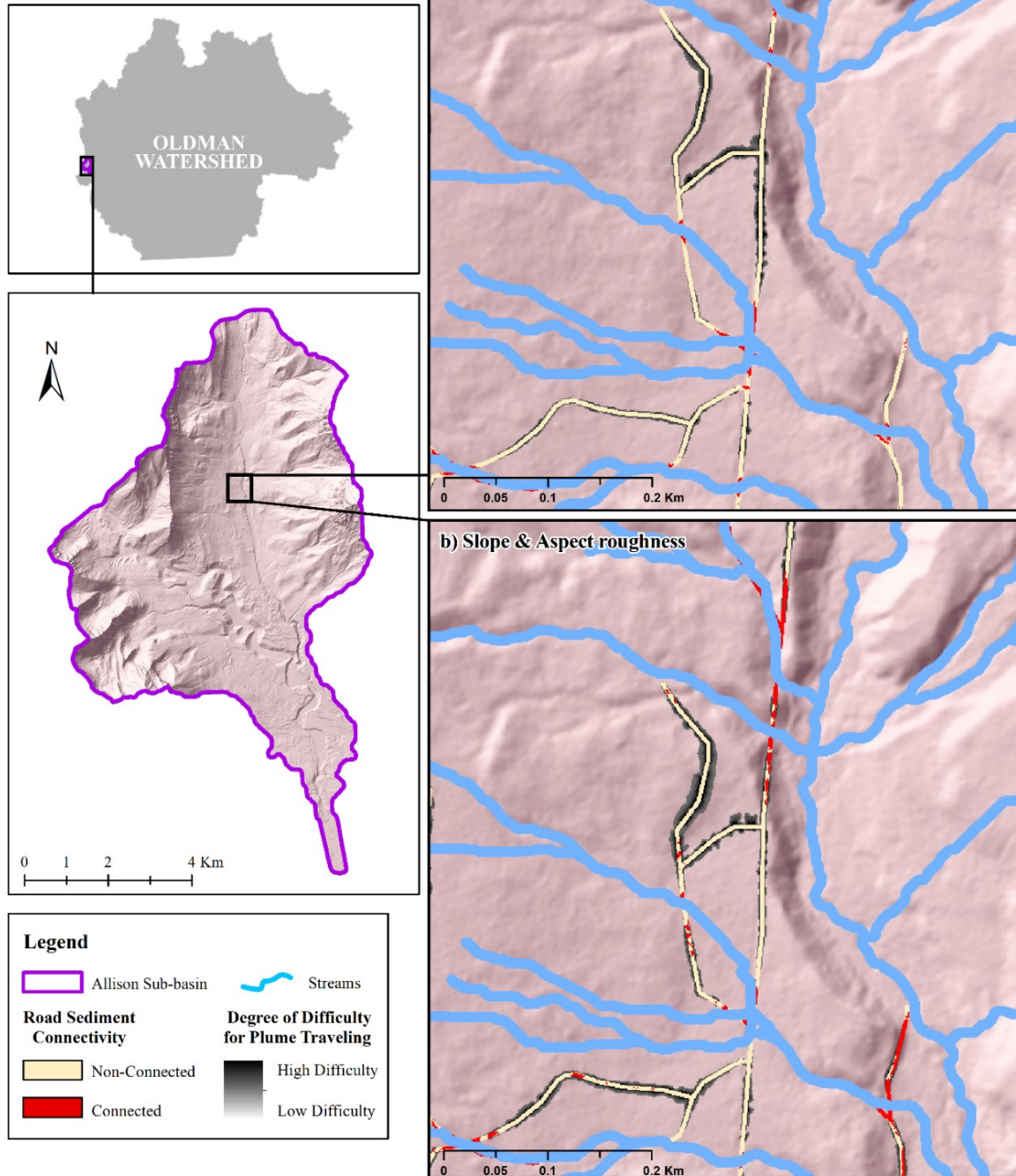


Figure 3-8. Allison Sub-basin. Sediment connectivity comparison using the Mad flow directional roughness and the Slope & Aspect roughness (directional statistics). Roughness weighed Sediment connectivity was classified in connected (red) and non-connected (light orange) for easy visualization in the present map. The black and grey ramp shows the level of traveling difficulty for sediment plume departing from the road surface and reaching the streams: no movement (black ramp) and potential for movement (gray – or no color).

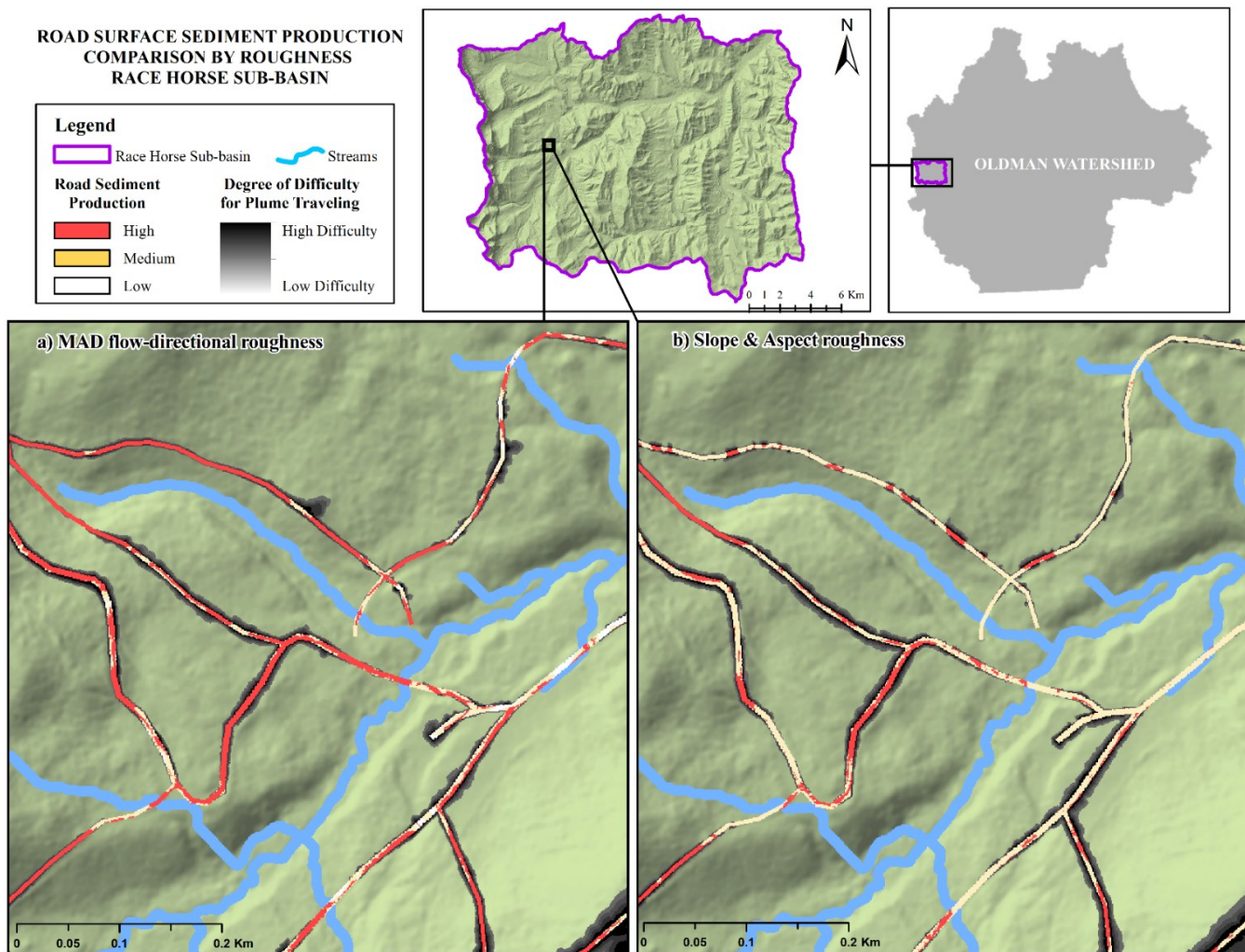


Figure 3-9. Race Horse Sub-basin. Road sediment production comparison using the Mad flow directional roughness and the Slope & Aspect roughness (directional statistics). For visualization purposes only, roughness weighed sediment production was classified in high (red), medium (light orange), and low production (white). The sediment plume length is represented by the back -grey ramp showing the level of difficulty for sediment movement to streams: no movement (black ramp) and potential for movement (gray or no color).

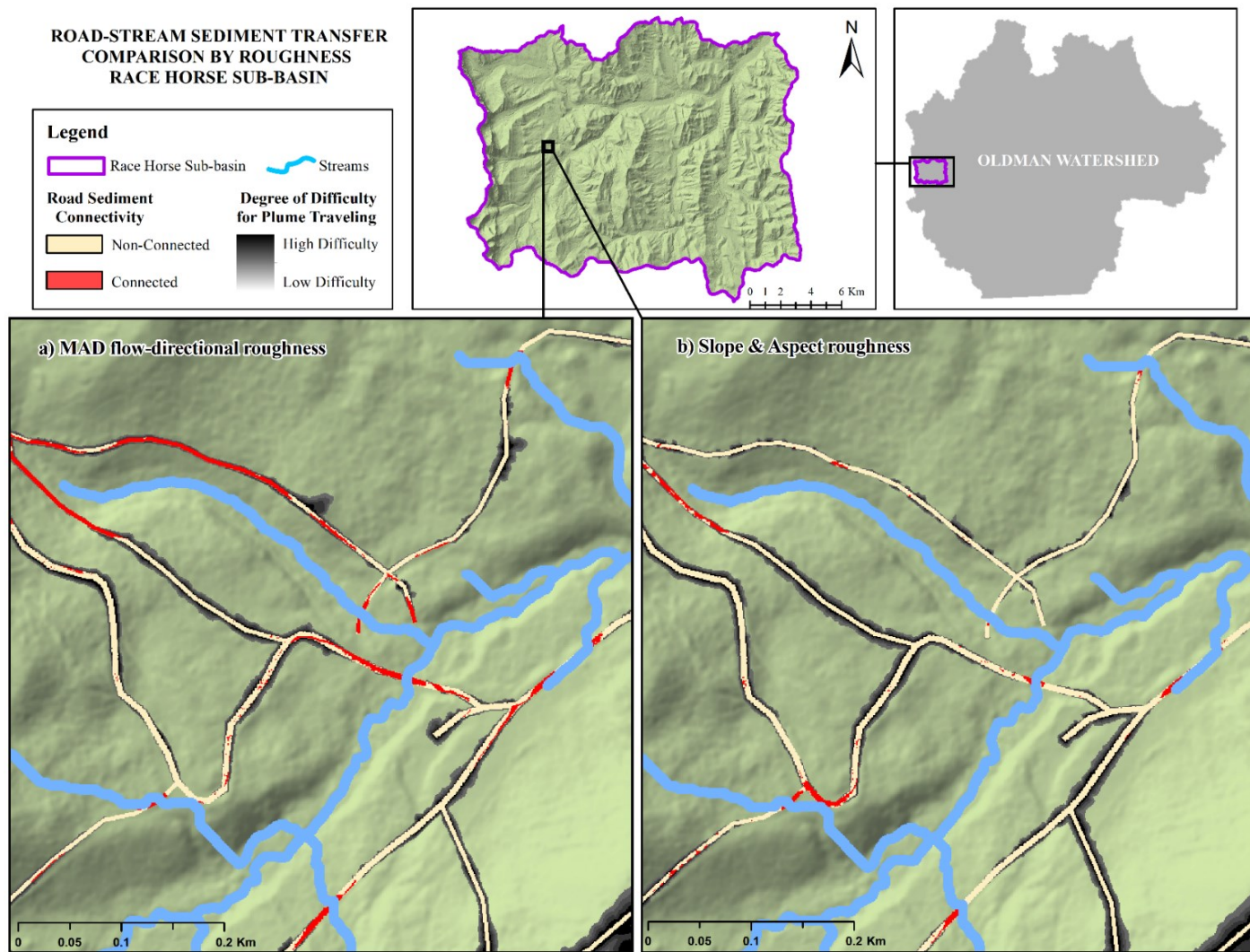


Figure 3-10. Race Horse Sub-basin. Road sediment connectivity comparison using the Mad flow directional roughness and the Slope & Aspect roughness (directional statistics). High sediment connectivity is represented in red and low connectivity in white. The sediment plume length is represented by the back -grey ramp showing the level of difficulty for sediment movement to streams: no movement (black ramp) and potential for movement (gray or no color).

References

- Ahmad Fadzil, M. H., Dinesh, S., & Vijanth Sagayan, A. (2011). A method for computation of surface roughness of digital elevation model terrains via multiscale analysis. *Computers and Geosciences*, *37*(2), 177–192. <https://doi.org/10.1016/j.cageo.2010.05.021>
- Ahmad Fadzil, M. H., Dinesh, S., & Vijanth Sagayan, A. (2012). Computing surface roughness of individual cells of digital elevation models via multiscale analysis. *Computers and Geosciences*, *43*, 137–146. <https://doi.org/10.1016/j.cageo.2011.09.015>
- Alexander, C. (2009). Delineating tree crowns from airborne laser scanning point cloud data using Delaunay triangulation. *International Journal of Remote Sensing*, *30*(14), 3843–3848. <https://doi.org/10.1080/01431160902842318>
- Benda, L., Miller, D., Andras, K., Bigelow, P., Reeves, G., & Michael, D. (2007). NetMap: A new tool in support of watershed science and resource management. *Forest Science*, *53*(2), 206–219. <https://doi.org/doi.org/10.1093/forestscience/53.2.206>
- Berti, M., Corsini, A., & Daehne, A. (2013). Comparative analysis of surface roughness algorithms for the identification of active landslides. *Geomorphology*, *182*, 1–18. <https://doi.org/10.1016/j.geomorph.2012.10.022>
- Borselli, L., Cassi, P., & Torri, D. (2008). Prolegomena to sediment and flow connectivity in the landscape: A GIS and field numerical assessment. *Catena*, *75*(3), 268–277. <https://doi.org/10.1016/j.catena.2008.07.006>
- Bracken, Louise J., and Croke, J. (2007). The concept of hydrological connectivity and its contribution to understanding runoff-dominated geomorphic systems, *21*, 2267–2274. <https://doi.org/10.1002/hyp.6313>
- Bracken, L. J., Turnbull, L., Wainwright, J., & Bogaart, P. (2015). Sediment connectivity: A framework for understanding sediment transfer at multiple scales. *Earth Surface Processes and Landforms*, *40*(2), 177–188. <https://doi.org/10.1002/esp.3635>
- Brubaker, K. M., Myers, W. L., Drohan, P. J., Miller, D. A., & Boyer, E. W. (2013). The use of LiDAR terrain data in characterizing surface roughness and microtopography. *Applied and Environmental Soil Science*, *2013*. <https://doi.org/10.1155/2013/891534>
- Carson, B., Maloney, D., Chatwin, S., Carver, M., & Beaudry, P. (2009). *Protocol for Evaluating the Potential Impact of Forestry and Range Use on Water Quality (Water Quality Routine Effectiveness Evaluation)*. Victoria, BC. Retrieved from <http://www.publications.gov.bc.ca>
- Cavalli, M., Goldin, B., Comiti, F., Brardinoni, F., & Marchi, L. (2017). Assessment of erosion and deposition in steep mountain basins by differencing sequential digital terrain models. *Geomorphology*, *291*, 4–16. <https://doi.org/10.1016/j.geomorph.2016.04.009>
- Cavalli, M., & Marchi, L. (2008). Characterization of the surface morphology of an alpine alluvial fan using airborne LiDAR. *Natural Hazards and Earth System Science*, *8*(2),

323–333. <https://doi.org/10.5194/nhess-8-323-2008>

- Cavalli, M., Trevisani, S., Comiti, F., & Marchi, L. (2013). Geomorphometric assessment of spatial sediment connectivity in small Alpine catchments. *Geomorphology*, *188*, 31–41. <https://doi.org/10.1016/j.geomorph.2012.05.007>
- Chen, Q., Jia, L., Hutjes, R., & Menenti, M. (2015). Estimation of aerodynamic roughness length over an oasis in the Heihe river basin by utilizing remote sensing and ground data. *Remote Sensing*, *7*(4), 3690–3709. <https://doi.org/10.3390/rs70403690>
- Esri (2018). ArcMap Release 10.6.1. Computer software. Redlands, CA: Environmental Systems Research Institute.
- Foerster, S., Wilczok, C., Brosinsky, A., & Segl, K. (2014). Assessment of sediment connectivity from vegetation cover and topography using remotely sensed data in a dryland catchment in the Spanish Pyrenees. *Journal of Soils and Sediments*, *14*(12), 1982–2000. <https://doi.org/10.1007/s11368-014-0992-3>
- Frankel, K. L., & Dolan, J. F. (2007). Characterizing arid region alluvial fan surface roughness with airborne laser swath mapping digital topographic data. *Journal of Geophysical Research: Earth Surface*, *112*(2), 1–14. <https://doi.org/10.1029/2006JF000644>
- Government of Alberta. (2016). Alberta Range Plants and Their Classification. Retrieved from agriculture.alberta.ca
- Government of Alberta (2018) LiDAR (Bare_Earth_DEM_asc) & (Full Feature DSM asc) (2016 SPOT6 RGB 1.5m) In AOI. (Raster digital data). Edmonton, AB: Alberta Environment and Parks – Informatics Branch. Data access through DMR# 1704M08, Project: Testing Erosion Prediction Tools in Alberta Road Networks.
- Grohmann, C. H., & Riccomini, C. (2009). Comparison of roving-window and search-window techniques for characterizing landscape morphometry. *Computers and Geosciences*, *35*(10), 2164–2169. <https://doi.org/10.1016/j.cageo.2008.12.014>
- Grohmann, C. H., & Sawakuchi, A. O. (2013). Influence of cell size on volume calculation using digital terrain models: A case of coastal dune fields. *Geomorphology*, *180–181*, 130–136. <https://doi.org/10.1016/j.geomorph.2012.09.012>
- Grohmann, C. H., Smith, M. J., & Riccomini, C. (2011). Multiscale analysis of topographic surface roughness in the Midland Valley, Scotland. *IEEE Transactions on Geoscience and Remote Sensing*, *49*(4), 1200–1213. <https://doi.org/10.1109/TGRS.2010.2053546>
- Hammond, D. S., Chapman, L., & Thornes, J. E. (2012). Roughness length estimation along road transects using airborne LIDAR data. *Meteorological Applications*, *19*(4), 420–426. <https://doi.org/10.1002/met.273>
- Haneberg, W.C., Creighton, A.L., Medley, E.W., and Jonas, D.A. (2005). Use of LiDAR to assess slope hazards at the Lihir gold mine, Papua New Guinea. In and E. E. O. Hungr, R. Fell, R. Couture (Ed.), *International Conference on Landslide Risk Management*.

Vancouver, Canada. <https://doi.org/10.1.1.473.8751>

- Hill, R. A., Smith, G. M., Fuller, R. M., & Veitch, N. (2002). Landscape modeling using integrated airborne multi-spectral and laser scanning data. *International Journal of Remote Sensing*, 23(11), 2327–2334. <https://doi.org/10.1080/01431160110119722>
- Hoja, D., Reinartz, P., & Lehner, L. (2005). DSM generation from high-resolution satellite imagery using additional information contained in existing DSM. In ISPRS (Ed.), *High-Resolution Earth Imaging for Geospatial Information*. Hannover, 17-20. May 2005: ISPRS Hannover Workshop 2005. Retrieved from <https://elib.dlr.de/18839/>
- Lane, S. N., Reaney, S. M., & Heathwaite, A. L. (2009). Representation of landscape hydrological connectivity using a topographically driven surface flow index. *Water Resources Research*, 45(8), 1–10. <https://doi.org/10.1029/2008WR007336>
- Marr, P. G. (2014). Directional (Circular) Statistics. Retrieved from <http://webspace.ship.edu/pgmarr/Geo441/Lectures/Lec 16 - Directional Statistics.pdf>
- Menenti, M., & Ritchie, J. C. (1994). Estimation of effective aerodynamic roughness of Walnut Gulch watershed with laser altimeter measurements. *Water Resources Research*, 30(5), 1329–1337. <https://doi.org/10.1029/93WR03055>
- Mitasova, H., & Iverson, L. R. (1996). Modeling topographic potential for erosion and deposition using GIS. *INT. J. Geographical Information System*, 10(5), 629–641. Retrieved from https://www.nrs.fs.fed.us/pubs/jrnl/1996/ne_1996_mitasova_001.pdf
- Nield, J. M., King, J., Wiggs, G. F. S., Leyland, J., Bryant, R. G., Chiverrell, R. C., ... Washington, R. (2013). Estimating aerodynamic roughness over complex surface terrain. *Journal of Geophysical Research Atmospheres*, 118(23), 12948–12961. <https://doi.org/10.1002/2013JD020632>
- Purves, R. (2016). Working with terrain models. Retrieved from http://www.geo.uzh.ch/microsite/geo372/PDF/week4_geo372_terrain.pdf
- Reid, S. C., Lane, S. N., Montgomery, D. R., & Brookes, C. J. (2007). Does hydrological connectivity improve modeling of coarse sediment delivery in upland environments? *Geomorphology*, 90(3–4), 263–282. <https://doi.org/10.1016/j.geomorph.2006.10.023>
- Roy, A. G., & Robert, A. (1990). Fractal techniques and the surface roughness of talus slopes: a comment. *Earth Surface Processes and Landforms*, 15(3), 283–285. <https://doi.org/10.1002/esp.3290150310>
- RStudio Team (2018). RStudio: Integrated Development for R. RStudio, Inc., Boston, MA URL <http://www.rstudio.com/>.
- Shepard, M. K., Campbell, B. A., Bulmer, M. H., Farr, T. G., Gaddis, L. R., & Plaut, J. J. (2001). The roughness of natural terrain: A planetary and remote sensing perspective. *Journal of Geophysical Research E: Planets*, 106(E12), 32777–32795. <https://doi.org/10.1029/2000JE001429>
- TerrainWorks Inc., & FRIAA (2018). *Identifying Unpaved Road Sediment Delivery to Critical*

Fish Habitats for Strategic Prioritization of Mitigation Actions in Alberta. Retrieved from www.terrainworks.com

- Thomas, I. A., Jordan, P., Shine, O., Fenton, O., Mellander, P. E., Dunlop, P., & Murphy, P. N. C. (2017). Defining optimal DEM resolutions and point densities for modeling hydrologically sensitive areas in agricultural catchments dominated by microtopography. *International Journal of Applied Earth Observation and Geoinformation*, *54*, 38–52. <https://doi.org/10.1016/j.jag.2016.08.012>
- Trevisani, S., & Cavalli, M. (2016). Topography-based flow-directional roughness: Potential and challenges. *Earth Surface Dynamics*, *4*(2), 343–358. <https://doi.org/10.5194/esurf-4-343-2016>
- Trevisani, S., & Rocca, M. (2015). MAD: Robust image texture analysis for applications in high-resolution geomorphometry. *Computers and Geosciences*, *81*, 78–92. <https://doi.org/10.1016/j.cageo.2015.04.003>
- Tsai, V. J. D. (1993). Delaunay triangulations in TIN creation: An overview and a linear-time algorithm. *International Journal of Geographical Information Systems*, *7*(6), 501–524. <https://doi.org/10.1080/02693799308901979>
- Whelley, P. L., Glaze, L. S., Calder, E. S., & Harding, D. J. (2014). LiDAR-derived surface roughness texture mapping: Application to Mount St. Helens pumice plain deposit analysis. *IEEE Transactions on Geoscience and Remote Sensing*, *52*(1), 426–438. <https://doi.org/10.1109/TGRS.2013.2241443>
- White, R. A., Dietterick, B. C., Mastin, T., & Strohman, R. (2010). forest roads mapped using LiDAR in steep forested terrain. *Remote Sensing*, *2*(4), 1120–1141. <https://doi.org/10.3390/rs2041120>

Chapter 4: Road-stream sediment connectivity for fish critical habitat assessment

4.1 Roads and the Fish Habitat Fragmentation and Degradation

Schiess (2001) suggests that the likelihood of road sediment input into streams depends on whether the sediment is produced by roads or by road use. In this study, I focused on sediment produced by roads and evaluated the terrain metrics to characterize sediment production from surface erosion by means of DEM data.

The study area is located in the eastern slopes of the Rocky Mountains in the Oldman Watershed, Alberta (Figure 2-7, 2-8) and is the native habitat for cold-water salmonid species. In recent years, roads have increased salmonid habitat isolation and degradation by intersecting at stream crossings and supplying fine sediment to streams (Hurkett, 2009). Extensive road networks and forest removal in the area, created by forestry and oil and gas industries, have also diminished aquatic species occurrence and abundance as affirmed by Ripley et al. (2005) in a study carried out in the Kakwa River basin in Alberta.

Road sediment particles from 62.5 µm (Baird et al., 2012) up to 2 mm in size (Reid and Dunne, 1984) are the main fish biological productivity concern (ASRD, 2012). Fish spawning areas reduction, growth rates, and late maturity are some of these negative impacts caused by fine sediment (Hurkett, 2009). Valdal and Quinn (2011), in their study, carried out in the Kootenay River Watershed in British Columbia, reported the existence of negative relationships between Cutthroat trout abundance and road density, roads constructed on erodible soils, and roads at stream crossings. In Alberta, Bull trout (*Salvelinus confluentus*) and Cutthroat trout (*Oncorhynchus clarkii lewisi*) are native species to the streams, rivers, and lakes in the headwaters of the eastern slope of the Rocky Mountains. According to ASRD (2012), in Alberta, Bull trout ranged across 24,000 stream kilometers once, but now its habitat has been reduced to approximately 16,000 km (33%). Therefore, because of a significant population reduction, Bull trout management, and recoveries plans have been undertaken by the Government of Alberta since 1995 (ASRD and ACA, 2009), and as a *Species of Special*

Concern, special attention was given to its critical habitat conservation (Post and Johnston, 2002). Regarding the Cutthroat trout, the extent of its habitat in Alberta has been reduced to 20 000 km² limited to the Rocky Mountain and Parkland Natural Regions (ASRD and ACA, 2006). Therefore, the Committee on the Status of Endangered Wildlife in Canada (COSEWIC) designated to the remaining genetically pure native populations of Cutthroat trout as *Threatened* (ASRD and ACA, 2006). Despite the efforts in management and recoveries plans, it is believed that Bull trout and Cutthroat trout have remarkably reduced populations in Alberta's mountainous region headwaters and their habitats have been categorized as at high risk (Post and Johnston, 2002, ASRD and ACA, 2006, 2009; ASRD, 2012).

4.2 Effects of Roughness on Sediment Movement

In this study, I present a method to measure road to stream sediment plume traveling capacity under the influence of terrain attributes. By means of roughness and slope distance costs, the most efficient corridor for sediment to move was estimated. Slope (directional flow) and roughness can certainly influence the distance sediment plume travels through pathways governed by terrain heterogeneities. This notion agrees with Schiess and Krogstad (2000) who stated that distance and routing to streams are variables that need to be considered when evaluating sediment input into streams. Besides, Cavalli et al. (2013) and Trevisani and Rocca (2015) pointed out that roughness also influences the distance sediment can move under the influence of anisotropic surfaces.

Therefore, I evaluated different methods to measure roughness values, so that the predictions of sediment production and sediment plume length can be examined under anisotropic instead of isotropic surfaces (Trevisani and Cavalli, 2016) for a better approximation of reality.

4.3 Road Sediment Connectivity and LiDAR-derived DEM Metrics

Road-stream proximity can be considered a serious concern in forested watersheds. For example, Valdal and Quinn (2011) in a study carried out in the East Kootenay region of British Columbia found that roads on erodible soils within 100 m distance to streams significantly threaten salmonid population. In this study, from models applied to the evaluation of debris connectivity (Borselli et al., 2008; Cavalli et al., 2013), I present an adapted method to predict the road connection to streams. Furthermore, by applying roughness values as weighting factors

for road sediment production and sediment plume length, I evaluated road-stream sediment connectivity as the ratio between both components as in Cavalli et al. (2013).

From the statistical results, the use of MAD flow directional roughness for the upslope component as in Trevisani & Rocca (2015) resulted in 77% association with field data, and the SD Slope & Aspect roughness for downslope component provided a 64% association with field sediment plume length. To measure SD Slope & Aspect roughness, I adapted the circular distribution (Marr, 2014) to be used with DEM data derived from LiDAR.

Predicted values of sediment production at 196 sites distributed across the study area, showed that roads had the potential to produce approximately a minimum of 2.95 and maximum of 202.31 m³, where the average was 56.97 m³ per site evaluated. Likewise, from field data, sediment production estimations presented an average of 43.76 m³, with a minimum and maximum of 1.80 and 196.86 m³. The DEM-based sediment production was associated to field data at approximately $r^2=0.77$, where F-statistic = 682.3, residual standard error = 20.77, and p-value<0.05.

Predicted sediment plume length showed that sediment plumes can travel approximately an average of 5.68 m compared to the field measure of 8.42 m. Maximum predicted sediment plume length was 27.40 m compared to 37.40 from field measurements. Additionally, sediment plume length predictions were related to field measurements by $r^2=0.64$, where F-statistic = 88.9, and p-value<0.05. Benda et al. (2016), using the road erosion and delivery index (READI) model and sediment plume length data obtained an average sediment plume length of 14 m in the Simonette watershed in Alberta.

Furthermore, by applying the combination of MAD flow directional and SD Slope & Aspect roughness, called MSA, to the ratio between the sediment production and sediment plume length, road sediment connectivity resulted in a general average of 0.6 units (connectivity values are dimensionless quantities) for the total study area, which according to the connectivity classification in Carson et al. (2009) falls under “a lot” (range 0.51- 0.8 units).

Additionally, from a total of 44 sites, approximations in sediment delivery resulted in a maximum of 119.36 m³ and minimum of 1.74 m³, and an average of 33.61 m³ which confirms

that approximately more than 60% of the sediment generated from the road surface is transported and delivered to a different place.

The connectivity evidence from this study points to the likelihood that unpaved roads have "a lot" of connection to the streams. Furthermore, it seems likely that the sediment supply capacity to the stream zones can reach up to 60% (prone to increase) of the total sediment produced. This situation certainly can cause negative effects on Bull trout and Cutthroat trout habitats and population reductions in Alberta's headwaters.

4.4 Conclusion and Future Research

Highlighting achievements

This research underlines the importance of remote sensing techniques and GIS tools as an opportunity to estimate sediment connectivity across extensive areas. To guide reclamation and management the road erosion and connectivity is often assessed in the field, which can be expensive and time-consuming, thus, this research has devised a procedure to provide estimates of connectivity and therefore save time and money by means of LIDAR DEM metrics. With algorithms previously used to predict landslide sediment connectivity, this study presents an approach to estimate road sediment connectivity as the ratio between the sediment production and plume traveling distance downhill. This study highlights the use of topographic roughness to improve sediment connectivity modeling. Therefore, sediment production from road surface considers the MAD flow directional and the sediment plume traveling distance focuses on the SD Slope & Aspect roughness as weighing factors. Furthermore, this study provides a method to estimate sediment plume traveling distance from road to streams based on topographic roughness and slope cost distance and corridors.

Research Limitations

Based on the results I obtained and the methods I used, there are some aspects that might be useful to consider for future studies:

- The sediment connectivity model provides a general view of what the reality would be in terms of sediment production, transportation, and connection to streams across the sampling area only. Therefore, the findings might not be representative of areas out of the

sampling area. The model must be used as a general approach to evaluating potential sediment production, transportation, and connection to streams requiring further field evaluation to reduce outliers.

- The approach may present limitations in other parts of the world and may require further studies to examine the model performance; thus, caution must be exercised.
- The present study has only investigated road surface as a source of sediment; consequently, including cutslope, hillslope, and other sediment sources might provide more complete information on the amount of sediment produced and contributed to the streams.

Research Implications

The procedure could be applied to support protection management of streams values in the eastern slopes of the Canadian Rocky Mountains in the Oldman watershed, which is home to a threatened Bull trout (*Salvelinus confluentus*) and Cutthroat trout (*Oncorhynchus clarkii lewisii*) salmonid species. By using high-resolution DEM metric and GIS, the model can be used as an overview to examine roads connected to streams under the limitations of field data.

Considerations for future work

- Further work needs to be performed to establish whether other factors can affect the sediment connectivity model performance. The model is not restricted to the use of another type of information such as rainfall, road density, soil infiltration, and soil texture as weighting factors; however, new improvements to the model should maintain the idea on overcoming field data unavailability.
- Evaluations on different window sizes are recommended to verify the effectiveness of the model in terms of topographic roughness estimation.
- Evaluations on different stream buffer distance are suggested considering stream order to examine the influence stream area connected to roads. Besides, an updated road layer may be required.

Figures

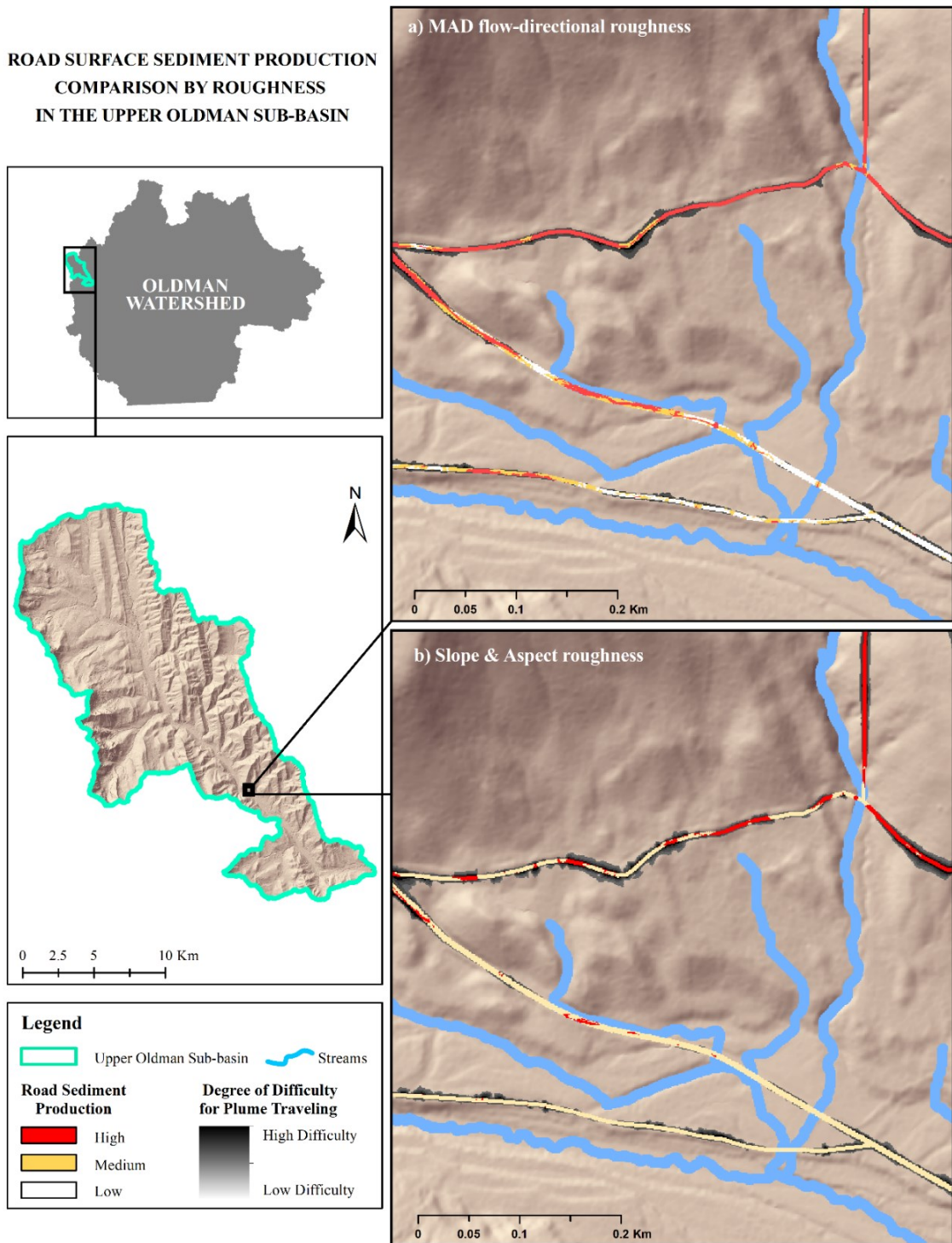


Figure 4-1. Upper Oldman Sub-basin. Road sediment production comparison using the MAD flow-directional roughness and the Slope & Aspect roughness (directional statistics). High sediment production is represented in red, medium in light orange, and low in white. The sediment plume length is represented by the back-grey ramp showing the level of difficulty for sediment movement to streams: no movement (black ramp) and potential for movement (gray or no color).

**ROAD-STREAM SEDIMENT CONNECTIVITY
BY ROUGHNESS COMPARISON
IN THE UPPER OLDMAN SUB-BASIN**

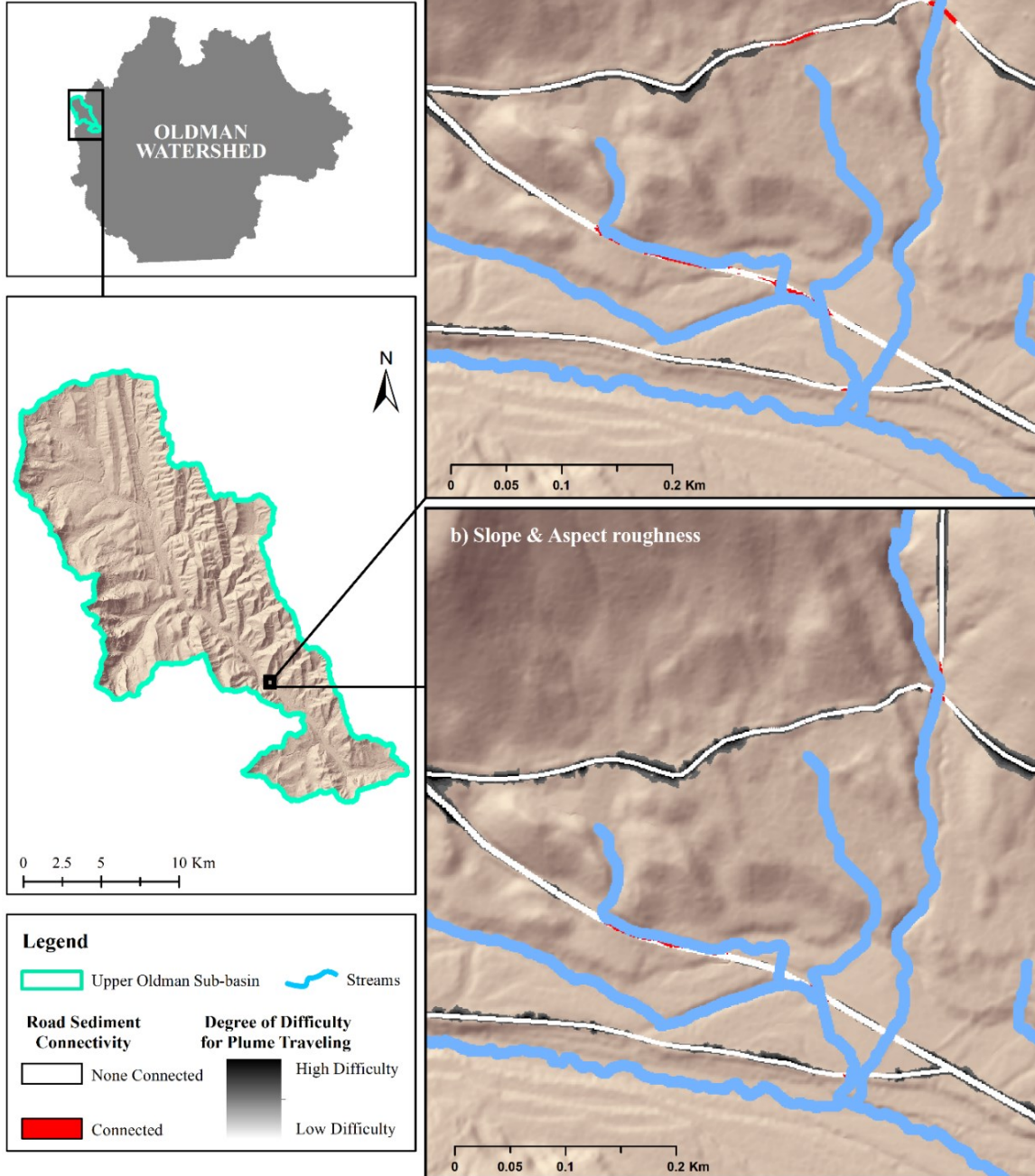


Figure 4-2. Upper Oldman Sub-basin. Road sediment connectivity comparison using the Mad flow directional roughness and the Slope & Aspect roughness (directional statistics). High sediment connectivity is represented in red and low connectivity in white. The back -grey ramp shows the level of difficulty for sediment movement to streams: no movement (black ramp) and potential for movement (gray or no color).

**ROAD SURFACE SEDIMENT PRODUCTION
&
ROAD-STREAM CONNECTIVITY
IN THE UPPER OLDMAN SUB-BASIN**

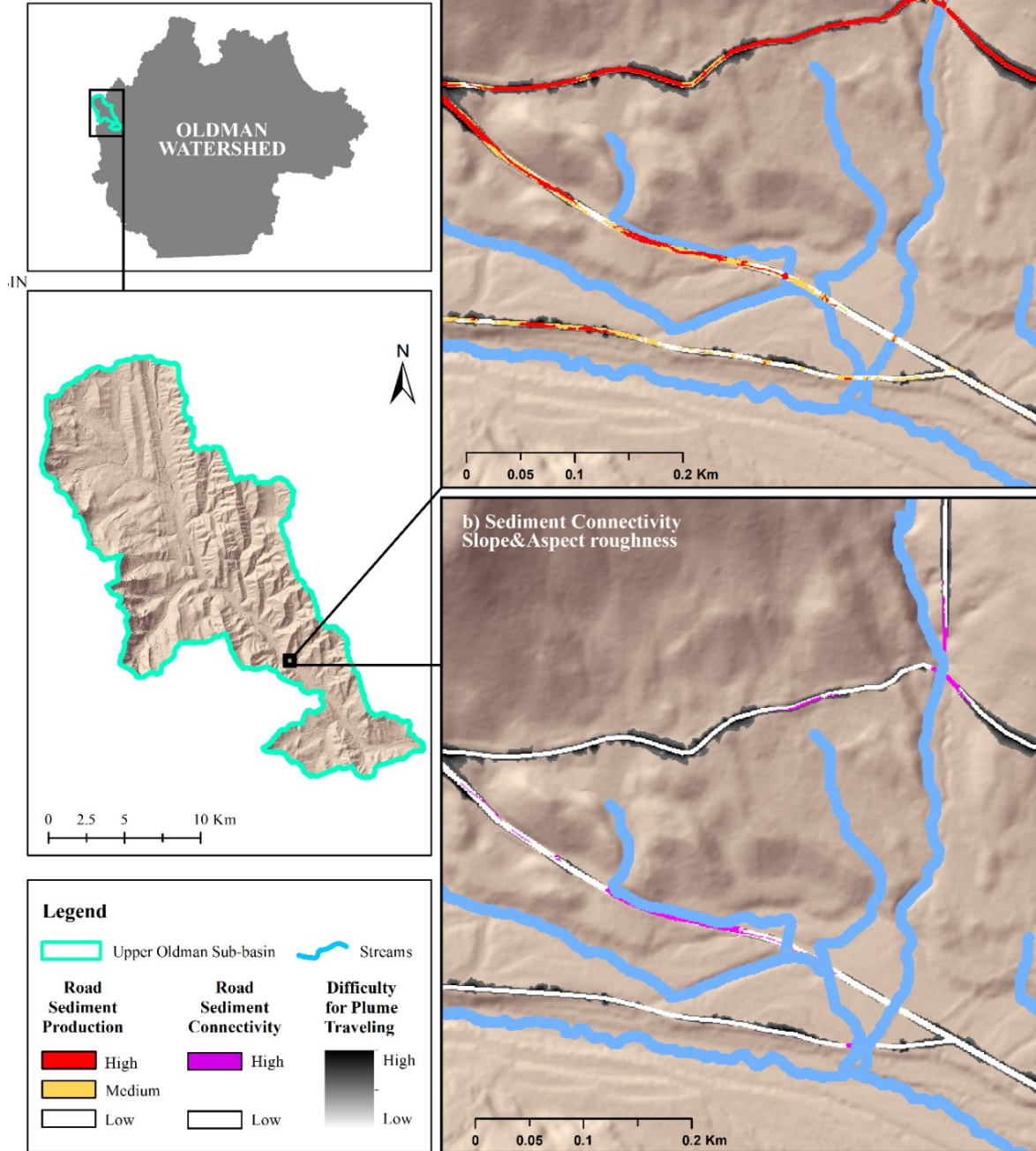


Figure 4-3. Upper Oldman Sub-basin. Sediment production, sediment plume length, sediment connectivity prediction by applying the MSA roughness. Colors sediment production high (red), medium (light orange), and low (white). High connected road areas (purple) and low connected (white). Sediment plume length shows low movement (black ramp) and high movement (gray or no color)

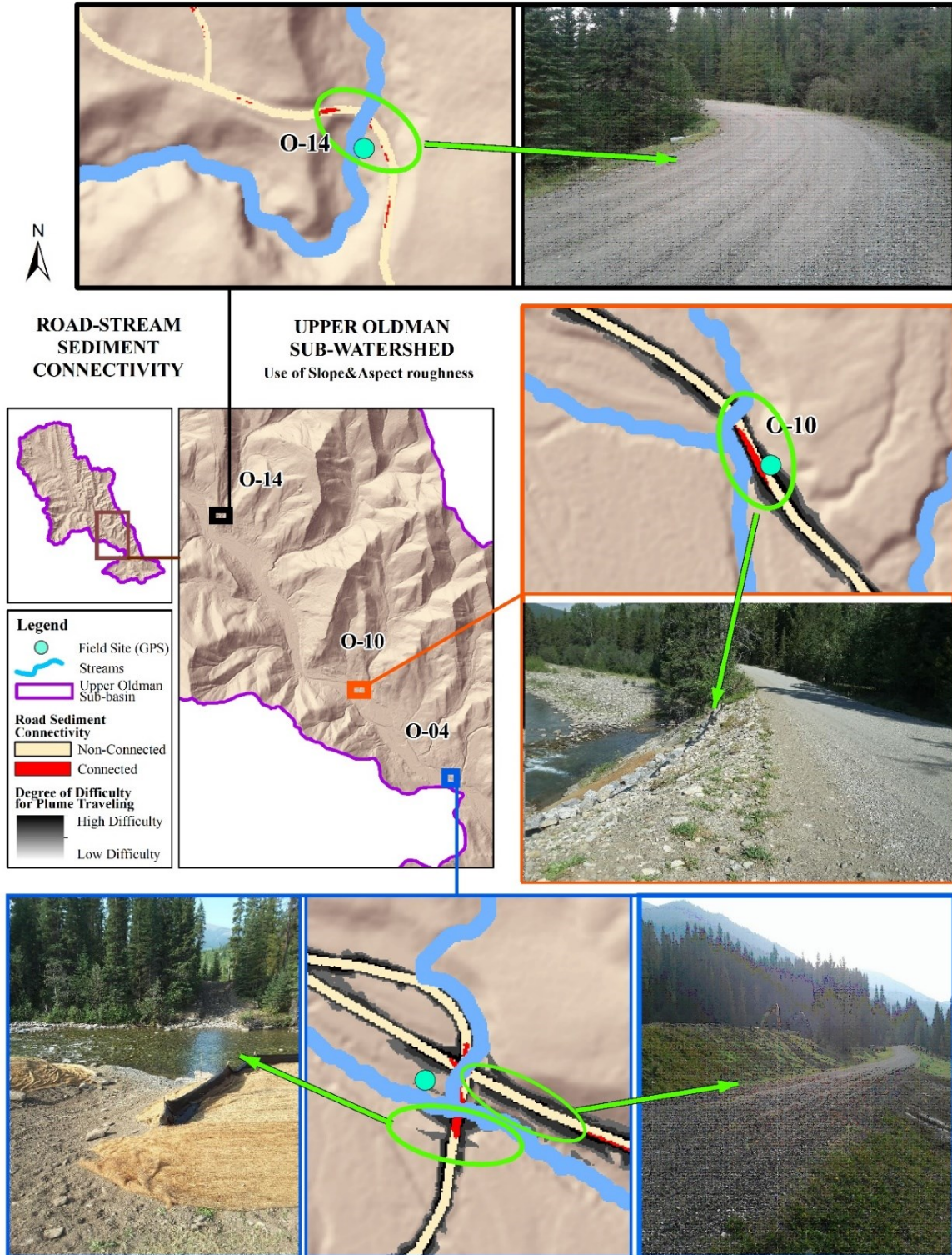


Figure 4-4. Upper Oldman Sub-basin. Prediction sediment connectivity mapping and pictures from the field. The zoomed-in areas show the road-stream connectivity (red – connected, light orange – unconnected) compared with the pictures taken at the sites. The capacity for sediment plume movement from road to streams is represented by the back and gray ramp.

References

- Alberta Sustainable Resource Development, (ASRD), & Alberta Conservation Association, (ACA). (2006). *Status of the Westslope Cutthroat Trout (Oncorhynchus clarkii lewisii) in Alberta*. Edmonton, AB: Alberta Sustainable Resource Development, Wildlife Status Report No. 61. Retrieved from <https://open.alberta.ca/publications/0778518694>
- Alberta Sustainable Resource Development, (ASRD), & Alberta Conservation Association, (ACA). (2009). *Status of the Bull Trout (Salvelinus confluentus) in Alberta : Update 2009* (Vol. 39). Edmonton, AB. Retrieved from <https://open.alberta.ca/publications/9780778591788>
- Alberta Sustainable Resource Development, (ASRD). (2012). Bull Trout Conservation Management Plan 2012-17. *Species at Risk Conservation Management Plan No. 8*. Edmonton, Alberta. [https://doi.org/ISBN: 978-1-4601-0230-5](https://doi.org/ISBN:978-1-4601-0230-5)
- Baird, E. J., Floyd, W., Van Meerveld, I., & Anderson, A. E. (2012). Road Surface Erosion, Part 1 : Summary of Effects, Processes, and Assessment Procedures. *Streamline Watershed Management Bulletin*, 15(1), 1–35. Retrieved from <http://www.forrex.org/publications/streamline%0AProject>
- Benda, L., Andras, K., Miller, D., Netmap, T., & Shasta, M. (2016). Road Cumulative Effects Analysis in the Simonette River Watershed. Retrieved from www.terrainworks.com
- Borselli, L., Cassi, P., & Torri, D. (2008). Prolegomena to sediment and flow connectivity in the landscape: A GIS and field numerical assessment. *Catena*, 75(3), 268–277. <https://doi.org/10.1016/j.catena.2008.07.006>
- Carson, B., Maloney, D., Chatwin, S., Carver, M., & Beaudry, P. (2009). Protocol for Evaluating the Potential Impact of Forestry and Range Use on Water Quality (Water Quality Routine Effectiveness Evaluation). Victoria, BC. Retrieved from <http://www.publications.gov.bc.ca>
- Cavalli, M., Trevisani, S., Comiti, F., & Marchi, L. (2013). Geomorphometric assessment of spatial sediment connectivity in small Alpine catchments. *Geomorphology*, 188, 31–41. <https://doi.org/10.1016/j.geomorph.2012.05.007>
- Hurkett, B. (2009). Bull Trout Population Assessment in the Upper Oldman River Drainage. Lethbridge, Alberta. Retrieved from <https://www.ab-conservation.com/publications/report-series/bull-trout-population-assessment-in-the-upper-oldman-river-drainage-2009/>
- Marr, P. G. (2014). Directional (Circular) Statistics. Retrieved from [http://webspace.ship.edu/pgmarr/Geo441/Lectures/Lec 16 - Directional Statistics.pdf](http://webspace.ship.edu/pgmarr/Geo441/Lectures/Lec%2016%20-%20Directional%20Statistics.pdf)
- Post, J. R., & Johnston, F. D. (2002). Status of the Bull Trout (Salvelinus confluentus) in Alberta. Edmonton, AB: Alberta Sustainable Resource Development, Fish and Wildlife Division, and Alberta Conservation Association, Wildlife Status Report No. 39. Retrieved from <https://open.alberta.ca/publications/0778518694>

- Reid, L. M., & Dunne, T. (1984). Sediment production from forest road surfaces. *Water Resources Research*, 20(11), 1753–1761. <https://doi.org/10.1029/WR020i011p01753>
- Ripley, T., Scrimgeour, G., & Boyce, M. S. (2005). Bull trout (*Salvelinus confluentus*) occurrence and abundance influenced by cumulative industrial developments in a Canadian boreal forest watershed. *Canadian Journal of Fisheries and Aquatic Sciences*, 62(11), 2431–2442. <https://doi.org/10.1139/f05-150>
- Schiess, P. (2001). Road Management Strategies to Reduce Habitat Impacts: A Case for Engineered Cable Yarding Operations and Harvest Schedules. In U. Arzberger & M. Grimoldi (Eds.), *New Trends in Wood Harvesting with Cable Systems for Sustainable Forest Management in The Mountains*. Ossiach, Austria June 18 to 24 June 2001: Forestry Training Centre, Government of Austria. Retrieved from <http://www.fao.org/3/Y9351E/Y9351E32.htm#ch32>
- Schiess, P., & Krogstad, F. (2000). Sediment and Road Density Reduction. In *Summit 2000, Washington Private Forests Forum*. Seattle, WA. Summer 2000: University of Washington. Retrieved from http://faculty.washington.edu/schiess/Publications/Road_Density/Forum_2000_paper.htm
- Trevisani, S., & Cavalli, M. (2016). Topography-based flow-directional roughness: Potential and challenges. *Earth Surface Dynamics*, 4(2), 343–358. <https://doi.org/10.5194/esurf-4-343-2016>
- Trevisani, S., & Rocca, M. (2015). MAD: Robust image texture analysis for applications in high-resolution geomorphometry. *Computers and Geosciences*, 81, 78–92. <https://doi.org/10.1016/j.cageo.2015.04.003>
- Valdal, E. J., & Quinn, M. S. (2011). Spatial Analysis of Forestry-Related Disturbance on Westslope Cutthroat Trout (*Oncorhynchus clarkii lewisi*): Implications for Policy and Management. *Applied Spatial Analysis and Policy*, 4(2), 95–111. <https://doi.org/10.1007/s12061-009-9045-5>

References

- Ahmad Fadzil, M. H., Dinesh, S., & Vijanth Sagayan, A. (2011). A method for computation of surface roughness of digital elevation model terrains via multiscale analysis. *Computers and Geosciences*, *37*(2), 177–192. <https://doi.org/10.1016/j.cageo.2010.05.021>
- Ahmad Fadzil, M. H., Dinesh, S., & Vijanth Sagayan, A. (2012). Computing surface roughness of individual cells of digital elevation models via multiscale analysis. *Computers and Geosciences*, *43*, 137–146. <https://doi.org/10.1016/j.cageo.2011.09.015>
- Akay, A. E., Erdas, O., Reis, M., & Yuksel, A. (2008). Estimating sediment yield from a forest road network by using a sediment prediction model and GIS techniques. *Building and Environment*, *43*(5), 687–695. <https://doi.org/10.1016/j.buildenv.2007.01.047>
- Alberta Agriculture and Forestry, University of New Brunswick, Forest Watershed Research Centre (2018) WAM-wet areas mapping of Alberta. Edmonton, AB: Alberta Environment and Parks – Informatics Branch. Data access through DMR# 1704M08, Project: Testing Erosion Prediction Tools in Alberta Road Networks.
- Al-Chokhachy, R., Black, T. A., Thomas, C., Luce, C. H., Rieman, B., Cissel, R., ... Kershner, J. L. (2016). Linkages between unpaved forest roads and streambed sediment: why context matters in directing road restoration. *Restoration Ecology*, *24*(5), 589–598. <https://doi.org/10.1111/rec.12365>
- Alberta Sustainable Resource Development, (ASRD), & Alberta Conservation Association, (ACA). (2006). Status of the Westslope Cutthroat Trout (*Oncorhynchus clarkii lewisii*) in Alberta. Edmonton, AB: Alberta Sustainable Resource Development, Wildlife Status Report No. 61. Retrieved from <https://open.alberta.ca/publications/0778518694>
- Alberta Sustainable Resource Development, (ASRD), & Alberta Conservation Association, (ACA). (2009). Status of the Bull Trout (*Salvelinus confluentus*) in Alberta : Update 2009 (Vol. 39). Edmonton, AB. Retrieved from <https://open.alberta.ca/publications/9780778591788>
- Alder, S., Prasuhn, V., Liniger, H., Herweg, K., Hurni, H., Candinas, A., & Gujer, H. U. (2015). A high-resolution map of direct and indirect connectivity of erosion risk areas to surface waters in Switzerland-A risk assessment tool for planning and policy-making. *Land Use Policy*, *48*, 236–249. <https://doi.org/10.1016/j.landusepol.2015.06.001>
- Alexander, C. (2009). Delineating tree crowns from airborne laser scanning point cloud data using Delaunay triangulation. *International Journal of Remote Sensing*, *30*(14), 3843–3848. <https://doi.org/10.1080/01431160902842318>
- Anderson, D. M., & MacDonald, L. H. (1998). Modelling road surface sediment production using a vector geographic information system. *Earth Surface Processes and Landforms*, *23*, 95–107. <https://doi.org/doi.org/10.1002>

- Anderson, P., & Anderson, R. (1987). Erosion potential index : a method for evaluating sheet erosion at stream crossings. Edmonton : Alberta Forestry, Lands and Wildlife,. <https://doi.org/10.5962/bhl.title.110391>
- Aruga, K., Sessions, J., & Miyata, E. S. (2005). Forest road design with soil sediment evaluation using a high-resolution DEM. *Journal of Forest Research*, 10(6), 471–479. <https://doi.org/10.1007/s10310-005-0174-7>
- ASRD. (2012). Bull Trout Conservation Management Plan 2012-17. Species at Risk Conservation Management Plan No. 8. Edmonton, Alberta. <https://doi.org/ISBN:978-1-4601-0230-5>
- Baartman, J. E. M., Masselink, R., Keesstra, S. D., & Temme, A. J. A. M. (2013). Linking landscape morphological complexity and sediment connectivity. *Earth Surface Processes and Landforms*, 38(12), 1457–1471. <https://doi.org/10.1002/esp.3434>
- Baird, E. J., Floyd, W., Van Meerveld, I., & Anderson, A. E. (2012). Road Surface Erosion , Part 1 : Summary of Effects , Processes , and Assessment Procedures. *Streamline Watershed Management Bulletin*, 15(1), 1–35. Retrieved from <http://www.forrex.org/publications/streamline%0AProject>
- Benda, L., Andras, K., Miller, D., Netmap, T., & Shasta, M. (2016). Road Cumulative Effects Analysis in the Simonette River Watershed. Retrieved from www.terrainworks.com
- Benda, L., James, C., Miller, D., & Andras, K. (2019). Road Erosion and Delivery Index (READI): A Model for Evaluating Unpaved Road Erosion and Stream Sediment Delivery. *Journal of the American Water Resources Association*. <https://doi.org/10.1111/1752-1688.12729>
- Benda, L., Miller, D., Andras, K., Bigelow, P., Reeves, G., & Michael, D. (2007). NetMap: A new tool in support of watershed science and resource management. *Forest Science*, 53(2), 206–219. <https://doi.org/doi.org/10.1093/forestscience/53.2.206>
- Berti, M., Corsini, A., & Daehne, A. (2013). Comparative analysis of surface roughness algorithms for the identification of active landslides. *Geomorphology*, 182, 1–18. <https://doi.org/10.1016/j.geomorph.2012.10.022>
- Beven, K. J., & Kirkby, M. J. (1979). A physically based, variable contributing area model of basin hydrology. *Hydrological Sciences Bulletin*, 24(1), 43–69. <https://doi.org/10.1080/02626667909491834>
- Bilby, R. E., Sullivan, K., & Duncan, S. H. (1989). The generation and fate of road-surface sediment in forested watersheds in southwestern Washington. *Forest Science*, 35(2), 453–468. <https://doi.org/doi.org/10.1093/forestscience/35.2.453>
- Borselli, L., Cassi, P., & Torri, D. (2008). Prolegomena to sediment and flow connectivity in the landscape: A GIS and field numerical assessment. *Catena*, 75(3), 268–277. <https://doi.org/10.1016/j.catena.2008.07.006>

- Bracken, Louise J., and Croke, J. (2007). The concept of hydrological connectivity and its contribution to understanding runoff-dominated geomorphic systems, *21*, 2267–2274. <https://doi.org/10.1002/hyp.6313>
- Bracken, L. J., Turnbull, L., Wainwright, J., & Bogaart, P. (2015). Sediment connectivity: A framework for understanding sediment transfer at multiple scales. *Earth Surface Processes and Landforms*, *40*(2), 177–188. <https://doi.org/10.1002/esp.3635>
- Brubaker, K. M., Myers, W. L., Drohan, P. J., Miller, D. A., & Boyer, E. W. (2013). The use of LiDAR terrain data in characterizing surface roughness and microtopography. *Applied and Environmental Soil Science*, *2013*. <https://doi.org/10.1155/2013/891534>
- Burnett, K. M., & Miller, D. J. (2007). Streamside policies for headwater channels: An example considering debris flows in the Oregon coastal province. *Forest Science*, *53*(2), 239–253. <https://doi.org/doi.org/10.1093/forestscience/53.2.239>
- Cantreul, V., Biellers, C., Calsamiglia, A., & Degré, A. (2017). How pixel size affects a sediment connectivity index in central Belgium. *Earth Surface Processes and Landforms*. <https://doi.org/10.1002/esp.4295>
- Carson, B., Maloney, D., Chatwin, S., Carver, M., & Beaudry, P. (2009). Protocol for Evaluating the Potential Impact of Forestry and Range Use on Water Quality (Water Quality Routine Effectiveness Evaluation). Victoria, BC. Retrieved from <http://www.publications.gov.bc.ca>
- Cavalli, M., Goldin, B., Comiti, F., Brardinoni, F., & Marchi, L. (2017). Assessment of erosion and deposition in steep mountain basins by differencing sequential digital terrain models. *Geomorphology*, *291*, 4–16. <https://doi.org/10.1016/j.geomorph.2016.04.009>
- Cavalli, M., & Marchi, L. (2008). Characterisation of the surface morphology of an alpine alluvial fan using airborne LiDAR. *Natural Hazards and Earth System Science*, *8*(2), 323–333. <https://doi.org/10.5194/nhess-8-323-2008>
- Cavalli, M., Trevisani, S., Comiti, F., & Marchi, L. (2013). Geomorphometric assessment of spatial sediment connectivity in small Alpine catchments. *Geomorphology*, *188*, 31–41. <https://doi.org/10.1016/j.geomorph.2012.05.007>
- Chen, Q., Jia, L., Hutjes, R., & Menenti, M. (2015). Estimation of aerodynamic roughness length over oasis in the Heihe river basin by utilizing remote sensing and ground data. *Remote Sensing*, *7*(4), 3690–3709. <https://doi.org/10.3390/rs70403690>
- Crema, S., & Cavalli, M. (2018). SedInConnect: a stand-alone, free and open source tool for the assessment of sediment connectivity. *Computers and Geosciences*, *111*(December 2016), 39–45. <https://doi.org/10.1016/j.cageo.2017.10.009>
- Croke, J. C., & Hairsine, P. B. (2006). Sediment delivery in managed forests: a review. *Environmental Reviews*, *14*(1), 59–87. <https://doi.org/10.1139/a05-016>
- Croke, J., & Mockler, S. (2001). Gully initiation and road-to-stream linkage in a forested

- catchment southeastern Australia. *Earth Surface Processes and Landforms*, 26(2), 205–217. [https://doi.org/10.1002/1096-9837\(200102\)26:2<205::AID-ESP168>3.0.CO;2-G](https://doi.org/10.1002/1096-9837(200102)26:2<205::AID-ESP168>3.0.CO;2-G)
- Croke, J., Mockler, S., Fogarty, P., & Takken, I. (2005). Sediment concentration changes in runoff pathways from a forest road network and the resultant spatial pattern of catchment connectivity. *Geomorphology*, 68(3–4), 257–268. <https://doi.org/10.1016/j.geomorph.2004.11.020>
- Demirci, A., & Karaburun, A. (2012). Estimation of soil erosion using RUSLE in a GIS framework: A case study in the Buyukcekmece Lake watershed, northwest Turkey. *Environmental Earth Sciences*, 66(3), 903–913. <https://doi.org/10.1007/s12665-011-1300-9>
- Esri (2018). ArcMap Release 10.6.1. Computer software. Redlands, CA: Environmental Systems Research Institute.
- Faivre, R., Colin, J., & Menenti, M. (2017). Evaluation of methods for aerodynamic roughness length retrieval from very high-resolution imaging LIDAR observations over the Heihe Basin in China [Remote Sens., 9, (2017) 63]. *Remote Sensing*, 9(2), 1–25. <https://doi.org/10.3390/rs9020157>
- Fiera Biological Consulting Ltd (Fiera). (2014). Oldman Watershed Headwaters Indicator Project - Final Report (Version 2014.1). Edmonton, Alberta. Fiera Biological Consulting Report #1346. Retrieved from <https://oldmanwatershed-council.squarespace.com/s/HeadwatersIndicatorsProject.pdf>
- Foerster, S., Wilczok, C., Brosinsky, A., & Segl, K. (2014). Assessment of sediment connectivity from vegetation cover and topography using remotely sensed data in a dryland catchment in the Spanish Pyrenees. *Journal of Soils and Sediments*, 14(12), 1982–2000. <https://doi.org/10.1007/s11368-014-0992-3>
- Frankel, K. L., & Dolan, J. F. (2007). Characterizing arid region alluvial fan surface roughness with airborne laser swath mapping digital topographic data. *Journal of Geophysical Research: Earth Surface*, 112(2), 1–14. <https://doi.org/10.1029/2006JF000644>
- Gay, A., Cerdan, O., Mardhel, V., & Desmet, M. (2016). Application of an index of sediment connectivity in a lowland area. *Journal of Soils and Sediments*, 16(1), 280–293. <https://doi.org/10.1007/s11368-015-1235-y>
- Gomes, R. A. T., Guimarães, R. F., Carvalho, O. A., Fernandes, N. F., Vargas, E. A., & Martins, É. S. (2008). Identification of the affected areas by mass movement through a physically based model of landslide hazard combined with an empirical model of debris flow. *Natural Hazards*, 45(2), 197–209. <https://doi.org/10.1007/s11069-007-9160-z>
- Government of Alberta. (2009). Alberta Recreation Corridor and Trails Classification System. Alberta Tourism, Parks and Recreation. Retrieved from www.tpr.gov.alberta.ca
- Government of Alberta. (2016). Alberta Range Plants and their Classification. Retrieved from

- Government of Alberta (2018) WAM derived Stream Features (vector digital data). Edmonton, AB: Alberta Environment and Parks – Informatics Branch. Data access through DMR# 1704M08, Project: Testing Erosion Prediction Tools in Alberta Road Networks.
- Government of Alberta (2018) Cutlines and Trails of Alberta (vector digital data). cited 2017. Edmonton, AB: Alberta Environment and Parks. Retrieved from: <https://maps.alberta.ca/genesis/rest/services/Access/Latest/MapServer>
- Government of Alberta (2014) Watersheds of Alberta (vector digital data). cited 2018. Edmonton, AB: Alberta Environment and Parks. Retrieved from: https://maps.alberta.ca/genesis/rest/services/Watersheds_of_Alberta/Latest/MapServer
- Grace, J. . I., & Clinton, B. . (2007). Protecting soil and water in forest road management. *Transactions of the American Society of Agricultural and Biological Engineers ASABE*, 50(5), 1579–1584. Retrieved from <http://digitalcommons.unl.edu/usdafsfacpub/58>
- Grace, J. . I., Rummer, B., Stokes, B. J., & Wilhoit, J. (1998). Evaluation of Erosion Control Techniques on Forest Roads. *American Society of Agricultural Engineers*, 41(2), 383–391. Retrieved from <https://www.fs.usda.gov/treesearch/pubs/65>
- Grauso, S., Pasanisi, F., & Tebano, C. (2018). Assessment of a Simplified Connectivity Index and Specific Sediment Potential in River Basins by Means of Geomorphometric Tools. *Geosciences*, 8(2), 48. <https://doi.org/10.3390/geosciences8020048>
- Grohmann, C. H., & Riccomini, C. (2009). Comparison of roving-window and search-window techniques for characterising landscape morphometry. *Computers and Geosciences*, 35(10), 2164–2169. <https://doi.org/10.1016/j.cageo.2008.12.014>
- Grohmann, C. H., & Sawakuchi, A. O. (2013). Influence of cell size on volume calculation using digital terrain models: A case of coastal dune fields. *Geomorphology*, 180–181, 130–136. <https://doi.org/10.1016/j.geomorph.2012.09.012>
- Grohmann, C. H., Smith, M. J., & Riccomini, C. (2011). Multiscale analysis of topographic surface roughness in the Midland Valley, Scotland. *IEEE Transactions on Geoscience and Remote Sensing*, 49(4), 1200–1213. <https://doi.org/10.1109/TGRS.2010.2053546>
- Hammond, D. S., Chapman, L., & Thornes, J. E. (2012). Roughness length estimation along road transects using airborne LIDAR data. *Meteorological Applications*, 19(4), 420–426. <https://doi.org/10.1002/met.273>
- Haneberg, W.C., Creighton, A.L., Medley, E.W., and Jonas, D.A. (2005). Use of LiDAR to assess slope hazards at the Lihir gold mine, Papua New Guinea. In and E. E. O. Hungr, R. Fell, R. Couture (Ed.), *International Conference on Landslide Risk Management*. Vancouver, Canada. <https://doi.org/10.1.1.473.8751>
- Hartcher, M. G., & Post, D. A. (2005). Reducing Uncertainty in Sediment Yield Through

- Improved Representation of Land Cover: Application to Two Sub-catchments of the Mae Chaem, Thailand. In *International Congress on Modelling and Simulation: Advances and Applications for Management and Decision Making* (pp. 1147–1153). Melbourne, VIC; Australia; 12 Dec-15 Dec: MODSIM05. Retrieved from <https://pdfs.semanticscholar.org/0659/fa09533a249be75b59b119c0c977a783b9bd.pdf>
- Hill, R. A., Smith, G. M., Fuller, R. M., & Veitch, N. (2002). Landscape modelling using integrated airborne multi-spectral and laser scanning data. *International Journal of Remote Sensing*, 23(11), 2327–2334. <https://doi.org/10.1080/01431160110119722>
- Hoja, D., Reinartz, P., & Lehner, L. (2005). DSM generation from high resolution satellite imagery using additional information contained in existing DSM. In ISPRS (Ed.), *High Resolution Earth Imaging for Geospatial Information*. Hannover, 17-20. May 2005: ISPRS Hannover Workshop 2005. Retrieved from <https://elib.dlr.de/18839/>
- Hooke, J. (2003). Coarse sediment connectivity in river channel systems: A conceptual framework and methodology. *Geomorphology*, 56(1–2), 79–94. [https://doi.org/10.1016/S0169-555X\(03\)00047-3](https://doi.org/10.1016/S0169-555X(03)00047-3)
- Hurkett, B. (2009). Bull Trout Population Assessment in the Upper Oldman River Drainage. Lethbridge, Alberta. Retrieved from <https://www.ab-conservation.com/publications/report-series/bull-trout-population-assessment-in-the-upper-oldman-river-drainage-2009/>
- Kemp, P., Sear, D., Collins, A., Naden, P., & Jones, I. (2011). The impacts of fine sediment on riverine fish. *Hydrological Processes*, 25(11), 1800–1821. <https://doi.org/10.1002/hyp.7940>
- La Marche, J. L., & Lettenmaier, D. P. (2001). Effects of forest roads on flood flows in the Deschutes River, Washington. *Earth Surface Processes and Landforms*, 26(2), 115–134. [https://doi.org/10.1002/1096-9837\(200102\)26:2<115::AID-ESP166>3.0.CO;2-O](https://doi.org/10.1002/1096-9837(200102)26:2<115::AID-ESP166>3.0.CO;2-O)
- Lane, P. N. J., & Sheridan, G. J. (2002). Impact of an unsealed forest road-stream crossing: Water quality and sediment sources. *Hydrological Processes*, 16(13), 2599–2612. <https://doi.org/10.1002/hyp.1050>
- Lane, S. N., Reaney, S. M., & Heathwaite, A. L. (2009). Representation of landscape hydrological connectivity using a topographically driven surface flow index. *Water Resources Research*, 45(8), 1–10. <https://doi.org/10.1029/2008WR007336>
- Lisle, T. E. (1989). Sediment transport and resulting deposition in spawning gravels, north coastal California. *Water Resources Research*, 25(6), 1303–1319. <https://doi.org/10.1029/WR025i006p01303>
- López-Vicente, M., & Álvarez, S. (2018). Influence of DEM resolution on modelling hydrological connectivity in a complex agricultural catchment with woody crops. *Earth Surface Processes and Landforms*, 43(7), 1403–1415. <https://doi.org/10.1002/esp.4321>
- Luce, C. H., & Black, T. a. (1999). Sediment production from forest roads in western Oregon.

- Water Resources Research*, 35(8), 2561. <https://doi.org/10.1029/1999WR900135>
- Luce, C. H., & Black, T. A. (2001). Effects of traffic and ditch maintenance on forest road sediment production. In *Seventh Federal Interagency Sedimentation Conference* (pp. 67–74). Reno, Nevada. Retrieved from <http://www.treesearch.fs.fed.us/pubs/23963>
- MacDonald, L. H., & Coe, D. B. R. (2008). Road Sediment Production and Delivery: Processes and Management. In *First World Landslide Forum* (pp. 381–384). 18-21 November. Tokyo, Japan: United Nations University. Retrieved from <https://ucanr.edu/sites/forestry/files/138028.pdf>
- Marchi, L., & Dalla Fontana, G. (2005). GIS morphometric indicators for the analysis of sediment dynamics in mountain basins. *Environmental Geology*, 48(2), 218–228. <https://doi.org/10.1007/s00254-005-1292-4>
- Marr, P. G. (2014). Directional (Circular) Statistics. Retrieved from <http://webpace.ship.edu/pgmarr/Geo441/Lectures/Lec 16 - Directional Statistics.pdf>
- McCaffery, M., Switalski, T. A., & Eby, L. (2007). Effects of Road Decommissioning on Stream Habitat Characteristics in the South Fork Flathead River, Montana. *Transactions of the American Fisheries Society*, 136(3), 553–561. <https://doi.org/10.1577/T06-134.1>
- Menenti, M., & Ritchie, J. C. (1994). Estimation of effective aerodynamic roughness of Walnut Gulch watershed with laser altimeter measurements. *Water Resources Research*, 30(5), 1329–1337. <https://doi.org/10.1029/93WR03055>
- Miller, D. J., & Burnett, K. M. (2007). Effects of forest cover, topography, and sampling extent on the measured density of shallow, translational landslides. *Water Resources Research*, 43(3), 1–23. <https://doi.org/10.1029/2005WR004807>
- Miller, D. J., & Burnett, K. M. (2008). A probabilistic model of debris-flow delivery to stream channels, demonstrated for the Coast Range of Oregon, USA. *Geomorphology*, 94(1–2), 184–205. <https://doi.org/10.1016/j.geomorph.2007.05.009>
- Miller, R. H. (2014). *Influence of log truck traffic and road hydrology on sediment yield in western Oregon*. Oregon State University in. Retrieved from <http://ir.library.oregonstate.edu/xmlui/handle/1957/49899>
- Mitasova, H., & Iverson, L. R. (1996). Modeling topographic potential for erosion and deposition using GIS. *INT..J. Geographical Information System*, 10(5), 629–641. Retrieved from https://www.nrs.fs.fed.us/pubs/jrnl/1996/ne_1996_mitasova_001.pdf
- Montgomery, D. R., & Dietrich, W. E. (1994). A physically based model for the topographical control on shallow landsliding. *Water Resources Research*, 30(4), 1153–1171. <https://doi.org/10.1029/93WR02979>
- Moore, I. D., & Burch, G. J. (1986). Physical Basis of the Length-slope Factor in the Universal Soil Loss Equation. *Soil Science Society of America Journal*, 50(5), 1294. <https://doi.org/10.2136/sssaj1986.03615995005000050042x>

- Nield, J. M., King, J., Wiggs, G. F. S., Leyland, J., Bryant, R. G., Chiverrell, R. C., ... Washington, R. (2013). Estimating aerodynamic roughness over complex surface terrain. *Journal of Geophysical Research Atmospheres*, *118*(23), 12948–12961. <https://doi.org/10.1002/2013JD020632>
- O'Loughlin, E. M. (1986). Prediction of Surface Saturation Zones in Natural Catchments by Topographic Analysis. *Water Resources Research*, *22*(5), 794–804. <https://doi.org/10.1029/WR022i005p00794>
- Oldman Watershed Council. (2010). *Oldman River State of the Watershed Report 2010*. Lethbridge, Alberta. Retrieved from www.oldmanbasin.org
- Post, J. R., & Johnston, F. D. (2002). Status of the Bull Trout (*Salvelinus confluentus*) in Alberta. Edmonton, AB: Alberta Sustainable Resource Development, Fish and Wildlife Division, and Alberta Conservation Association, Wildlife Status Report No. 39. Retrieved from <https://open.alberta.ca/publications/0778518694>
- Purves, R. (2016). Working with terrain models. Retrieved from http://www.geo.uzh.ch/microsite/geo372/PDF/week4_geo372_terrain.pdf
- Qin, C., Zhu, A. X., Pei, T., Li, B., Zhou, C., & Yang, L. (2007). An adaptive approach to selecting a flow-partition exponent for a multiple-flow-direction algorithm. *International Journal of Geographical Information Science*, *21*(4), 443–458. <https://doi.org/10.1080/13658810601073240>
- Rainato, R., Picco, L., Cavalli, M., Mao, L., Neverman, A. J., & Tarolli, P. (2017). Coupling Climate Conditions, Sediment Sources and Sediment Transport in an Alpine Basin. *Land Degradation and Development*. <https://doi.org/10.1002/ldr.2813>
- Ramos-Scharrón, C. E., & MacDonald, L. H. (2005). Measurement and prediction of sediment production from unpaved roads, St John, US Virgin Islands. *Earth Surface Processes and Landforms*, *30*(10), 1283–1304. <https://doi.org/10.1002/esp.1201>
- Raupach, M. R. (1994). Simplified expressions for vegetation roughness length and zero-plane displacement as functions of canopy height and area index. *Boundary-Layer Meteorology*, *71*(1–2), 211–216. <https://doi.org/10.1007/BF00709229>
- Reid, L. M., & Dunne, T. (1984). Sediment production from forest road surfaces. *Water Resources Research*, *20*(11), 1753–1761. <https://doi.org/10.1029/WR020i011p01753>
- Reid, S. C., Lane, S. N., Montgomery, D. R., & Brookes, C. J. (2007). Does hydrological connectivity improve modelling of coarse sediment delivery in upland environments? *Geomorphology*, *90*(3–4), 263–282. <https://doi.org/10.1016/j.geomorph.2006.10.023>
- Renard, K. G., Foster, G. R., Weesies, G. a., & Porter, J. P. (1991). RUSLE: Revised universal soil loss equation. *Journal of Soil and Water Conservation*, *46*(1), 30–33. Retrieved from <http://www.jswnonline.org/content/46/1/30.short>
- Rex, J. F., & Petticrew, E. L. (2011). Fine Sediment Deposition at Forest Road Crossings: An

- Overview and Effective Monitoring Protocol. In D. A. Manning (Ed.), *Sediment Transport in Aquatic Environments* (2011th ed., p. 332). INTECH. Retrieved from <http://www.intechopen.com/books/sediment-transport-in-aquatic-environments%0AIn>
- Ripley, T., Scrimgeour, G., & Boyce, M. S. (2005). Bull trout (*Salvelinus confluentus*) occurrence and abundance influenced by cumulative industrial developments in a Canadian boreal forest watershed. *Canadian Journal of Fisheries and Aquatic Sciences*, 62(11), 2431–2442. <https://doi.org/10.1139/f05-150>
- Roy, A. G., & Robert, A. (1990). Fractal techniques and the surface roughness of talus slopes: a comment. *Earth Surface Processes and Landforms*, 15(3), 283–285. <https://doi.org/10.1002/esp.3290150310>
- RStudio Team (2018). RStudio: Integrated Development for R. RStudio, Inc., Boston, MA URL <http://www.rstudio.com/>.
- Sawatzky, C. D. (2016). Information in support of a recovery potential assessment of Bull Trout (*Salvelinus confluentus*) (Saskatchewan – Nelson rivers populations) in Alberta. *DFO Can. Sci. Advis. Sec. Res. Doc.*, 2016/113(December).
- Schäuble, H., Marinoni, O., & Hinderer, M. (2008). A GIS-based method to calculate flow accumulation by considering dams and their specific operation time. *Computers and Geosciences*, 34(6), 635–646. <https://doi.org/10.1016/j.cageo.2007.05.023>
- Schiess, P. (2001). Road Management Strategies to Reduce Habitat Impacts: A Case for Engineered Cable Yarding Operations and Harvest Schedules. In U. Arzberger & M. Grimoldi (Eds.), *New Trends in Wood Harvesting with Cable Systems for Sustainable Forest Management in The Mountains*. Ossiach, Austria June 18 to 24 June 2001: Forestry Training Centre, Government of Austria. Retrieved from <http://www.fao.org/3/Y9351E/Y9351E32.htm#ch32>
- Schiess, P., & Krogstad, F. (2000). Sediment and Road Density Reduction. In *Summit 2000, Washington Private Forests Forum*. Seattle, WA. Summer 2000: University of Washington. Retrieved from http://faculty.washington.edu/schiess/Publications/Road_Density/Forum_2000_paper.htm
- Shepard, M. K., Campbell, B. A., Bulmer, M. H., Farr, T. G., Gaddis, L. R., & Plaut, J. J. (2001). The roughness of natural terrain: A planetary and remote sensing perspective. *Journal of Geophysical Research E: Planets*, 106(E12), 32777–32795. <https://doi.org/10.1029/2000JE001429>
- Sosa-Pérez, G., & MacDonald, L. H. (2017). Reductions in road sediment production and road-stream connectivity from two decommissioning treatments. *Forest Ecology and Management*, 398, 116–129. <https://doi.org/10.1016/j.foreco.2017.04.031>
- Sugden, B. D., & Woods, S. W. (2007). Sediment Production From Forest Roads in Western Montana. *JAWRA Journal of the American Water Resources Association*, 43(1), 193–

206. <https://doi.org/10.1111/j.1752-1688.2007.00016.x>

- Tarboton, D. G. (1997). A new method for the determination of flow directions and upslope areas in grid digital elevation models. *Water Resources Research*, 33(2), 309–319. <https://doi.org/10.1029/96WR03137>
- TerrainWorks Inc., & FRIAA (2018). Identifying Unpaved Road Sediment Delivery to Critical Fish Habitats for Strategic Prioritization of Mitigation Actions in Alberta. Retrieved from www.terrainworks.com
- Thomas, I. A., Jordan, P., Shine, O., Fenton, O., Mellander, P. E., Dunlop, P., & Murphy, P. N. C. (2017). Defining optimal DEM resolutions and point densities for modeling hydrologically sensitive areas in agricultural catchments dominated by microtopography. *International Journal of Applied Earth Observation and Geoinformation*, 54, 38–52. <https://doi.org/10.1016/j.jag.2016.08.012>
- Thompson, C. J., Takken, I., & Croke, J. (2008). Hydrological and sedimentological connectivity of unsealed roads. In *Sediment Dynamics in Changing Environments* (pp. 524–531). Christchurch, New Zealand: International Association of Hydrological Sciences, IAHS Publ. 325, 2008.
- Trevisani, S., & Cavalli, M. (2016). Topography-based flow-directional roughness: Potential and challenges. *Earth Surface Dynamics*, 4(2), 343–358. <https://doi.org/10.5194/esurf-4-343-2016>
- Trevisani, S., & Rocca, M. (2015). MAD: Robust image texture analysis for applications in high-resolution geomorphometry. *Computers and Geosciences*, 81, 78–92. <https://doi.org/10.1016/j.cageo.2015.04.003>
- Tsai, V. J. D. (1993). Delaunay triangulations in TIN creation: An overview and a linear-time algorithm. *International Journal of Geographical Information Systems*, 7(6), 501–524. <https://doi.org/10.1080/02693799308901979>
- Valdal, E. J., & Quinn, M. S. (2011). Spatial Analysis of Forestry-Related Disturbance on Westslope Cutthroat Trout (*Oncorhynchus clarkii lewisi*): Implications for Policy and Management. *Applied Spatial Analysis and Policy*, 4(2), 95–111. <https://doi.org/10.1007/s12061-009-9045-5>
- van Meerveld, H. J., Baird, E. J., & Floyd, W. C. (2014). Controls on sediment production from an unpaved resource road in a Pacific maritime watershed. *Water Resources Research*, 50(6), 4803–4820. <https://doi.org/10.1002/2013WR014605>
- Wemple, B. C., Jones, J. a., & Grant, G. E. (1996). Channel network extension by logging roads in two basins, western Cascades, Oregon. *Water Resources Bulletin*, 32(6), 1195–1207. <https://doi.org/10.1029/2002WR001744>
- Whelley, P. L., Glaze, L. S., Calder, E. S., & Harding, D. J. (2014). LiDAR-derived surface roughness texture mapping: Application to Mount St. Helens pumice plain deposit analysis. *IEEE Transactions on Geoscience and Remote Sensing*, 52(1), 426–438.

<https://doi.org/10.1109/TGRS.2013.2241443>

White, B., Ogilvie, J., Campbell, D. M. H., Hiltz, D., Gauthier, B., Chisholm, H. K. H., ...
Arp, P. A. A. (2012). Using the Cartographic Depth-to-Water Index to Locate Small
Streams and Associated Wet Areas across Landscapes. *Canadian Water Resources
Journal / Revue Canadienne Des Ressources Hydriques*, 37(4), 333–347.

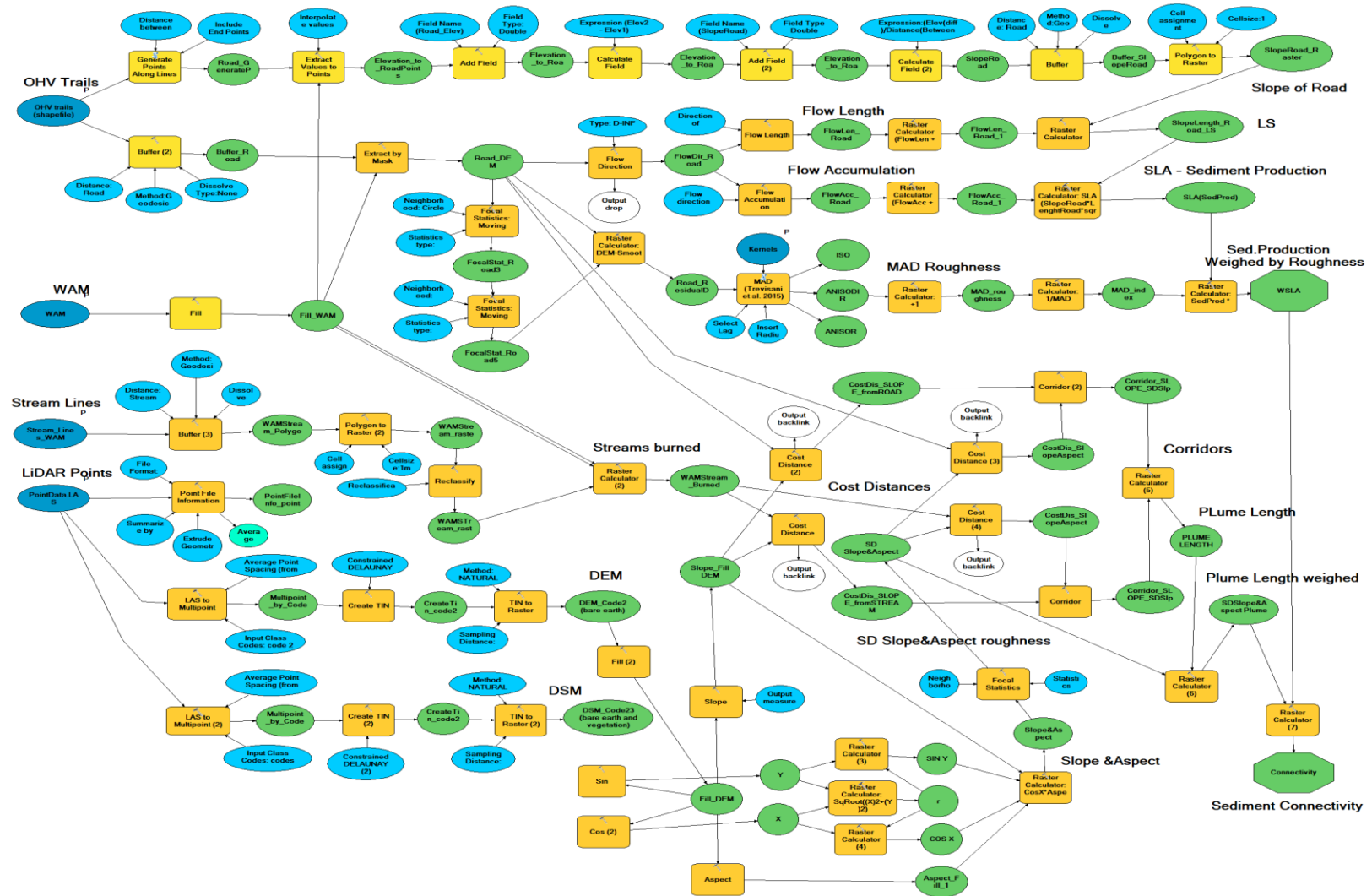
<https://doi.org/10.4296/cwrj2011-909>

White, R. A., Dietterick, B. C., Mastin, T., & Strohmman, R. (2010). forest roads mapped using
LiDAR in steep forested terrain. *Remote Sensing*, 2(4), 1120–1141.

<https://doi.org/10.3390/rs2041120>

Wischmeier, W. H., & Smith, D. D. (1978). Predicting rainfall erosion losses. *Agriculture
Handbook No. 537*, (537), 285–291. <https://doi.org/10.1029/TR039i002p00285>

Appendix A. Sediment Connectivity Model



Appendix B. Field Form for data collection.

IC FIELD EVALUATION FORM																									
Watershed Name		Dutch Creek						Road/District Name		Dutch						Site ID		D05							
Site Type (Stream crossings, cut bank, culverts, road failures):				Road Surface				Coordinates		East				675627.033				UTM Zone		11					
Road Type (Truck trail, Cut line):				On_highway				Coordinates		North				5530636.789				UTM Zone		11					
Erosion Characterization												Connection			Plum characteristics										
Characteristics	Soil & water management: Poor (0), Average (0.5),	Status: Inactive (0), Temporarily or permanently deactivated (0.5),	Soil Type and %: (Silt, Sand, Clay)	Slope: 0-2% 2-10% >10%	Quality: (Improved, Native), Graveled, Native)	Erosion features (gullies, other): none (0) little (.2) half (0.5) a lot	Traffic: (High, medium, low, none)	Length (L) m	Width (W) m	Estimate portion of erodible (Pe) area %:	Total Erodible area (L*W*Pe) m ²	Drainage Type: Natural or Engineered	Class Drainage	Connectivity to drainage: none (0) little (.2) half (0.5) potential	Plume presence	Buffer, artificial barriers: none (0) little (.2) half (0.5) a lot (0.8) all (1)	Plume length m	Width m	Depth (cm)	Shape	Plum Slope: 0-2% 2-10% >10%	Type of Plum Material and %			
Source of erosion																									
Road surface	0	1	Silt, Clay	5.2%(3°)	Native, Imp	0.8	High	13.2	6.3	80	66.528	Natural	Diffuse	0.2	Yes	0	7.6	1.2	10	Rectangular	19.4%(11°)	Fines			
Ditch																									
Cutslope																									
Hillslope																									
Comments:		mud hole which fills and then over tops road																							